AD-A138 075 ACCURACY ESTIMATE FOR RADAR CROSS SECTION MEASUREMENTS OF TARGETS MODELLE..(U) AIR FORCE INST OF TECH WRIGHT-PATTERSON AFB OH SCHOOL OF ENGI.. J N LINK 1/2

UNCLASSIFIED DEC 83 AFIT/GE/EE/83D-39 F/G 17/9 NL

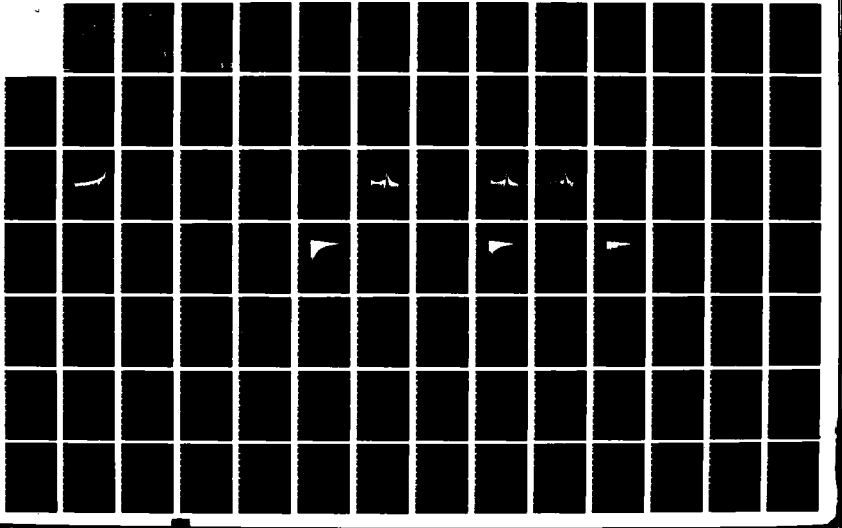

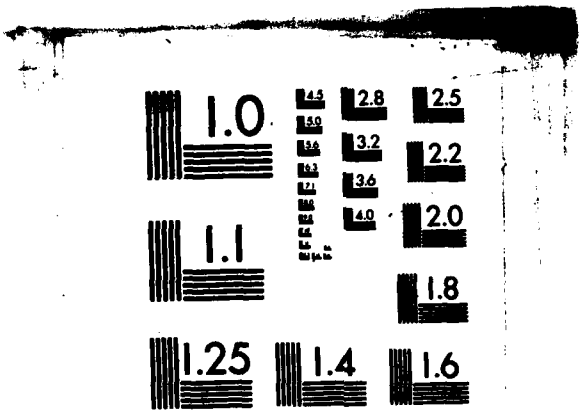

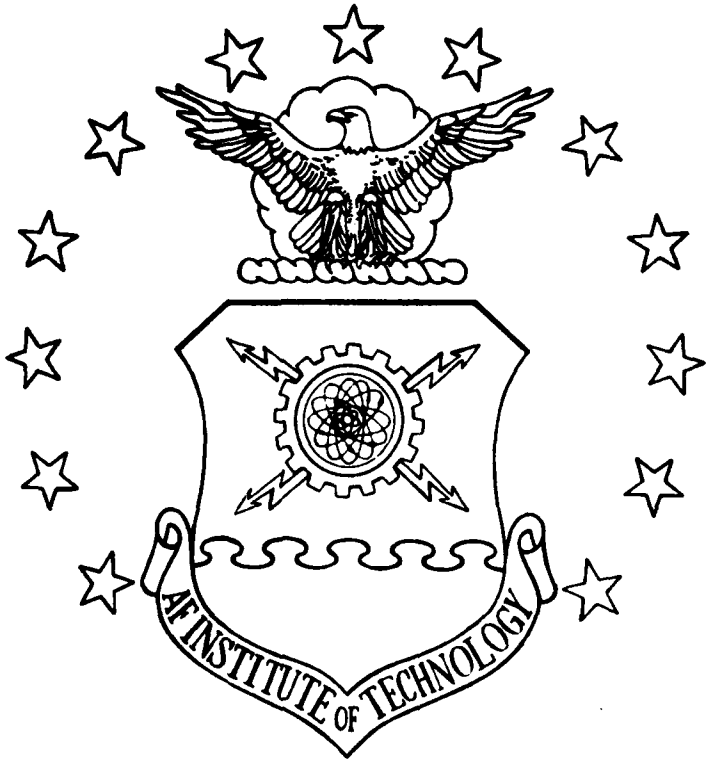

ACCURACY ESTIMATE FOR RADAR CROSS SECTION MEASUREMENTS OF TARGETS MODELLED BY MULTIPLE INDEPENDENT SCATTERERS IN CONSTANT CLUTTER

THESIS

AFIT/GE/EE/83D-39 Jon N. Link
2Lt USAF

DEPARTMENT OF THE AIR FORCE
AIR UNIVERSITY
AIR FORCE INSTITUTE OF TECHNOLOGY

Wright-Patterson Air Force Base, Ohio

AFIT/GE/EE/83D-39

ACCURACY ESTIMATE FOR RADAR CROSS SECTION MEASUREMENTS OF TARGETS MODELLED BY MULTIPLE INDEPENDENT SCATTERERS IN CONSTANT CLUTTER

THESIS

AFIT/GE/EE/83D-39 Jon N. Link
2Lt USAF

AFIT/GE/EE/83D-39

ACCURACY ESTIMATE FOR RADAR CROSS SECTION MEASUREMENTS OF TARGETS MODELLED BY MULTIPLE INDEPENDENT SCATTERERS IN CONSTANT CLUTTER

THESIS

Presented to the Faculty of the School of Engineering
of the Air Force Institute of Technology
Air University
in Partial Fulfillment of the
Requirements for the Degree of
Master of Science

by
Jon N. Link, B.S.
2Lt USAF
Graduate Electrical Engineering
December 1983

Preface

I would like to thank my sponsor, Mr. William Kent, ASD/ENAMA, for his support and help. Thanks are also due to my advisor, Captain Thomas Johnson, for his patience and guidence through this ordeal. Finally, a special note of thanks to my friends and family for their patience in putting up with me.

"the hammer drops,
the tire smokes,
the starship is lanched into
its next flight of fantasy."

Contents

Contents (continued)

List of Figures

List of Figures (continued)

List of Figures (continued)

List of Figures (continued)

List of Figures (continued)

Notation

Symbol		Definition
σ_t	. . .	Free space target radar cross section
σ_m	. . .	Measured radar cross section (includes effects from target and clutter)
σ_c	. . .	Clutter radar cross section
ϕ	. . .	Phase
$\bar{\sigma}_x$	. . .	Mean of cross section of x
s_x	. . .	Standard deviation of cross section of x
$\hat{\sigma}_x$	. . .	Estimate of cross section of x
$\bar{\hat{\sigma}}_x$	. . .	Mean of estimate of cross section of x
$s_{\hat{x}}$	. . .	Standard deviation of estimate of cross section of x
S/C	. . .	Signal to clutter ratio
X	. . .	Signal to clutter ratio
pdf	. . .	Probability density function
E[x]	. . .	Expected value of x
r_{xy}	. . .	Correlation Coefficient of x and y
$f_x(x)$	. . .	Probability density function of x
$f_{xy}(x\|y)$	. . .	Conditional probability density function of x given y
$f_{xy}(x,y)$	. . .	Joint Probability function of x and y

Abstract

The error bounds for accuracy of radar cross section (RCS) measurements of targets in clutter are examined in detail. Traditional error bounds are based on precision at every individual aspect angle and on two deterministic sources (target and clutter). In this thesis a model is developed that describes the target and clutter probabilistically. The requirement of accuracy at every point is replaced by a requirement for accuracy of a running average of measured RCS values. The probability distribution of the ratio of the averaged, measured RCS to the averaged, true, free space target RCS is calculated. The standard deviation of this ratio represents how much the averaged, measured RCS data diverages from the averaged, true, free space target RCS.

The results show that accuracy improves for increasing signal to clutter ratios, and also for increasing levels of averaging. Even averaging as few as eleven points, this new measure is shown to give more confidence in the measured, averaged results than the traditional approach.

ACCURACY ESTIMATE FOR RADAR CROSS SECTION MEASUREMENTS OF TARGETS MODELLED BY MULTIPLE INDEPENDENT SCATTERERS IN CONSTANT CLUTTER

I. Introduction

Background

An important design consideration of modern airframes must be their Radar Cross Section (RCS). Essentially, this RCS is a measure of how well a radar will be able to locate the airframe, or rather, the radar target. Because of its extremely complicated nature, the only reliable method of determining a target's RCS involves actually measuring it. As with any physical measurement, errors must be accounted for. One source of errors in the RCS measurement is the unwanted radar echo returns from background clutter.

The RCS of a target, simply put, is a measure of the electromagnetic energy scattered or reflected from the target divided by the electromagnetic energy incident upon the target. There are two main sources that contribute to the RCS of the target. The first, specular reflection, comes

about from large, flat surfaces. Specular reflection is analogous to light that is reflected from a common mirror. Generally, this type of scattering dominates the characteristic RCS of a target. However, today there is a trend to reduce cross sections as much as possible. Low RCS targets are especially attractive in the military environment. A target, or more specifically, an airplane, has a much higher chance of survival in a hostile enviroment if it has a lower probability of being detected by the enemy's radar.

With RCS's continually being reduced, the second type of scattering, which normally causes a much smaller return, becomes significant. One important subset of this category is called diffracting scattering, Diffracting scattering is due to electromagnetic effects of sharp corners, edges, and other discontinuities in the target's surface at high frequency (usually microwave frequencies and higher). A real target's RCS is made up of a combination of specular and diffracting scatterers.

The target's RCS pattern will have regions governed by specular scatterers and regions governed by diffracting scatterers. Regardless of whether a particular region of the RCS pattern is governed by specular or diffracting scatterers it can be modelled as a collection of independent scatterers. However, when there are very many of these independent scatterers they become probabilistic in nature and also generally create a lower level of cross section. Because the

magnitude of the radar return in these areas is lower, it is more affected by measurement errors.

When a target's RCS is measured, the background clutter, that is also illuminated by the radar, creates errors. These errors arise from a portion of the radar's energy being returned from objects other than the target. During RCS measurement, unwanted radar returns are often caused by nearby structures, target supports, ground interference, and certain atmospheric conditions. Therefore, knowledge of how background clutter affects the accuracy of the measurement becomes an important consideration in RCS measurement.

Background errors are among the most serious source of errors in RCS measurements. The background cross section is defined as the cross section measured without the target present. Most measurement ranges can be cleared of objects that cause errors and if these objects can not be cleared, the error causing radar return can usually be eliminated by using range gating on the radar. The only component of the background error that can not be dealt with directly is the error from the target support. The target support is a "necessary evil" that must be dealt with differently. In general, the measured cross section results from the vector sum of the scattered fields from the background (target support) and the target. If the presence of the target does not greatly change the background fields, the target support's cross section can be measured separately and then subtracted off leaving only the cross section of the target.

This, however, is usually not the case. In general, there will be interaction between the target and target support. This interaction comes in two forms, direct interaction between the individual scattered fields, and interaction from multiple "bounces" between the target and the target support. The error from this interaction (which turns out to be random) becomes significant as the levels of the target and background become closer, or rather, as the level of the cross ssection of the target becomes smaller as RCS reduction techniques improve. In the remainder of this paper we will assume that all background clutter is caused by the target support. As a result, all models that are presented that deal with the error causing background are actually models representing the target support.

Problem

The goal of this thesis is to apply statistical techniques to solve the general problem of a target modelled as multiple independent scatterers with constant background clutter and to develop an accuracy estimate as a function of signal to clutter ratio.

Assumptions

The development and solution of this thesis depends on the following assumptions:

1. Targets and background clutter can be probabilistically modeled as a collection of distinct scattering points.
2. The target and clutter are sufficiently far from the source and receiver to approximate the incident electromagnetic waves as planar.
3. The Geometric Theory of Diffraction (GTD) is an accurate and reliable method of modelling this class of electromagnetic scattering problems. GTD is not necessary for the development of the theoretical models. It is, however, necessary for the computer simulation models.
4. There is no distortion or noise from anything except the background clutter and this background clutter is solely from the target support.

Review of Literature

To date, the contribution of errors from background clutter has been dealt with in two ways. the first, and most general, is summarized by Ruck [Ref 12:913-923] and Crispin [Ref 4:381-386]. Here, an estimate for the maximum error is developed based on the ratio of the radar cross section measured to the background clutter. Their error estimate is developed assuming a general background and fixed target and background signal levels. The graphs showing this maximum error estimate present the "worst case" error bounds based on no knowledge of clutter sources and requiring accuracy at every point of aspect angle. This technique is reviewed in depth in Chapter II. We are more interested in a specific background error contributor, the target support, and we are interested in an estimate that is not limited to the maximum error.

The second way of dealing with the background error is to develop an expression for the clutter's cross section. The most important error contribution comes, of course, from the target support and has been found for the deterministic case by several people. One of the first was Senior [Ref 13]. He developed several expressions for the radar cross section of foamed plastic target supports. With these expressions Senior could design foamed plastic supports for various heights, diameters, and cross sections. He showed that the cross section from these target supports was very frequency sensitive and by changing the relative permittivity and size,

the radar cross section could be "tuned" between succesive maxima and minima. This was important at that time, but is not very important today, because the state of the art in target supports has surpassed the height and weight limitations of foamed plastic columns, thus making them obsolete. Senior did make one significant observation, however. He showed that a "christmas tree" shaped, or rather, a serrated cone shaped, support pedestal will be less frequency sensitive (because of the serrations) and, because of the angle of the leading surface, will direct the backscatter away from the receiver. Serrations are not of interest anymore, but leaning the target support has been shown to be an effective way of minimizing the direct backscatter.

Another person who developed expressions for the radar cross section of target supports was Freeny [Ref 6]. Freeny, like Senior, found the cross section of plastic column supports given various height, weight, and dielectric constant limitations. He also found the radar cross section of suspension line supports. For each different kind of target support, Freeny graphed the maximum background error vs. the target cross section. As before, Freeny's work was significant at the time but modern supports, such as metal knife-edged columns, have a lower cross section, can be built taller, and can support a heavier weight.

Another factor in previous work on the cross sections of various target supports is their assumption that the cross

sections were entirely deterministic. At best, Freeny assumed uniform phase distribution between the background and target return. These earlier target supports were far from deterministic. But all of the previous work has neglected the possibility that the target support has probabilistic components other than a simple random phase distribution. An additional assumption that was present in these general approaches was that the location and value of every RCS peak and of every minimum should not be affected by the background. If the pattern data is analyzed from the viewpoint that a running median or running average over some window (say one degree) is evaluated, the hard requirements of accuracy at every point of the traditional approach no longer apply.

General Approach

The approach to solving this thesis can be broken up into the following main divisions:

1. Derive the statistics of the target's free space cross section.
2. Derive the statistics of the target with target support cross section.
3. Develop a new approach to analyzing the accuracy estimate of the measured cross section data.
4. Derive the statistics of this new approach and compare them with the traditional approach.
5. Use the results from the new approach to derive a new measure of confidence that can be placed on the measured cross section data.

Development

In this paper several probabilistic models of the target and target support will be analyzed. To provide a basis for comparision, computer generated data will be used. This data can be generated for a variety of average signal to clutter ratios all representing a diffracting source. The procedure used to obtain and process this computer generated data is explained in Chapter II.

An indepth review of the tradtional approach is presented in Chapter III. The statistics for two general sources, N general sources, and Rayleigh distributed N sources will be

formulated. This last model, that of the Rayleigh distributed target, will be used to represent the target in free space. This probablility density function (pdf) will be compared to a pdf curve obtained from the computer generated data.

In Chapter IV the new model for the target and target support is introduced. This model will be simply a Rayleigh distributed target added to a constant, deterministic clutter. The pdf and statistics will be derived for this new model and compared to the pdf obtained from the computer generated data.

Using this new model, a new approach for analyzing the accuracy of the measured cross section will be derived in Chapter V. This new approach will then be compared to the traditional approach as well as the computer generated data.

Finally in Chapter VI the results are summarized. Also the measure of confidence that can be placed in the measured data is discussed and compared to the traditional measure of confidence.

II. Computer Simulation Models of Target and Target Support

In this chapter the techniques using the computer to generate simulated RCS data are summarized. This data is important because it will be compared to the theortical results.

The heart of the computer generated data is a FORTRAN program written by R. J. Marhefka. This program, called "Radar Cross Section Basic Scattering Code," or "RCSBSC," is a very versatile program designed to find the radar cross section of any target that can be modelled as a collection of multiple flat plates and multiple finite cylinders. The code can simulate many high frequencies, here the data was generated assuming a frequency of 9 GHz, and many axes of rotation. The code is based on uniform asymptotic techniques formulated in terms of the Uniform Geometrical Theory of Diffraction (UTD).

This code is not with out limitations, however. The code only accounts for the double diffracted fields from corner to edge, edge to corner, and corner to corner. The code does not contain the higher order scattering effects such as edge waves (corner to corner trapped along the edge) and triple diffraction. The higher order effects primarily add to the fine detail of the cross section patterns. Another

disadvantage of the code is that it works only for finite flat plates. As a result, there is no way to model an infinte ground plane to be under the target model.

Target and Target Support Models

The model that represents the target is a flat isosceles triangular plate. This flat plate is of length 0.91 meters and has a base of 0.55 meters. It is oriented such that the apex of the triangle is pointed toward the radar at 0 degrees aspect angle. It is also oriented such that the normal of the flat plate is parallel to the normal of the imaginary ground plane, or rather, the flat plate lies flat, parallel to the ground (see Figure II-1). This model is used as input for the RCSBSC program to generate data that represents the target in free space.

The target support is modelled as another flat triangular plate. The top of the support model, where the support is attached to the target, is 0.30 meters wide. The support model is 2.40 meters long and comes to a point at the bottom (see Figure II-1). The background clutter level is obtained by finding the value of the cross section of the target support alone at 0 degrees aspect. This clutter level can be adjusted by varying the tilt angle of the support (see Figure II-2). As can be seen, changing the tilt angle of the support by just a small amount can have a dramatic effect on the background clutter level.

Ideally, the computer model would consist of a target on a target support and the entire system on an infinite ground plane. This ground plane is desired because in actual conditions, the ground plane affects the antenna pattern from the radar. For vertical polarization, the polarization of the incident field assumed to generate the data, the ground plane will force the antenna pattern to have a null at the ground. The ground plane also affects the system by allowing radiated energy to reflect off of the ground. The reflection can not be modeled with the computer code, but the antenna pattern can be modeled by forcing the support to contribute less and less of a return the further down the support until at the bottom of the support, where the model comes to a point, there is no contribution to the reflected energy.

The computer program was designed to find the radar cross section of a modelled target in free space. That is, the program rotates the entire target with respect to aspect angle. In this case, however, the radar cross section of the target and target support system is needed. The target needs to be rotated while leaving the support stationary. To do this the original RCSBSC program was modified. As a result, the program takes considerably more time to run but it does allow for rotating only part of the system.

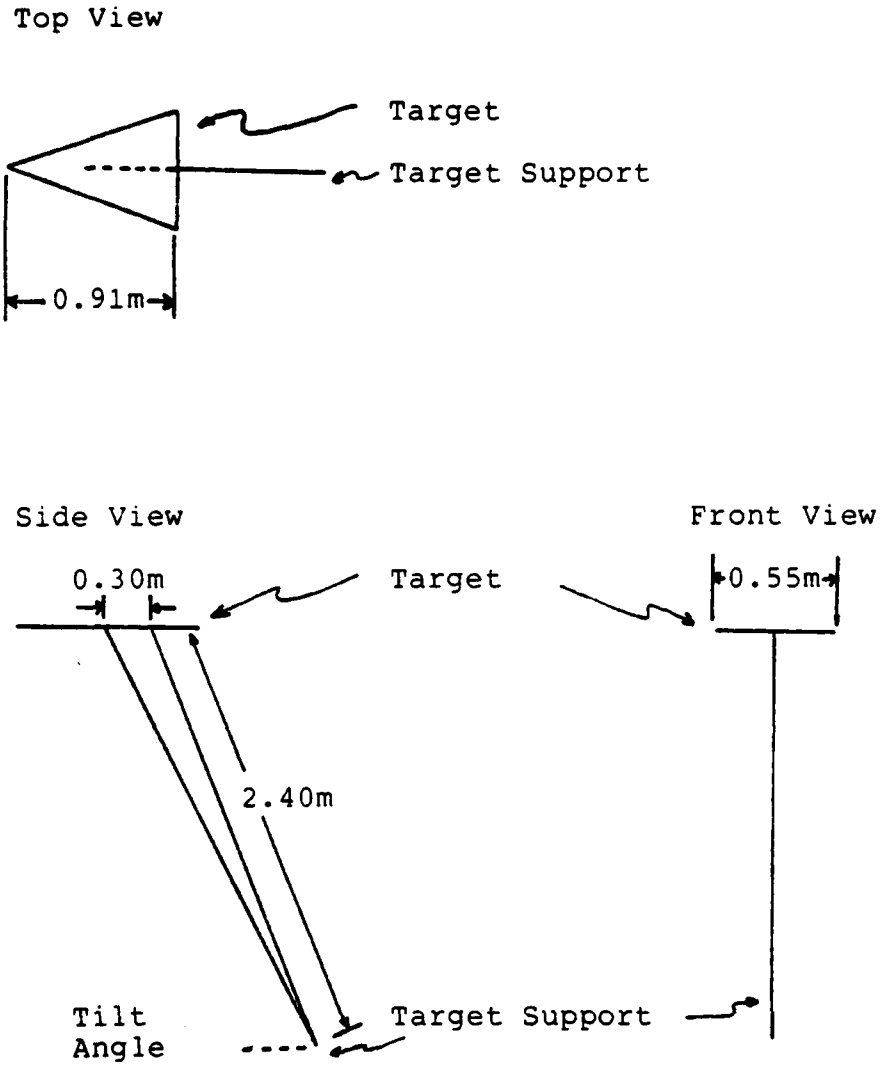

Figure II-1 Target and Target Support Computer Simulation Models

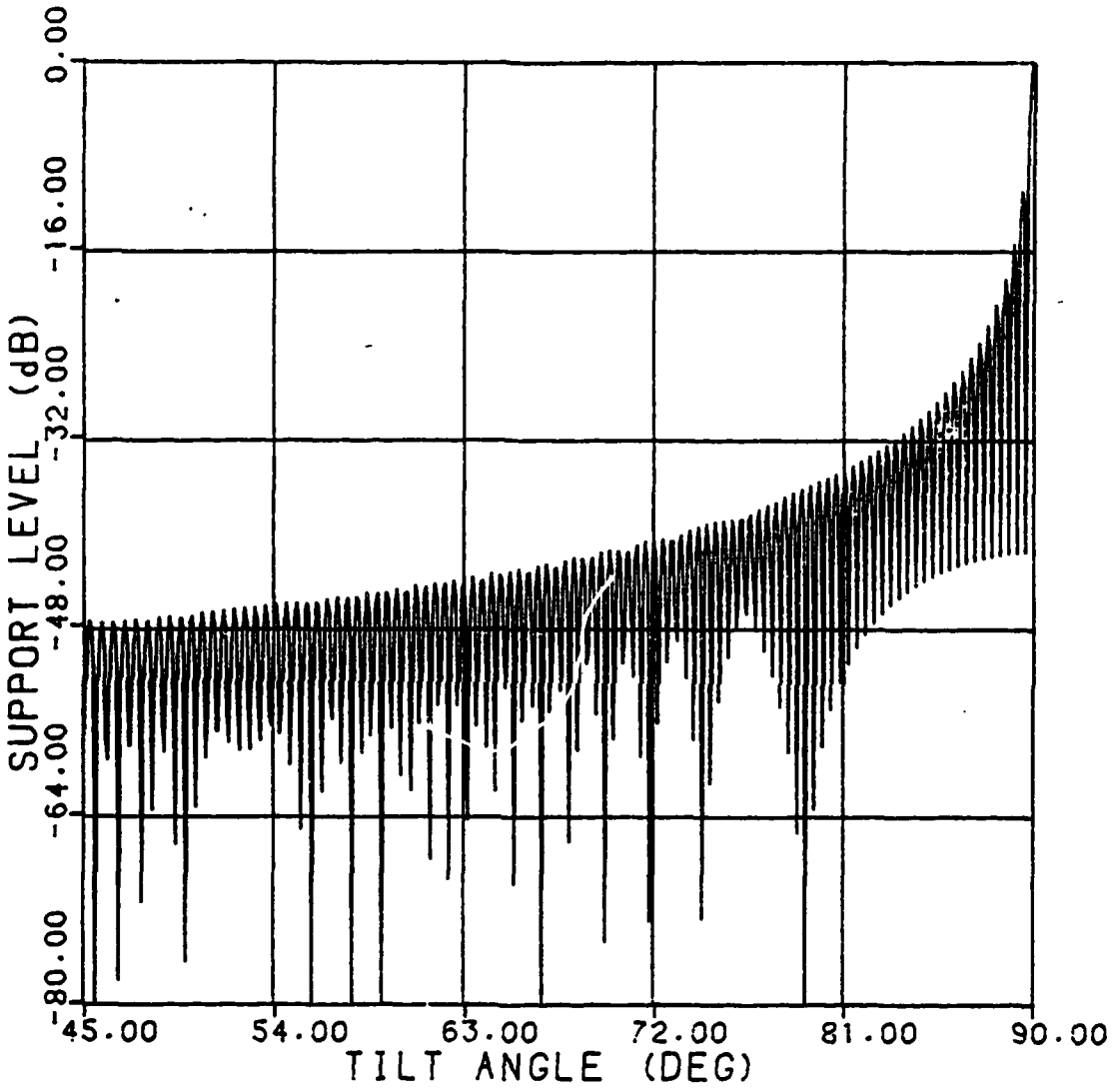

Figure II-2 Support Background Clutter Level vs. Tilt Angle

Cross Section Patterns and Signal to Clutter Ratios

The modified RCSBSC program can be run for any degree increment. However, when this program is run at increments of a hundreth of a degree the cross section data points become correlated. In order to get sufficient independent data points the program must be run with tenth of a degree increments. Independence in the cross section data points is an assumption that is made later in the development of several probabilistic models. The computer generated plot of the target's free space radar cross section pattern for every tenth of a degree is shown in Figure II-3.

Because only vertical polarization is being used, large returns from back edges of the target are expected. The vertically polarized electromagnetic wave passes by the leading edge of the target unaffected. As the wave progresses across the target it creates a surface current in the target. When the wave meets the back edge the surface current is very suddenly terminated. It is this sudden termination that creates the large scattering return. The pattern is just as expected. The large spike-like return at 0 degrees aspect is produced by the base edge of the triangular model. The other large return occurs at an aspect angle of about 107 degrees. This too represents the return from a back edge. Also, because of the symmetry of the target, the radar cross section pattern will be symmetric about 0 or 180 degrees aspect angle.

This paper assumes a target that can be represented as a

diffracting scatterer. The large returns, however, are caused by a "specular diffraction". "Specular diffraction" is a phrase sometimes loosely associated with the return, in vertical polarization, from edge that is perpendicular to the direction of the wavefront. Therefore, these areas are not wanted in this analysis. The region between 15 and 95 degrees aspect angle will be used. This region is sufficiently far from the points of "specular diffraction." The pattern in this region is dominated by the lower level, rapidly varying, fine structure which is characteristic of a diffracting scatterer. The average cross section level in this diffracting region is needed to find the average signal to clutter ratio. This can be done by plotting the pattern after it has been processed by a running average program. This program finds the average within a window, then moves the window one increment, then again finds the average within the window, and so on.

Figure II-4 shows a plot of the target's free space radar cross section pattarn after the data has been processed by this running average program. The averaging window was 51 points wide, which represents a window of just over 5 degrees. It can be seen from this figure that the average cross section level of the target is about -47 dB. It can also be seen that not only does taking a running average across the entire pattern smooth out the diffracting regions, it also significantly reduces the specular regions.

When the target support is added to the system, the

target is , of course no longer in free space. The support will contribute to the radar cross section pattern not only directly but also from its interaction with the target. Data for several different clutter or support levels was obtained by varying the tilt angle of the support. Below is a table summarizing the support levels, tilt angles, and resultant average signal to clutter ratios (S/C).

Tilt Angle (deg)	Clutter Level (dB)	S/C	S/C (dB)
66.0	-49.1	1.6	2.1
68.0	-60.6	22.9	13.6
70.0	-44.6	0.6	-2.4
80.0	-53.9	4.9	6.9

Table II-1 Summary of Tilt Angles and Clutter Levels from Computer Generated Data

It is important to realize that the signal to clutter ratios above are merely average values. It is possible to obtain only a rough estimate of the average signal to clutter ratio from this data. The signal to clutter ratio can only be estimated because the actual data varies rapidly from point to point. The true signal to clutter ratio may vary considerably.

Figure II-5 shows the radar cross section pattern of the target and target support with a high average signal to clutter ratio. It can be seen that the target support does not effect the pattern a great deal. This is contrasted to

Figure II-6 which shows a target and target support with very low average signal to clutter ratio. As the clutter becomes stronger, it dramatically affects the cross section pattern. This effect is most significant in the diffraction region. Not only does the clutter affect the values of the nulls and peaks, it also affects their exact loacton.

The question that needs to be answered is what average signal to clutter ratio is necessary for a given error level assuming an a priori knowledge of the target and target support. The data that is generated with this "RCSBSC" program will be used to verify the results obtained theortically.

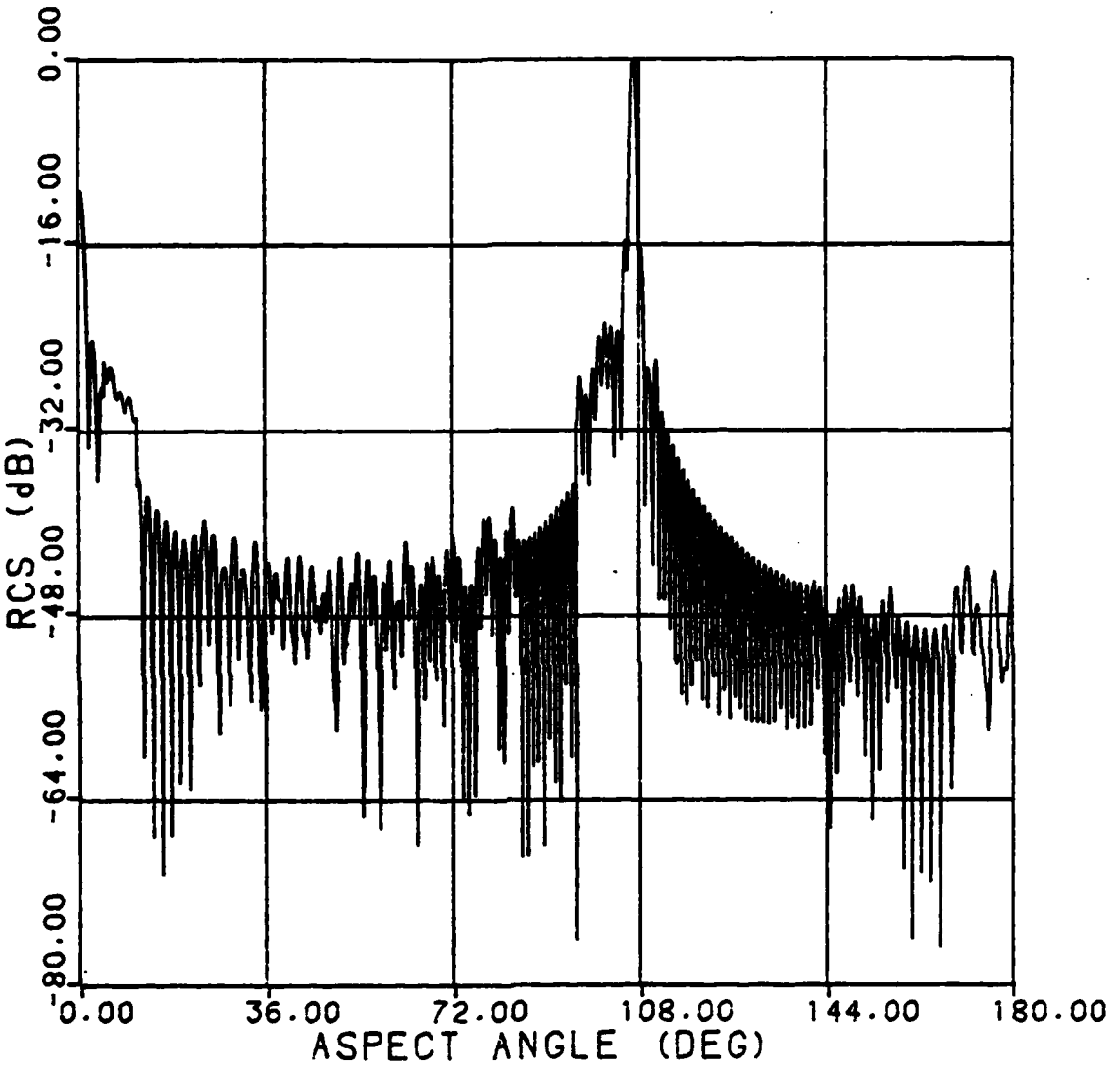

Figure II-3 Target Free Space Cross Section Pattern

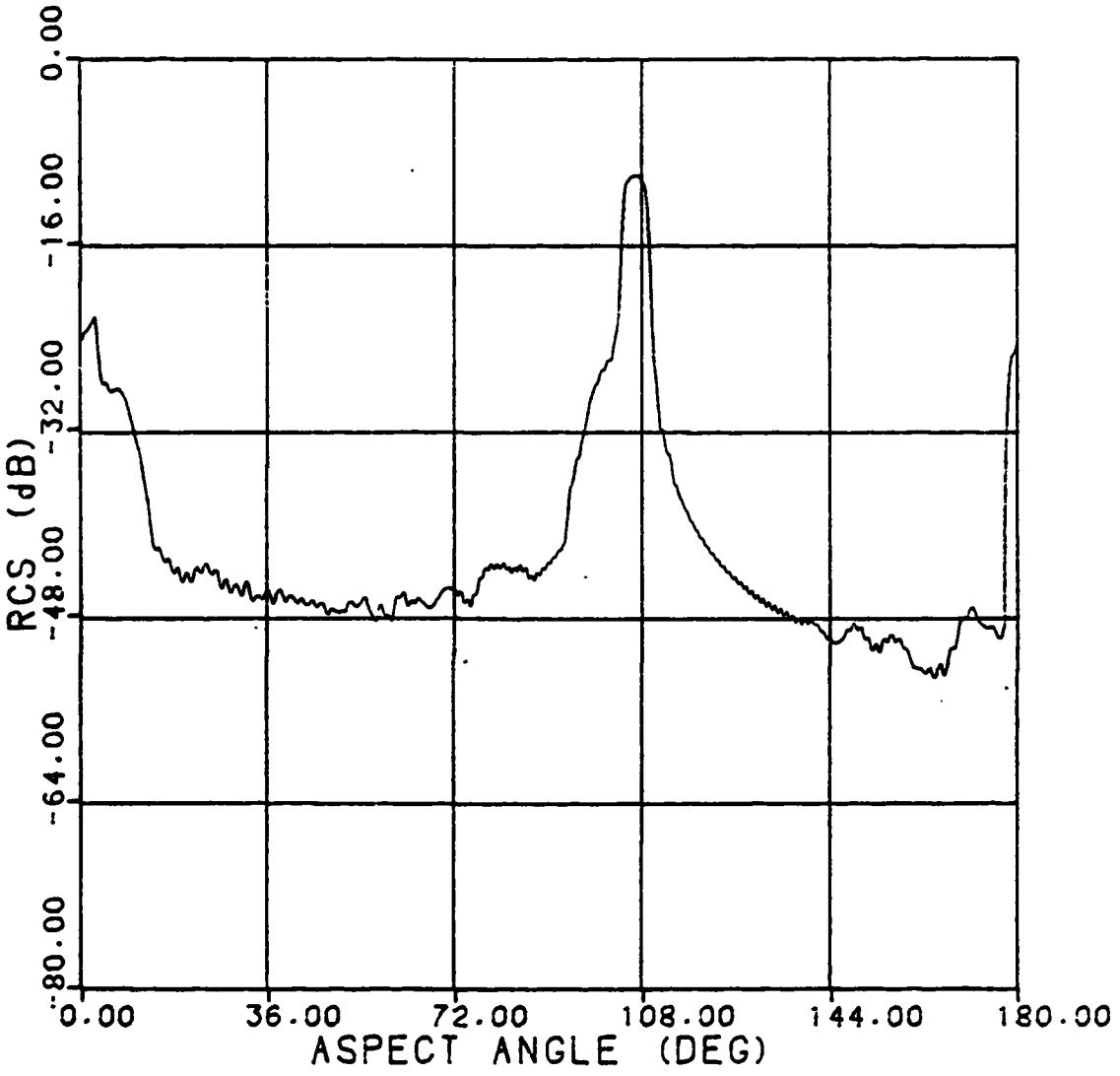

Figure II-4 Averaged Target Free Space Cross Section Pattern

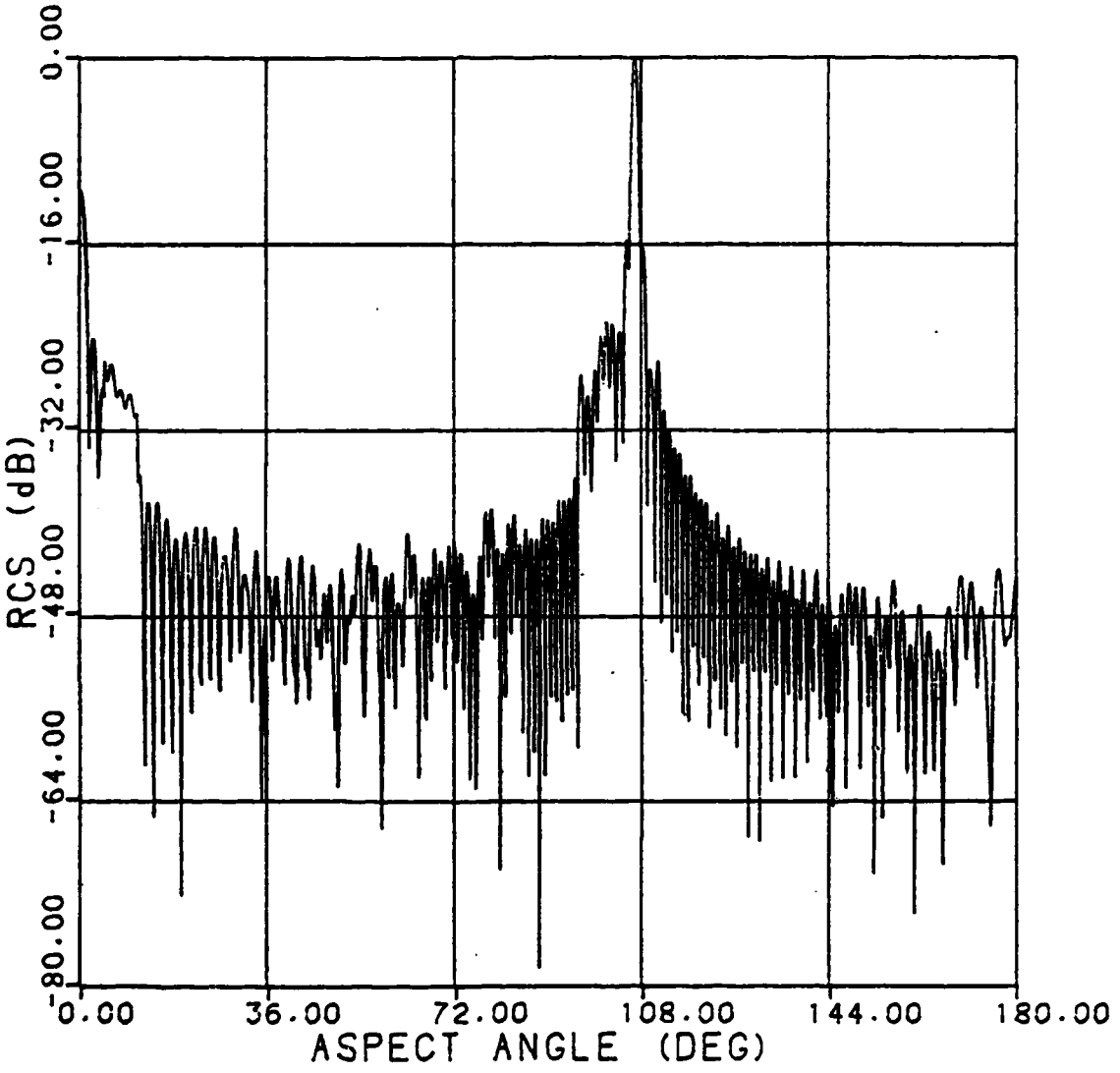

Figure II-5 Target With Target Support Cross Section Pattern For High Signal to Clutter Ratio (13.6 dB)

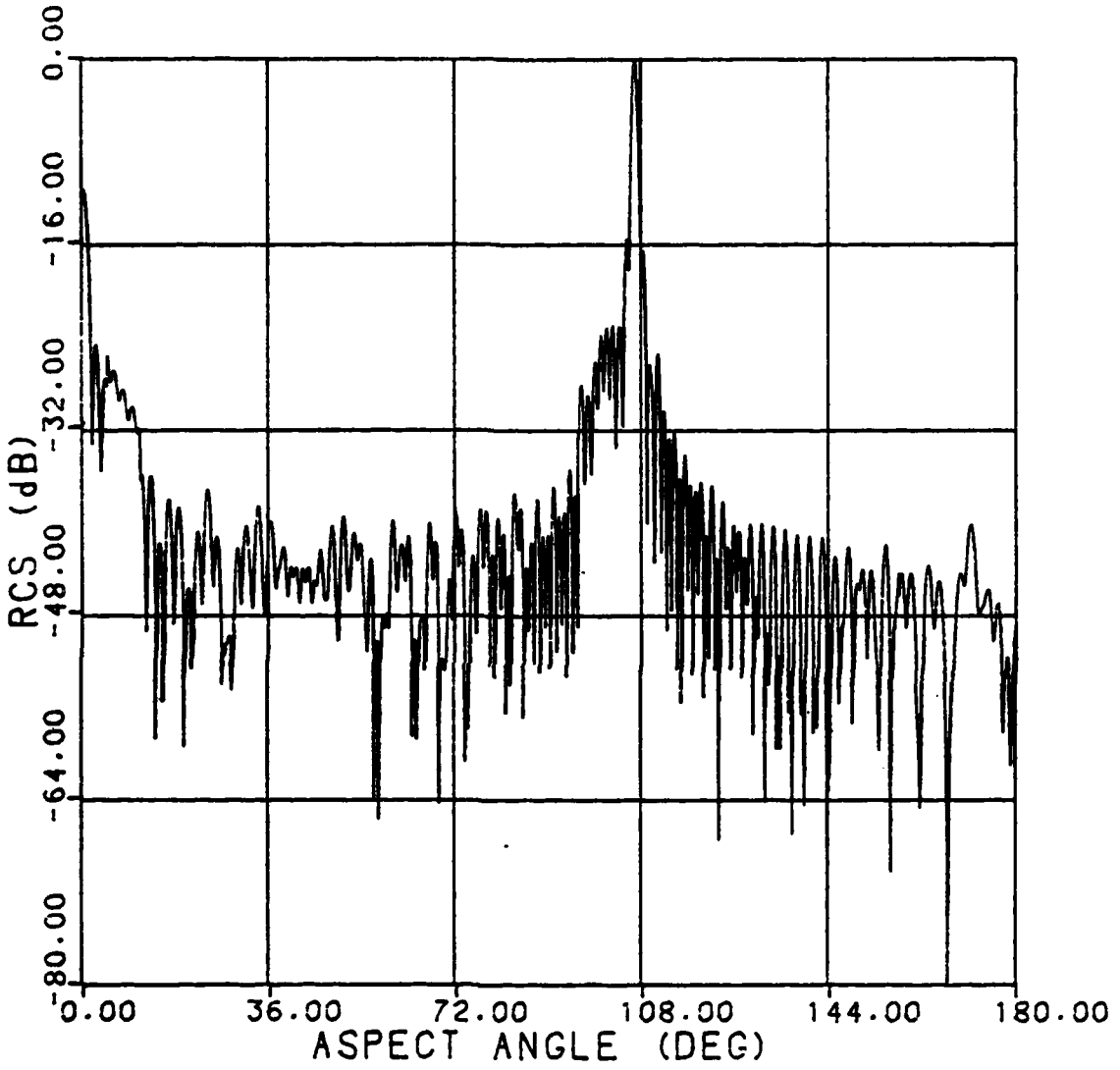

Figure II-6 Target With Target Support Cross Section Pattern For Low Signal to Clutter Ratio (2.1 dB)

III. Traditional Approach

The traditional approach is summarized by Ruck [Ref 12:913-923] and Crispin [Ref 4:381-386]. Here, they develop the maximum possible error and a "rms error" based on the ratio of the measured radar cross section to the average measured cross section. These maximum and rms errors are then calculated for a range of signal to clutter ratios. The maximum error is the "worst case" error bounds based on no knowledge of the clutter sources and requiring accuracy at every point of aspect angle. The traditional approach also assumes that the sources are all deterministic in nature. Crispin's "rms error" is similar to the maximum error except here the swing is not based on the "worst case," but rather, on the bounds of one standard deviation on either side of the mean of the measured cross section. This rms error is a measure of the confidence that can be put in to the measured cross section values. The narrower the rms error curves, the closer the values will be spaced around the mean of the measured cross section.

To gain useful knowledge from RCS measurement data, whether gathered theoetically or experimentally, an averaging technique must be used. Some of these techniques include: averaging with respect to phase, averaging with respect to

wavelength, and averaging with respect to aspect [Ref 3:980]. One of the most common methods is the first and is referred to as the "Random Phase Method." This is the averaging technique that is used in the traditional approach.

In this chapter the statistics of several different models will be summarized and for the first model, the two source model, the theortical results will be compared to results from the computer generated data. The traditional approach requires accuracy at every point and therefore is deterministic in nature. All of the sources' signal voltages, for the models are based on random phase, uniformly distributed between 0 and 2 . The deterministic amplitudes of the signal are proportional to the square root of the source's cross section. This is because the radar cross section is defined as being proportional to the square of the scattered electric field magnitude over the square of the incident electric field magnitude. The magnitude of the source's signal voltage will be proportional to the electric field magnitude, and thus proportional to the square root of the cross section.

The cross section models that will be used are:

1. Two sources with deterministic amplitudes.
2. N sources with deterministic amplitudes.
3. One source with Rayleigh distribution for the amplitudes.

Two Sources (Deterministic)

In this section, a simple model of two sources will be used. This is the traditional approach of viewing the target and support, one source represents the target and the other represents the target support. Each of the sources will have a deterministic amplitude and each will have a random phase, uniformly distributed between 0 and 2π .

Since the sources' signal voltages are proportional to the square root of their cross section, the measured cross section is simply the square of the complex sum of the two complex source voltages.

$$\sigma_m = \left| \sqrt{\sigma_1}\, e^{j(\phi_1)} + \sqrt{\sigma_2}\, e^{j(\phi_2)} \right|^2 \qquad \text{(III-1)}$$

where

σ_m = measured cross section
σ_1 = cross section of the first source (deterministic)
ϕ_1 = phase of the first source (uniform random)
σ_2 = cross section of the second source (deterministic)
ϕ_2 = phase of the second source (uniform random)

The measured cross section can also be written as:

$$\sigma_m = \left(\sqrt{\sigma_1}\, e^{j(\phi_1)} + \sqrt{\sigma_2}\, e^{j(\phi_2)} \right) * \left(\sqrt{\sigma_1}\, e^{-j(\phi_1)} + \sqrt{\sigma_2}\, e^{-j(\phi_2)} \right) \qquad \text{(III-2)}$$

$$\sigma_m = \sigma_1 + \sigma_2 + \sqrt{\sigma_1\sigma_2}\, e^{j(\phi_1-\phi_2)} + \sqrt{\sigma_1\sigma_2}\, e^{-j(\phi_1-\phi_2)} \qquad \text{(III-3)}$$

$$\sigma_m = \sigma_1 + \sigma_2 + 2\sqrt{\sigma_1\sigma_2}\cos(\phi) \qquad \text{(III-4)}$$

where

ϕ = relative phase between first and second source

Next, the mean of the measured cross section is found. The mean is taken to be the expected value of the measured cross section.

$$\bar{\sigma}_m = E[\sigma_m] \qquad \text{(III-5)}$$

$$\bar{\sigma}_m = E[\sigma_1 + \sigma_2 + 2\sqrt{\sigma_1\sigma_2}\cos(\phi)] \qquad \text{(III-6)}$$

The expected value of the two determinstic cross sections, of course, is simply their value. And as a consequence of assuming a uniform distribution for the relative phase between the two components, the mean of the measured cross section is simply the sum of the component cross sections.

$$\bar{\sigma}_m = \sigma_1 + \sigma_2 + 2\sqrt{\sigma_1\sigma_2}\,E[\cos(\phi)] \qquad \text{(III-7)}$$

$$\bar{\sigma}_m = \sigma_1 + \sigma_2 \qquad \text{(III-8)}$$

Also, of interest is the maximum and minimum value of the measured cross section. These are obtained by letting the difference between the phases of the signals to be 0 and π. When these limits are substituted into Equation (III-4) the measured cross section falls between the bounds given by:

$$\sigma_m = \sigma_1 + \sigma_2 \pm 2\sqrt{\sigma_1\sigma_2} \qquad \text{(III-9)}$$

Of interest also is the standard deviation of the measured cross section. The standard deviation is taken to be the square root of the variance, and the variance to be the expected value of the square of the difference between the measured cross section and its mean.

$$s_m^2 = E[(\sigma_m - \bar{\sigma}_m)^2] \qquad \text{(III-10)}$$

where

s_m^2 = variance of the measured cross section
s_m = standard deviation of the measured cross section

Into this equation the expression for the measured cross section, Equation (III-4), and the mean of the measured cross section, Equation (III-5) are substituted.

$$s_m^2 = E[(\sigma_1 + \sigma_2 + 2\sqrt{\sigma_1\sigma_2}\cos(\phi) - (\sigma_1 - \sigma_2))^2] \qquad \text{(III-11)}$$

$$s_m^2 = E[(2\sqrt{\sigma_1\sigma_2}\cos(\phi))^2] \qquad \text{(III-12)}$$

$$s_m^2 = 4\sigma_1\sigma_2 E[\cos^2(\phi)] \qquad \text{(III-13)}$$

As a consequence of assuming a uniform distribution over 0 and 2π for the relative phases, the expected value of the square of the cosine of their difference is 1/2.

$$s_m^2 = 2\sigma_1\sigma_2 \qquad \text{(III-14)}$$

As a result, the standard deviation of the measured cross section is simply the square root of twice the product of the components.

$$s_m^2 = \sqrt{2\sigma_1\sigma_2} \qquad \text{(III-15)}$$

For the case of two sources, the mean, the variance, the standard deviation, the maximum, and the minimum value of the measured cross section have been found. Figure III-1 shows a graph of these statistics. Where the maximum/minimum spread is given by:

$$\sigma_m = \sigma_1 + \sigma_2 \pm 2\sqrt{\sigma_1\sigma_2} \qquad \text{(III-16)}$$

And the rms spread is a standard deviation above and below the mean.

$$\sigma_m = \sigma_1 + \sigma_2 \pm \sqrt{2\sigma_1\sigma_2} \qquad \text{(III-17)}$$

The two inside curves represent the rms error bounds, and the two outside curves represent the maximum error bounds. These curves are plotted as the measured cross section in dB normalized by the average measured cross section versus the ratio of the two sources' cross section. If one source is taken to represent the target and the other to represent background clutter, the graph is a measure of how spread the measurements will be for a range of signal to clutter ratios.

According to Crispin and Moffett, experience [Ref 3:980] with measured data has shown that even with rapidly varing experimental data, the RCS curve, or rather, the RCS data points, will lie within the region defined by the RMS spread 50 to 60 percent of the time.

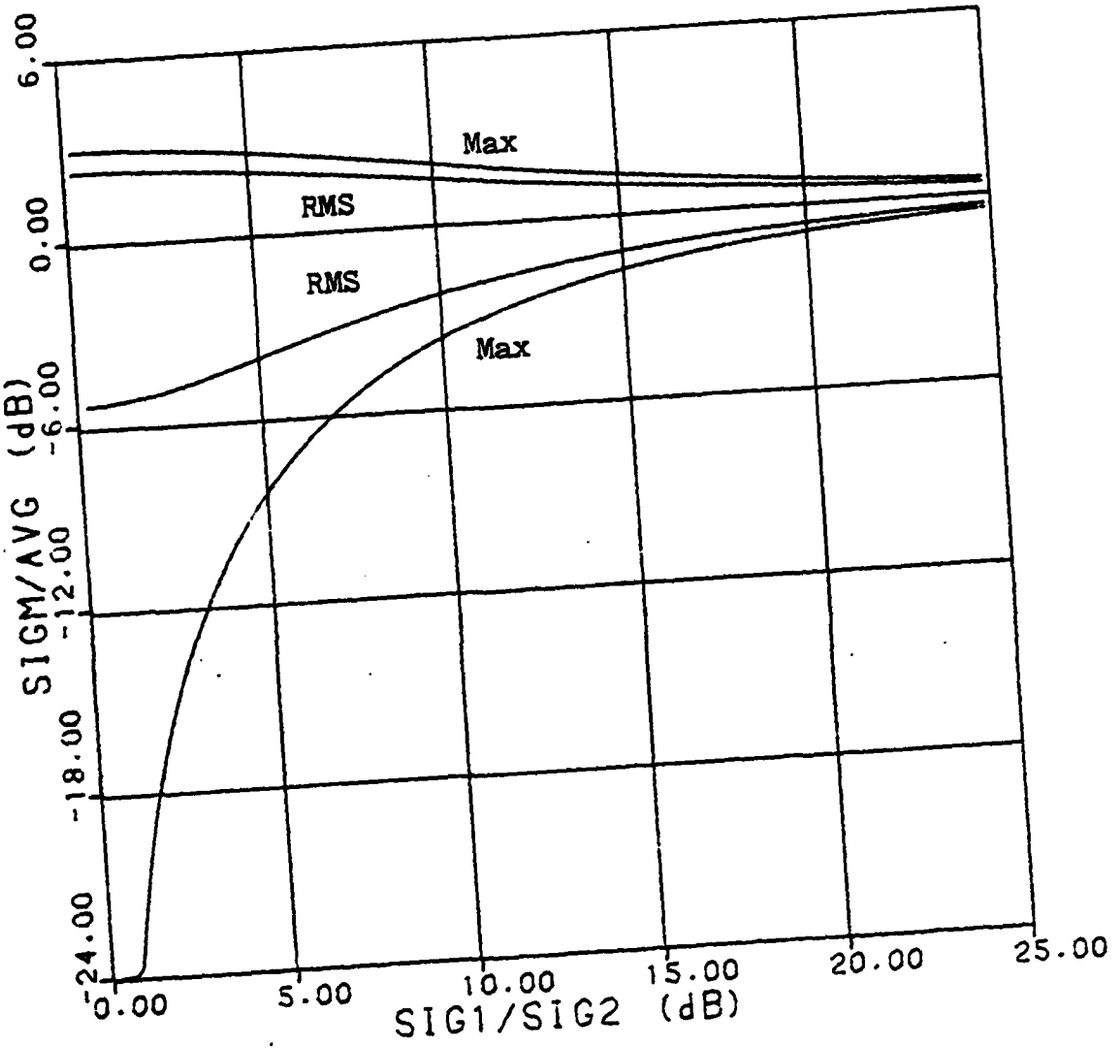

Figure III-1 Traditional Error (Maximum and RMS) Bounds

Comparison with Computer Generated Data

The results from assuming two determinsic sources will be compared to the results from the computer generated data in this section. As mentioned in Chapter II the computer data was obtained by using the RCSBSC program on a flat plate target rotated above a flat plate target support. The data was taken every tenth of a degree between 15 and 95 degrees aspect angle. This region represents the area where diffracting scatterers dominate.

The data used in this section was obtained by taking the amplitudes of the measured cross sections of the target with support from all four of the test clutter levels at each increment of aspect angle and normalizing it to the sum of the corresponding target amplitude cross section and the target support amplitude cross section. This sum, of course, is the point to point mean of the measured cross section. The processed data was plotted versus signal to clutter ratio, which is the ratio of the target cross section to the target support, or clutter cross section. This data is shown in Figure III-2

The maximum bounds of this graph lie exactly on the curves predicated by the theortical derivation. This same data was run through a program to plot the standard deviation above and below the normalized mean. This graph is shown on Figure III-3. This graph also lies exactly on the rms bounds predicated theortically.

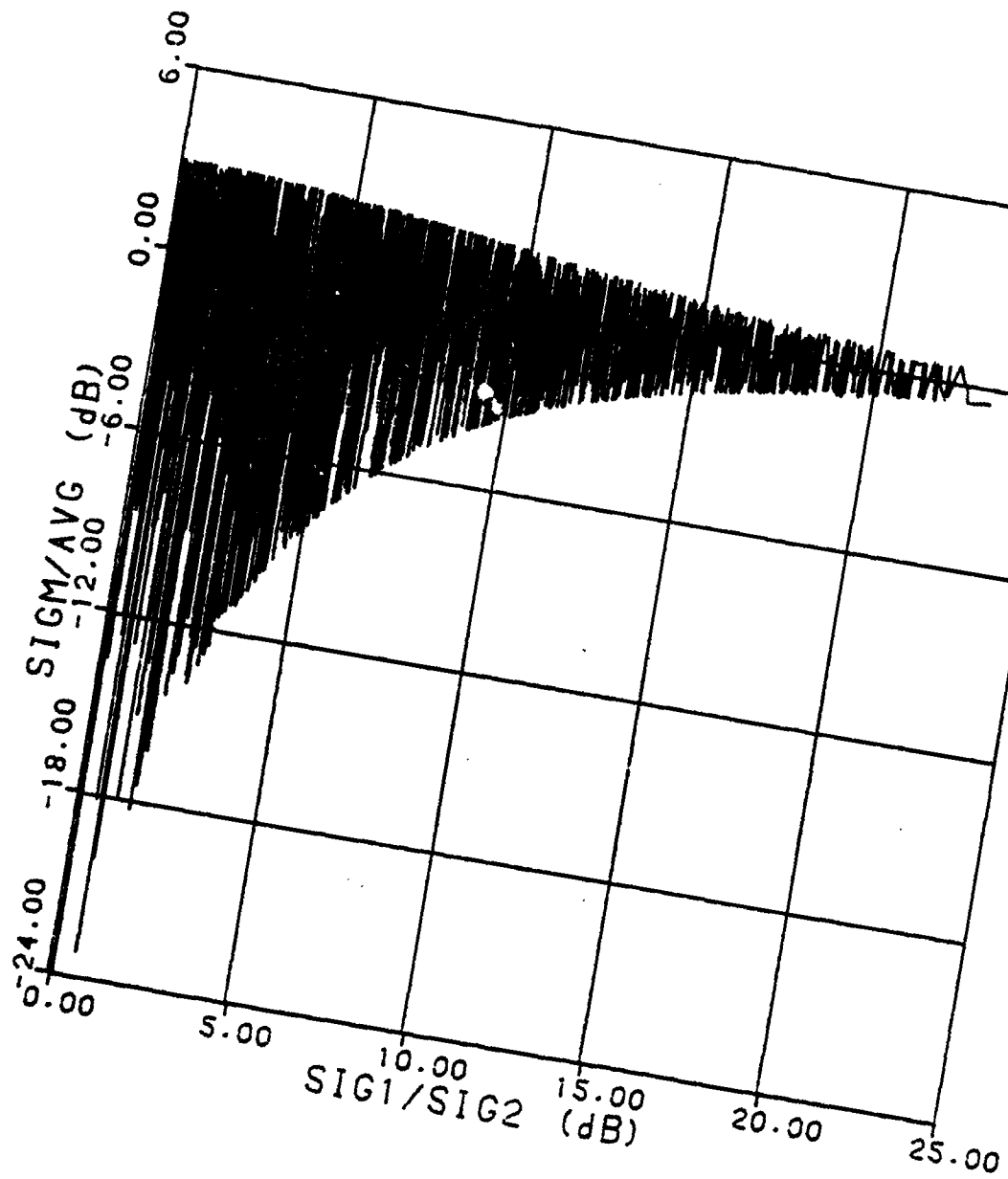

Figure III-2 Error Estimate (from Computer Generated Data)
Under Traditional Approach Assumptions

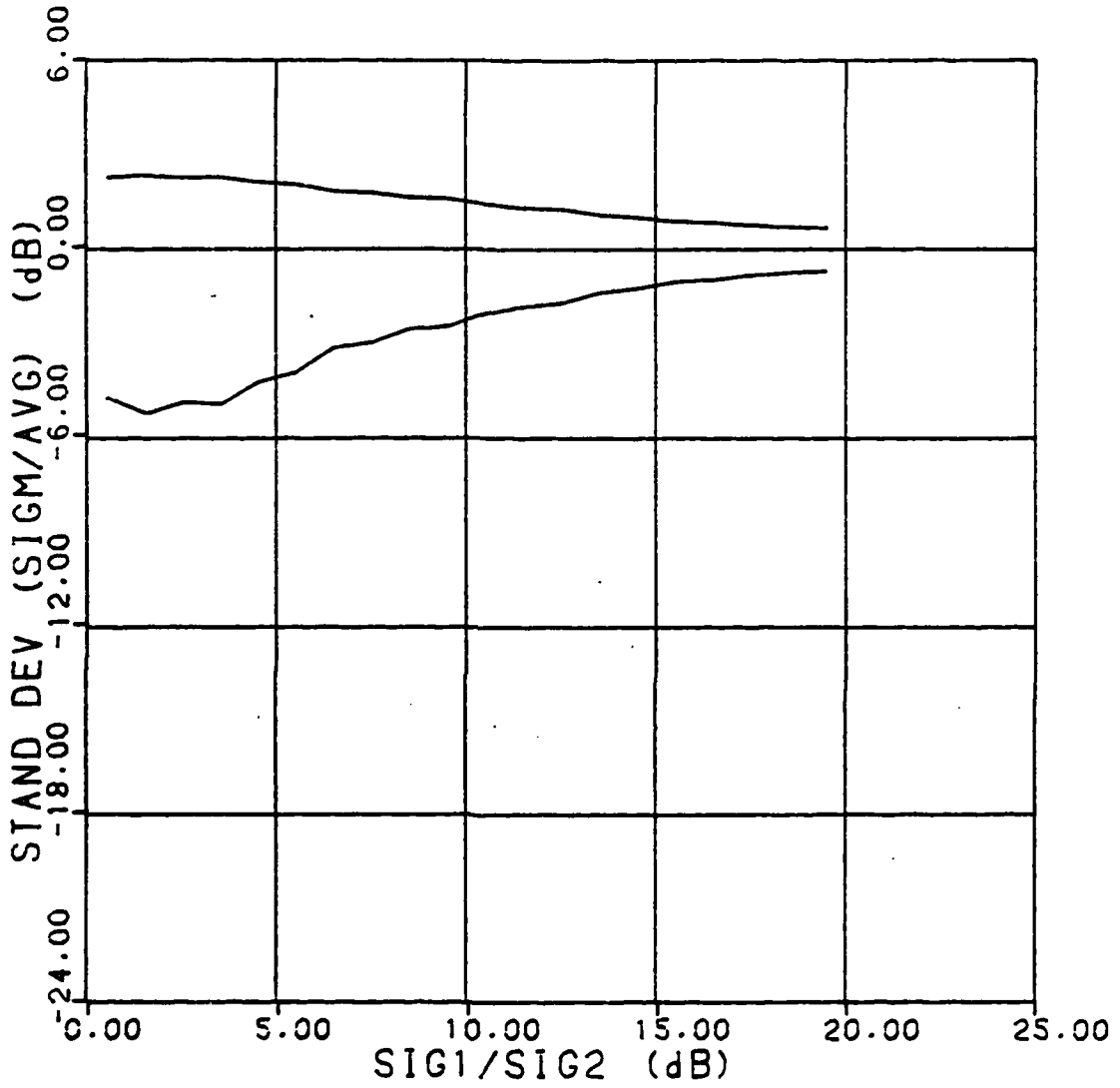

Figure III-3 RMS Curves (from Computer Generated Data) Under Traditional Approach Assumptions

It has been shown in the previous section that N similar and deterministic scatterers have the same distribution as a single source with Rayleigh amplitude distribution. A graph of this simulated pdf is shown in Figure III-9. Because this is a graph of the pdf of the signal amplitude of the cross section it should be Rayleigh distributed. It has been mentioned that the cross section data after being run through a running average processor could be of interest. The next set of graphs show the simulated pdf's of the signal amplitude of the cross sections after the cross sections have been processed by the running average program. Figure III-10 represents the pdf after the cross section data has been averaged over an 11 point window (just larger than a degree). Figures III-11 and III-12 represent the pdf's after averaging over a 25 point (2.5 degrees) and a 51 point (just larger than 5 degrees) window. Before averaging, the pdf has a definite Rayleigh shape, just as predicted theortically. After averaging, the pdf begins to center around the mean and take on a Gaussian shape, which is also predicted through the application of the Central Limit Theorem. Finally, after more averaging, the pdf of the amplitude of the cross section has a rough Gaussian shape.

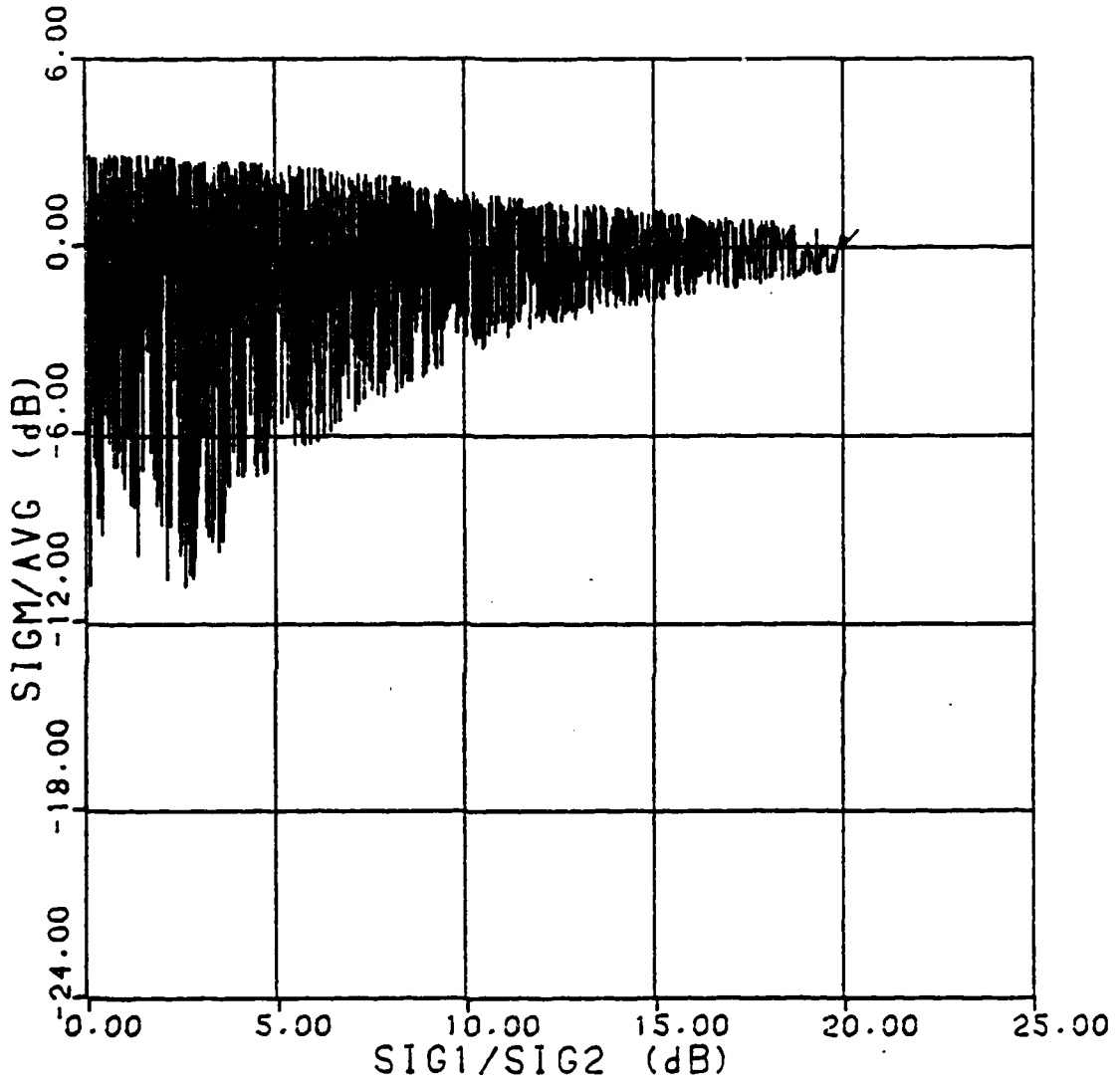

Figure III-4 Error Estimate (from Computer Generated Data) After Processing With an Averaging Window 11 Points (1.10 degrees) Wide Under Traditional Approach Assumptions

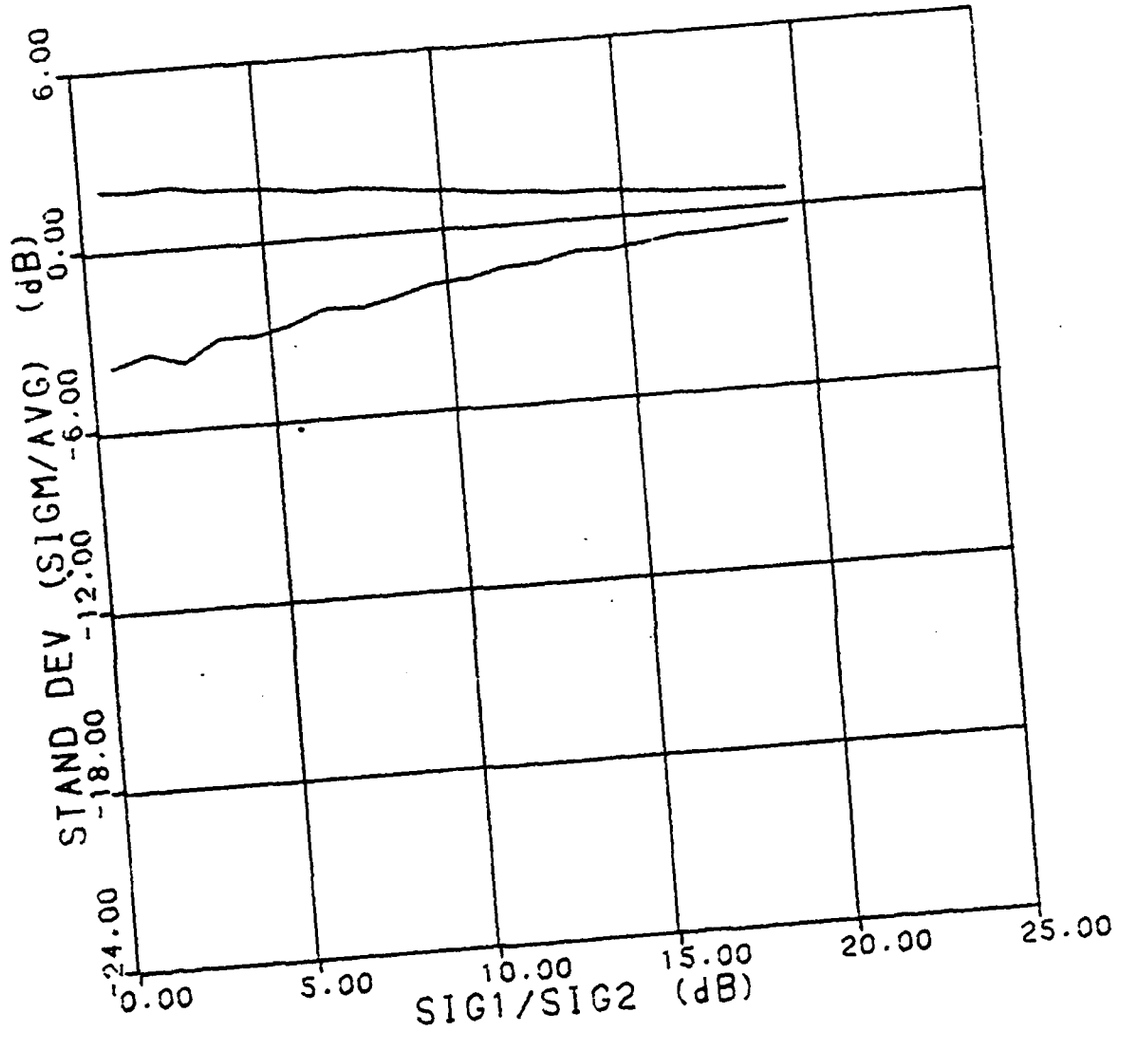

Figure III-5 RMS Curves (from Computer Generated Data) After Processing With an Averaging Window 11 Points (1.10 degrees) Wide Under Traditional Approach Assumptions

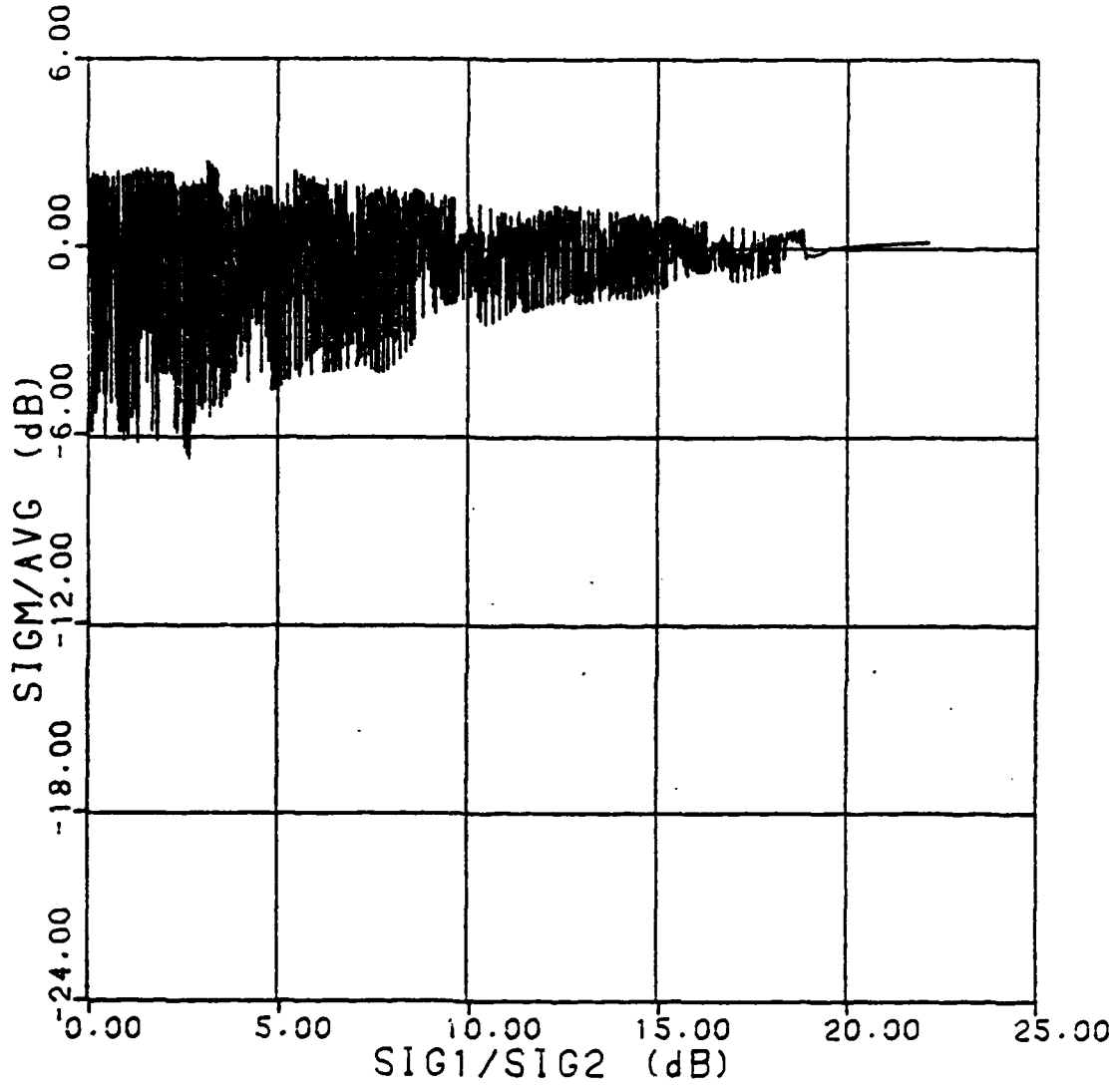

Figure III-6 Error Estimate (from Computer Generated Data) After Processing With an Averaging Window 21 Points (2.10 degrees) Wide Under Traditional Approach Assumptions

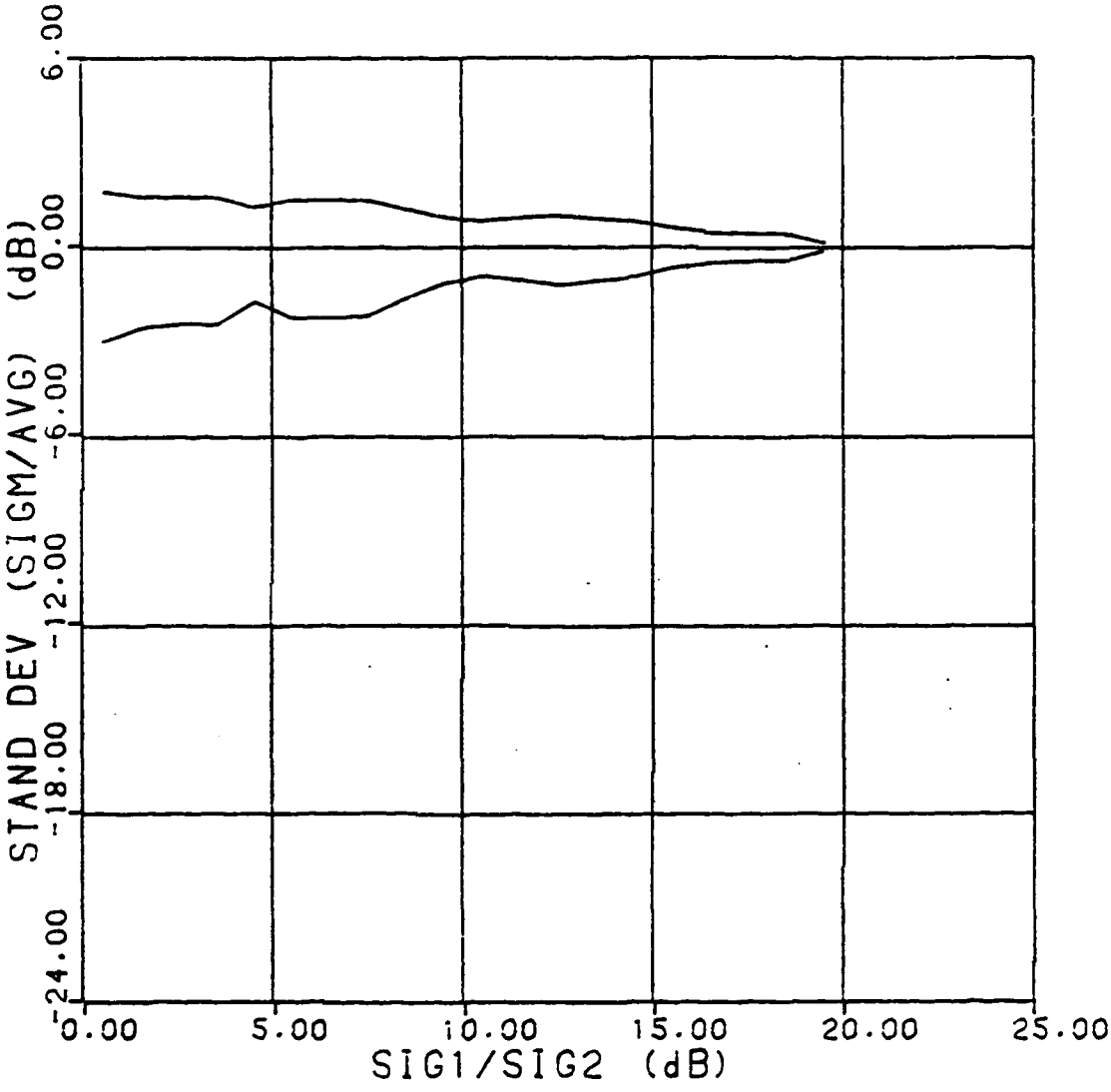

Figure III-7 RMS Curves (from Computer Generated Data) After Processing With an Averaging Window 21 Points (2.10 degrees) Wide Under Traditional Approach Assumptions

N Sources (Deterministic)

An extension on the two source model is to assume N sources. This model represents a target that is made up of many individual scattering sources. Again, each of the sources will have a deterministic amplitude,and each will have a random phase, uniformly distributed between 0 and 2π.

The measured cross section is given by: [Ref 3:974]

$$\sigma_m = \left| \sum_{i=1}^{N} \sqrt{\sigma_i}\ e^{j(\phi_i)} \right|^2 \qquad \text{(III-18)}$$

The measured cross section can also be written as:

$$\sigma_m = \left(\sum_{i=1}^{N} \sqrt{\sigma_i}\ e^{j(\phi_i)} \right) \left(\sum_{k=1}^{N} \sqrt{\sigma_k}\ e^{-j(\phi_i)} \right) \qquad \text{(III-19)}$$

$$\sigma_m = \sum_{i=1}^{N} \sum_{k=1}^{N} \sqrt{\sigma_i \sigma_k}\ e^{j(\phi_i - \phi_k)} \qquad \text{(III-20)}$$

Here, the terms where i=j can be separated from the cross terms where $i \neq j$.

$$\sigma_m = \sum_{i=1}^{N} \sigma_i + \sum_{\substack{i=1 \\ (i=k)}}^{N} \sum_{k=1}^{N} \sqrt{\sigma_i \sigma_k}\, e^{j(\phi_i - \phi_k)} \qquad \text{(III-21)}$$

$$\sigma_m = \sum_{i=1}^{N} \sigma_i + 2 \sum_{i=1}^{N-1} \sum_{k=i+1}^{N} \sqrt{\sigma_i \sigma_k}\, \cos(\phi_i - \phi_k) \qquad \text{(III-22)}$$

Now, the mean of the measured cross section is taken to be the expected value of the measured cross section. The expected value of the deterministic terms is simply their value.

$$\bar{\sigma}_m = \sum_{i=1}^{N} \sigma_i + 2 \sum_{i=1}^{N-1} \sum_{k=i+1}^{N} \sqrt{\sigma_i \sigma_k}\, E[\cos(\phi_i - \phi_k)] \qquad \text{(III-23)}$$

As a consequence of assuming a uniform distribution for the relative phase between the two components, the mean of the measured cross section is simply the sum of the individual cross sections.

$$\bar{\sigma}_m = \sum_{i=1}^{N} \sigma_i \qquad \text{(III-24)}$$

Next, the standard deviation of the measured cross section is found. The variance is taken to be the expected value of the square of the difference between the measured cross section and its mean.

$$s_m^2 = E[|\sigma_m - \bar{\sigma}_m|^2] \qquad \text{(III-25)}$$

Into this Equation substitute the expression for the measured cross section, Equation (III-22), and the mean of the measured cross section, Equation (III-24), to obtain:

$$s_m^2 = E[|\sum_{i=1}^{N}\sigma_i + 2\sum_{i=1}^{N-1}\sum_{k=i+1}^{N}\sqrt{\sigma_i\sigma_k}\cos(\phi_i-\phi_k) - \sum_{i=1}^{N}\sigma_i|^2] \qquad \text{(III-26)}$$

Cancelling the like terms and expanding the squared summation terms the variance becomes:

$$s_m^2 = 4E[\sum_{i=1}^{N-1}\sum_{k=i+1}^{N}\sum_{m=1}^{N-1}\sum_{n=m+1}^{N}\sqrt{\sigma_i\sigma_k\sigma_m\sigma_n}\cos(\phi_i - \phi_k)*\cos(\phi_m - \phi_n)] \qquad \text{(III-27)}$$

To simplify this expression, first examine those terms for $i=m$ and $k\neq n$. The square roots of the cross sections can be taken out of the expected value because they are

deterministic.

$$s_m^2 = 4 \sum_{i=1}^{N-1} \sum_{k=i+1}^{N} \sum_{m=1}^{N-1} \sum_{n=m+1}^{N} \sqrt{\sigma_i \sigma_k \sigma_m \sigma_n}\, E[\cos(\phi_{ik})\cos(\phi_{mn})] \quad \text{(III-28)}$$

where

$$\phi_{ik} = \phi_i - \phi_k \quad \text{(relative phase)}$$
$$\phi_{mn} = \phi_m - \phi_n \quad \text{(relative phase)}$$

Because the two cosine terms are independent of each other when $k \neq n$ the expected value of each one can be taken separately. Also, as a consequence of assuming a uniform random distribution for the relative phase, each of these cosine terms is equal to zero and the contribution to the variance from the terms of $i=m$ and $k \neq n$ is equal to zero.

$$s_m^2 = 4 \sum_{i=1}^{N-1} \sum_{\substack{k=i+1 \\ (i=m,k=n)}}^{N} \sum_{m=1}^{N-1} \sum_{n=m+1}^{N} \sqrt{\sigma_i \sigma_k \sigma_m \sigma_n}\, E[\cos(\phi_{ik})\cos(\phi_{mn})] = 0 \quad \text{(III-29)}$$

Similarly those terms for which $k=n$ and $i \neq m$ and the terms for which $k \neq n$ and $i \neq m$, the variance becomes zero. Also, as a consequence of assuming a uniform random phase distribution the expected value of the cosine terms becomes 1/2. All of this greatly simplifies the expression for the variance, leaving only the terms of $i=m$ and $k=n$.

$$s_m^2 = 2 \sum_{i=1}^{N-1} \sum_{\substack{k=i+1 \\ (i=m,\ k=n)}}^{N} \sum_{m=1}^{N-1} \sum_{n=m+1}^{N} \sqrt{\sigma_i \sigma_k \sigma_m \sigma_n} \qquad \text{(III-30)}$$

Also, since the variance only has a value for i=m and k=n, the sumations over m and n are redundant.

$$s_m^2 = 2 \sum_{i=1}^{N-1} \sum_{k=i+1}^{N} \sqrt{\sigma_i \sigma_k} \qquad \text{(III-31)}$$

As a result, the standard deviation of the measured cross section is simply the square root of the sum of twice the product of the cross terms of the components.

$$s_m = \sqrt{2 \sum_{i=1}^{N-1} \sum_{k=i+1}^{N} \sqrt{\sigma_i \sigma_k}} \qquad \text{(III-32)}$$

One Source (Rayleigh)

The next extension is to again assume that there are N individual scatterers, with each scatterer having deterministic amplitude and uniform distributed phase. These N scatterers will be the individual components that add up to form the model of target in free space. With many

deterministic scatterers it will turn out that the N scatterers appear to be one source which has a Rayleigh distribution on the amplitude. This assumption turns out to be a very good one if none of the individual scatterers are much larger than the rest. Again, the measured cross section is first used to find the statistics:

$$\sigma_m = \left| \sum_{i=1}^{N} \sqrt{\sigma_i}\, e^{j(\phi_i)} \right|^2 \qquad \text{(III-33)}$$

Rewritting the measured cross section as the sum of two squared terms:

$$\sigma_m = u_2 + v_2 \qquad \text{(III-34)}$$

Where u and v are simply the quadrature components of the measured cross section.

$$u = \sum_{i=1}^{N} \sqrt{\sigma_i}\, \cos(\phi_i) \qquad \text{(III-35)}$$

$$v = \sum_{k=1}^{N} \sqrt{\sigma_k}\, \sin(\phi_i) \qquad \text{(III-36)}$$

Since the distributions of the individual phases are the same, the Central Limit Theorem can be used to assume that both u and v are asymptotically normal. The square root of the sum of two normally distributed, zero mean, and independent random variables is Rayleigh distributed [Ref 10:195].

At this point a new term which is the square root of the measured cross section will be defined. This term, x, will represent the amplitude of the signal from the measured cross section. It is this signal amplitude which is Rayleigh distributed, or rather "asymptotically" Rayleigh distributed.

Now, the statistics on $|x|^2$ will be calculated. The probability density function, pdf, of x, which is Rayleigh distributed is given by [Ref 10:148]:

$$f_x(x) = 2x/\bar{\sigma}_m \exp(-x^2/\bar{\sigma}_m), \qquad x>0 \qquad \text{(III-37)}$$

Not only is this amplitude pdf needed, the pdf of the amplitude squared, or rather the cross section is needed. To do this the simple transformation below is used.

$$v = u^2 \qquad \text{(III-38)}$$

where

u = original random variable
v = new, transformed random variable

The distribution of v is given by [Ref 10:129]:

$$f_v(v) = 1/(2\sqrt{v})\ [f_u(\sqrt{v}) + f_u(-\sqrt{v})], \quad v>0 \qquad \text{(III-39)}$$

But in this case the original random variable is defined for positive values, leaving just the first term in the above expression:

$$f_v(v) = 1/(2\sqrt{v})\ f_u(\sqrt{v}), \qquad v>0 \qquad \text{(III-40)}$$

and making the following substitutions:

$v = \sigma_m$
$u = x^m$

The pdf of the Rayleigh amplitude distributed cross section is obtained. This pdf turns out to be a simple exponential distribution.

$$f_m(\sigma_m) = 1/\bar{\sigma}_m \exp(-\sigma_m/\bar{\sigma}_m). \qquad \sigma_m>0 \qquad \text{(III-41)}$$

The mean of the measured cross section for N individual scatterers is given by the sum of the individual cross sections, Equation (III-24).

Next, the variance of the measured cross section is found. Again, the variance is taken to be the expected value of the of the square difference between the measured cross section and its mean. But recall that the measured cross section is also x squared.

$$s_m = E[|x^2 - \bar{\sigma}_m|^2] \tag{III-42}$$

Expanding this and separating terms the variance becomes:

$$s_m^2 = E[x^4] - 2\sigma_m E[x^2] + \bar{\sigma}_m^2 \tag{III-43}$$

At this point the second and fourth moments of x are needed. The general expresion for the moments of a Rayleigh distributed random variable are given by [Ref 10:148]:

$$E[x^n] = \begin{cases} \sqrt{\pi}/2 \ (1\ 3\ 5\ \ldots\ n a^n), & n \text{ odd} \\ 2^{n/2}\ (n/2)!\ a^n, & n \text{ even} \end{cases} \tag{III-44}$$

Therefore, the second and fourth moments of x, or rather, the mean and second moments of the measured cross section are given by:

$$E[x^2] = E[\sigma_m] = \bar{\sigma}_m \qquad \text{(III-45)}$$

$$E[x^4] = E[\sigma_m^2] = 2\bar{\sigma}_m^2 \qquad \text{(III-46)}$$

Substituting Equations (III-45) and (III-46) into Equation (III-43) the variance, in its simplest form is obtained.

$$s_m^2 = \bar{\sigma}_m^2 \qquad \text{(III-47)}$$

The above Rayleigh approximation is good only for many scatterers. If any one of the individual scatterers is much larger than the rest, the assumptions that were used will no longer be valid and the Rayleigh approximation will be a poor one. This is discussed further in Chapter IV.

In actual practice, the Rayleigh approximation is reasonably good for as few as two or three scatterers [Ref 9:1355]. Even with this few of scatterers, 55 to 60 percent of the cross section values are contained within one standard deviation of the mean [Ref 3:980]. Of course, if the received signal were exactly Rayleigh distributed, 86.5 percent would be within one standard deviation of the mean.

There is some confusion in the terminology in the literature on RCS statistics. The chi-sqared distribution with two degrees freedom is called Rayleigh, which is the

distribution of x. The probability distribution of the square of such a variable, the measured cross section, would be chi-squared with four degrees of freedom, also called exponential. Many have chosen to call this "Rayleigh Power Distribution," then stating that the RCS under certain assumptions has a Rayleigh power distribution, and later casually dropping the word "Power" and misapplying the Rayleigh distribution to the RCS values [Ref 14:50].

Comparison with Computer Generated Data

In this section graphs that represent the probability density functions of the relative phase and the amplitude of the cross section of the target in free space are introduced. The data for these graphs was produced by obtaining the relative phase and cross section for every hundreth of a degree (between 15 and 95 degrees aspect angle) using the RCSBSC program on the triangular flat plate target model. The number of occurances of a particular range of phases or cross sections was plotted versus the range of the phase or the amplitude of the cross section values.

The relative phase is obtained by comparing the data from the measured cross section to the free space target cross section at each data point (see Equation III-4). Because of the limitations of the inverse cosine function on the computer, these relative phase values are plotted for 0 to π. As can be seen by Figure III-8 the phase appears to

have a uniform phase distribution. Recall that this uniform phase distribution assumption is essential in the development of the probablistic models of this paper. Figure III-8 only shows the relative phase for a particular level of signal to clutter ratio. This graph, however, is typical of any tilt angle or any signal to clutter ratio. If the phase were obtained from averaged data, however, one would find that the relative phase no longer is uniform. Instead, the phase will take on a Gaussian distribution centered around its most likely value, or mean, of $\pi/2$. The change from uniform to Gaussian distribution does not affect the assumptions made earlier in this chapter. These uniform phase distribution assumptions were made only on the data before averaging.

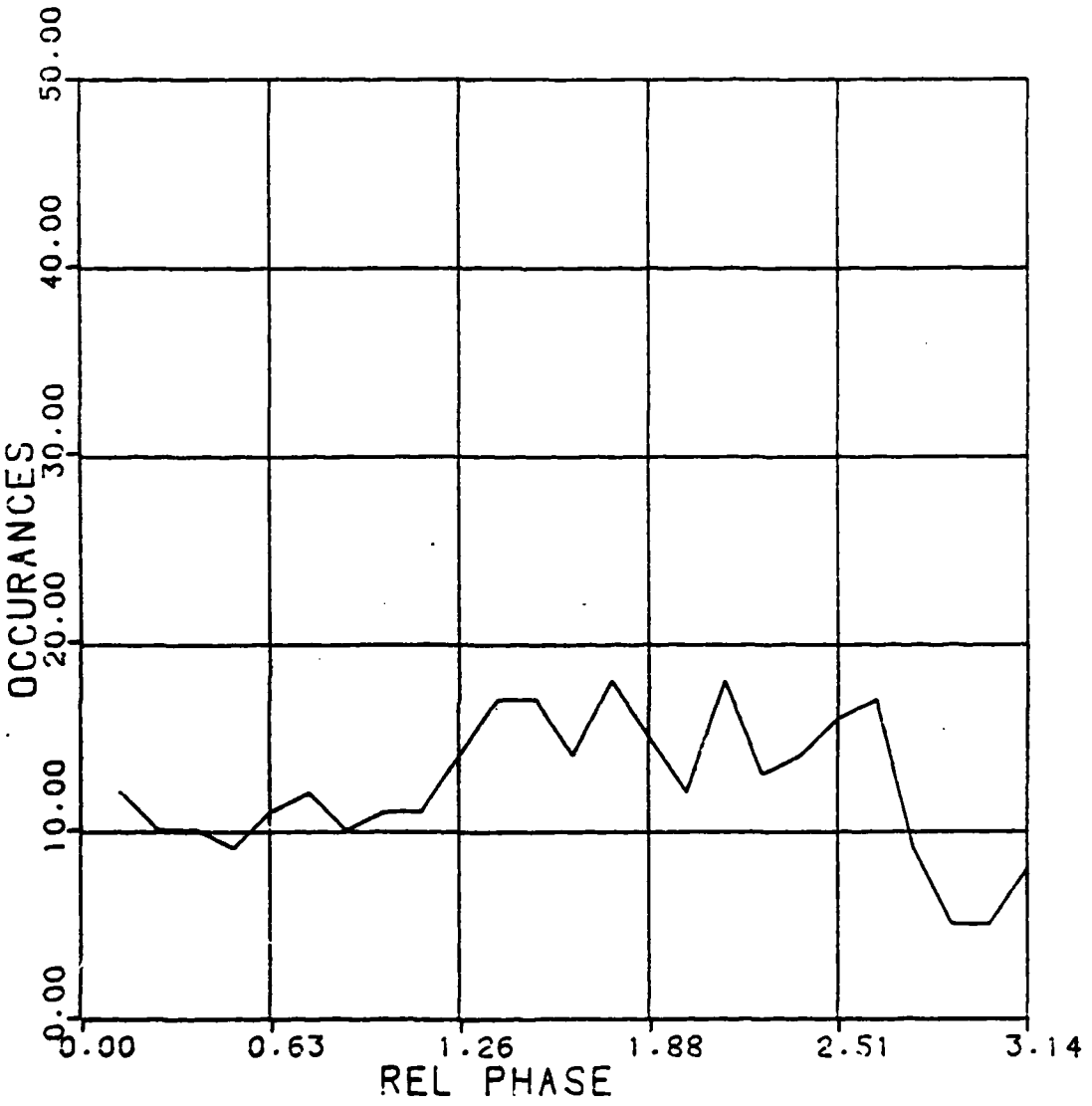

Figure III-8 Probability Density Function (from Computer Generated Data) of the Relative Phase Between the Measured Cross Section and the Free Space Target Cross Section (for S/C=1 dB)

It has also been mentioned that the traditional approach requires accuracy at every point. If this hard requirement were relaxed, the data from a running average processor could be analyzed. The raw data, taken every tenth of a degree, from all four test clutter levels was run through such a running average processor. This averaged data was also run through the standard deviation program to find the rms spread. Figure III-4 shows the data from the running average processor for an averaging window of 11 points, or a window just larger than a degree. Figure III-5 shows the rms curves from this averaged data. Figures III-6 and III-7 show similar results from processing the data with a 21 point, two degree, window.

Note that the more points the data is averaged over, the smaller the maximum swings on the data. Also, for more averaging, the rms curves approach the normalized mean. Essentially this means that even assuming the traditional approache's deterministic sources, the accuracy estimate on the maximum bounds and the rms bounds can be improved by processing the data through a running average program. Furthermore, the wider the averaging window, the better the accuracy estimate becomes.

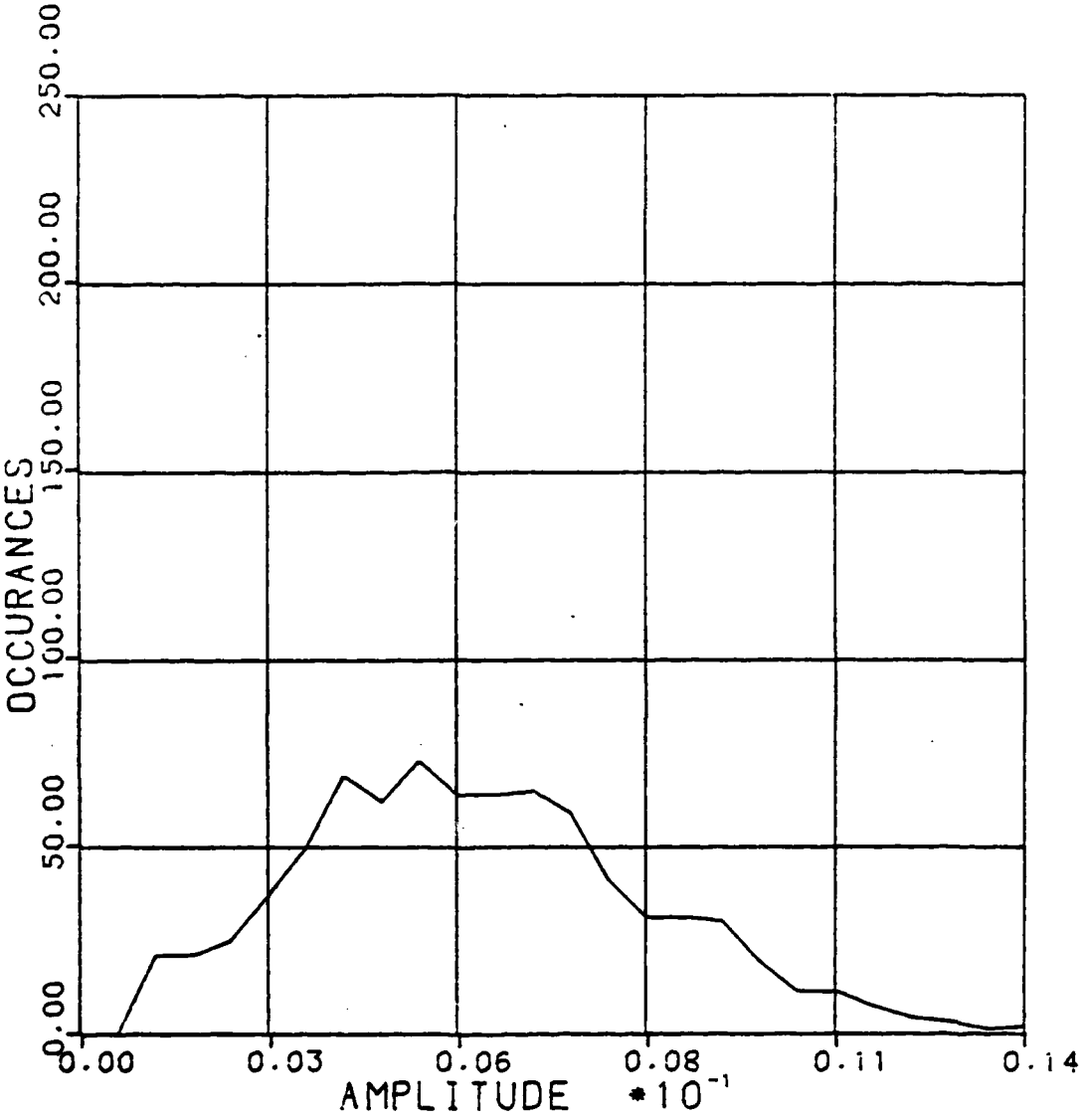

Figure III-9 Probability Density Function (from Computer Generated Data) of the Target's Free Space Cross Section Amplitude

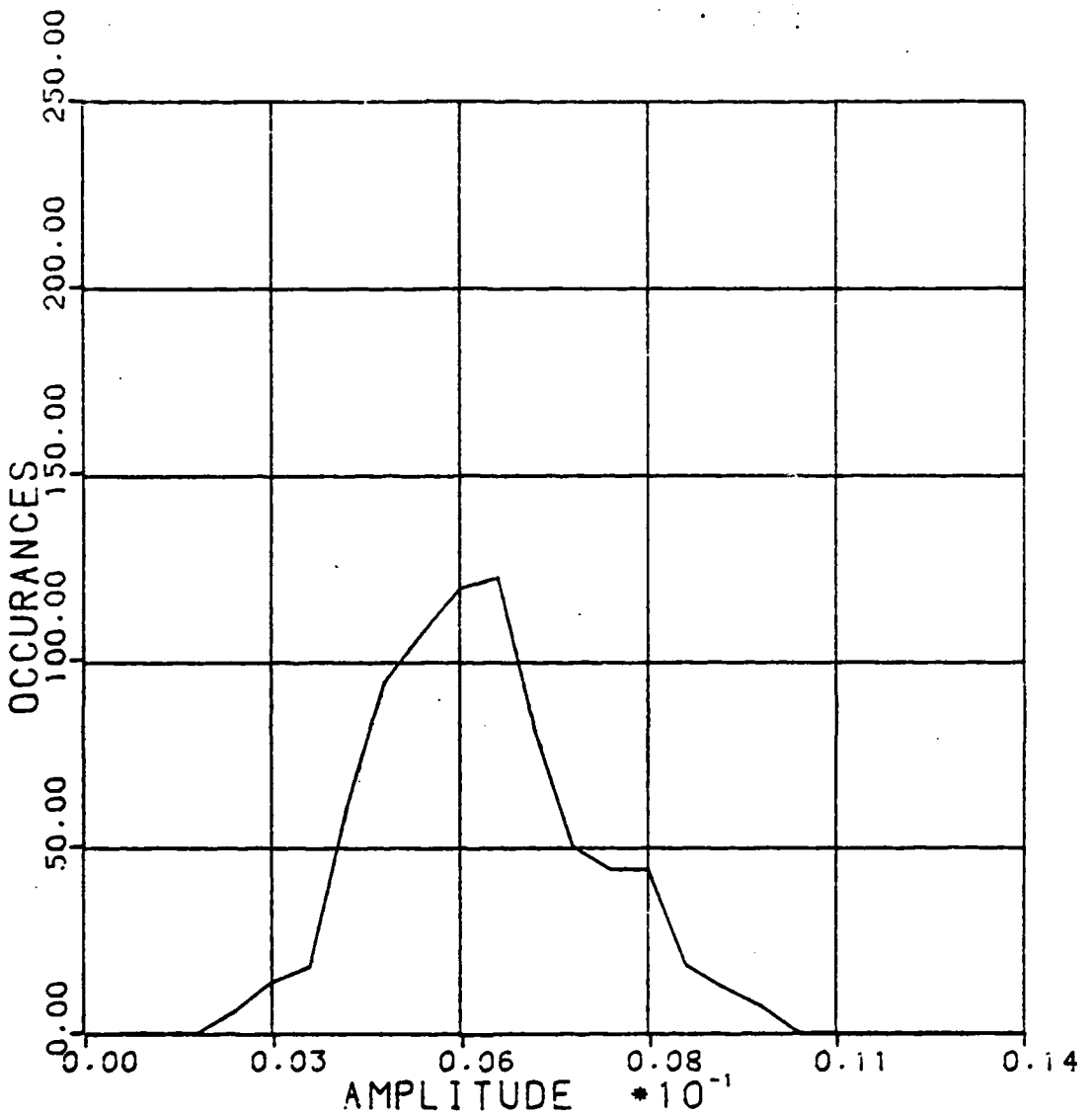

Figure III-10 Probability Density Function (from Computer Generated Data) of the Target's Free Space Cross Section Amplitude After Averaging Over an 11 Point (1.1 degree) Window

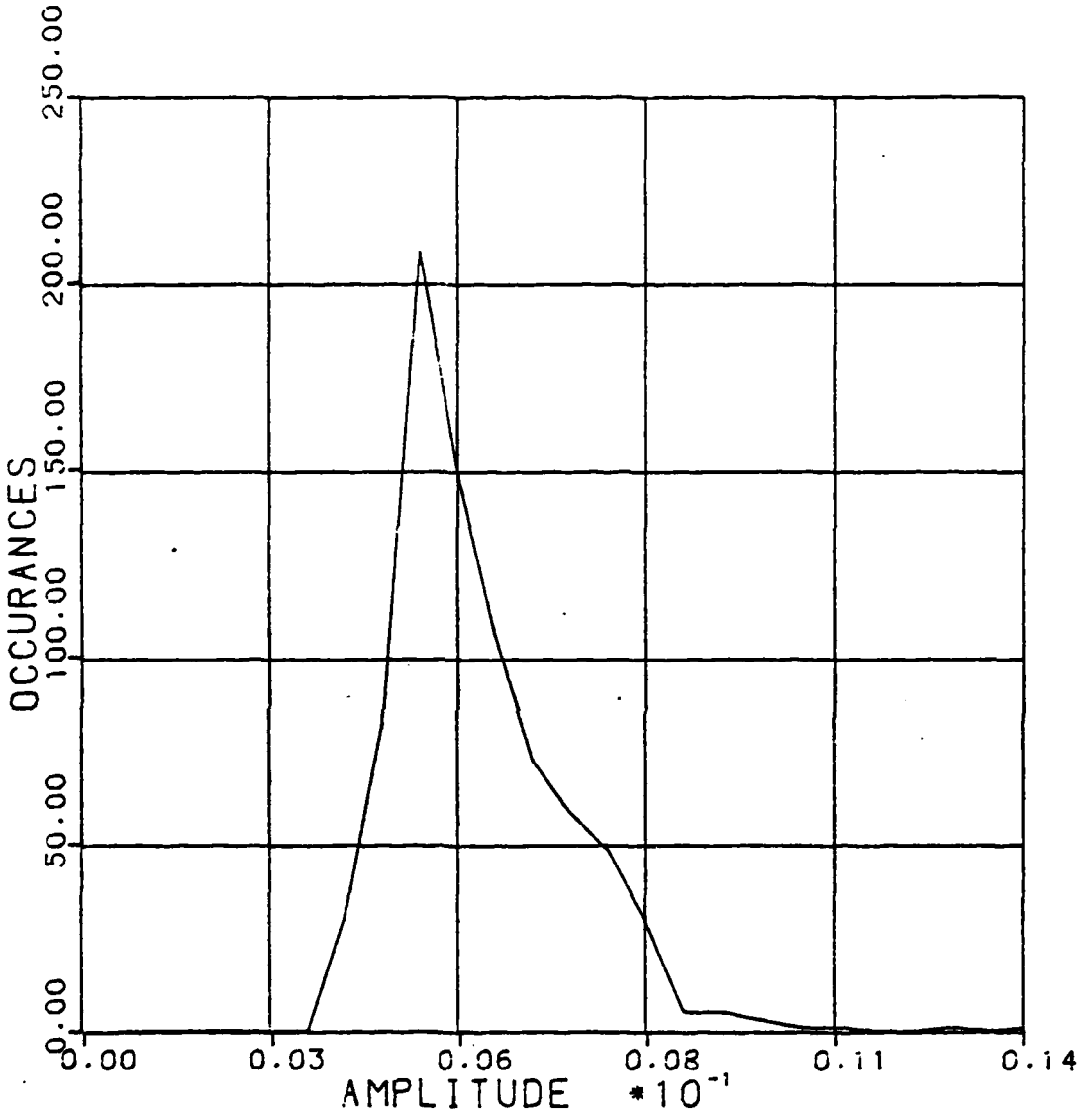

Figure III-11 Probability Density Function (from Computer Generated Data) of the Target's Free Space Cross Section Amplitude After Averaging Over a 25 Point (25 degree) Window

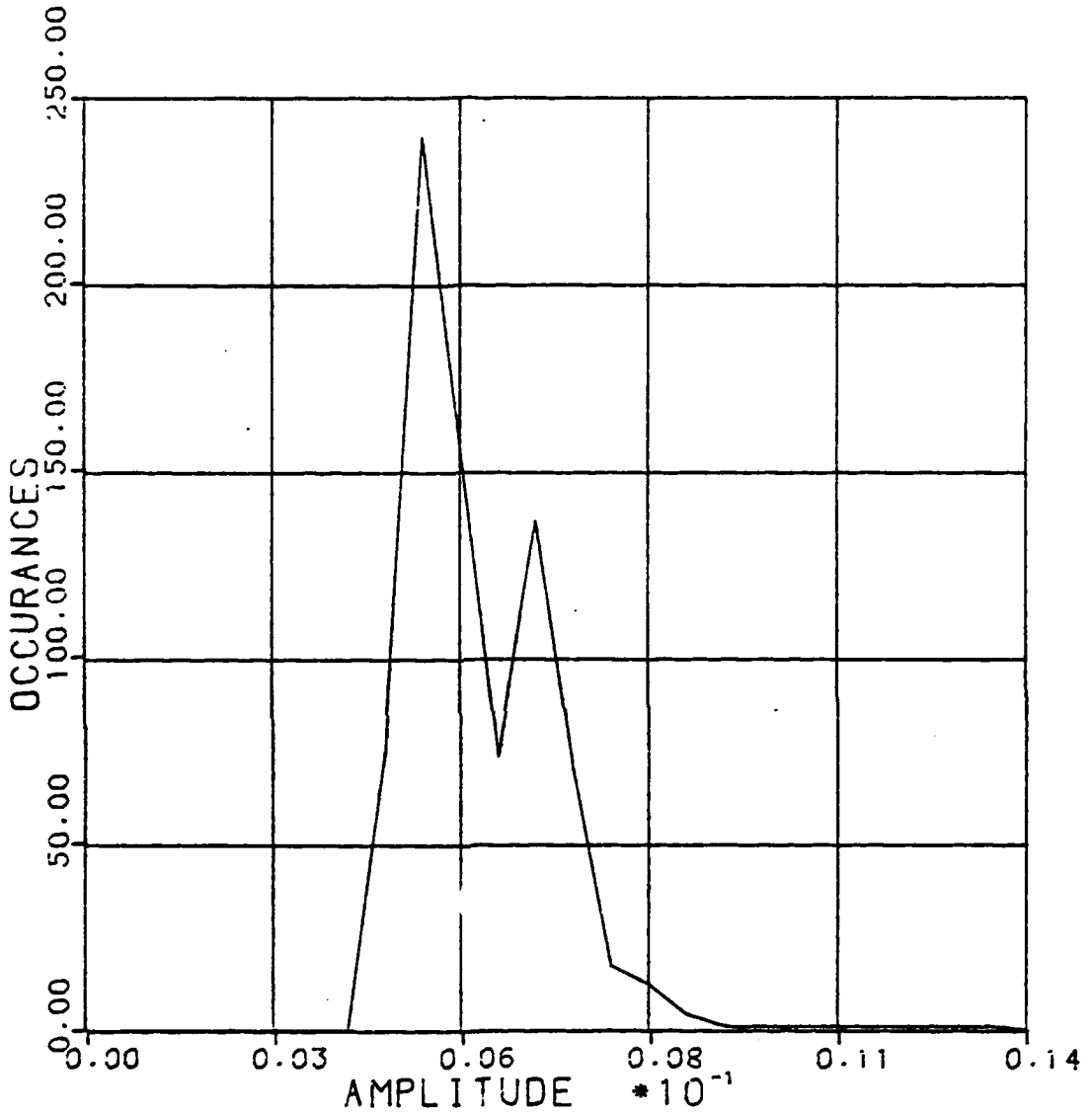

Figure III-12 Probability Density Function (from Computer Generated Data) of the Target's Free Space Cross Section Amplitude After Averaging over a 51 Point (5.1 degree) Window

IV. Analysis of the Probability Distributions of a Rayleigh Target in Constant Clutter

In Chapter III the traditional approach was summarized. There are several important assumptions to this approach. First, the traditional approach assumes deterministic amplitudes. In actual practice this can be an overly restrictive assumption. Most present targets can be modelled by multiple independent scatterers. The total return from these scatterers is far from deterministic at angles not close to the areas of "specular diffraction." The amplitudes of these sources can vary rapidly for small changes of aspect angle (see the cross section patterns in Figures II-2, II-3, II-5, and II-6). The RCS return is therefore best described probabilisticly. In Chapter III the derivation in assuming N sources was outlined. It was shown that these N sources, when taken as a whole, can be modelled as a single Rayleigh amplitude distributed source.

In this chapter a new model will be derived. This model will be based on a target and a target support. The target will be a Rayleigh amplitude distributed source and the target support, or clutter, will be a constant deterministic source. This is a new target with clutter model. Many other

target with clutter models have been suggested such as Swerling Cases III and IV (Chi-Squared distribution with four degrees of freedom) [Ref 15] and Log-Normal distribution [Ref 7]. But all of these previous target with clutter models assume the need to model the clutter probabilisticly. Also, some of the models are not justified by mathematical derivation, but rather from how closely they follow measured data. As a result, a new model is justified.

Two Sources (Rayleigh and Deterministic)

As explained previously the next extension is to assume that there are two sources of cross section, one with a Rayleigh distribution on the signal amplitude, and the other with a deterministic amplitude. Each source also has a random phase, uniformly distributed from 0 to 2π radians. This extension models the case that is of most interest. The random source represents the target, and the deterministic source represents the background clutter, or target support, which is assumed to be constant. Since both sources have a random phase, the phases of both sources can be combined into one random phase and can be attached to the deterministic source. The received signal, which is the square root of the measured cross section, can be represented simply as the sum of the two source signals.

$$x = y_t + y_c e^{j\phi} \qquad \text{(IV-1)}$$

where

ϕ = relative phase between sources
y_t = amplitude of the randomly distributed target
y_c = amplitude of the deterministic clutter

Each signal has a power, or rather a cross section, associated with it:

where

y_t has power σ_t
y_c has power σ_c

The measured cross section is, of course, given by:

$$\sigma_m = |x|^2 \qquad \text{(IV-2)}$$

Substituting Equation (IV-1) into Equation (IV-2) and simplifing the expression for the measured cross section:

$$\sigma_m = (y_t + y_c e^{j\phi})(y_t + y_c e^{-j\phi}) \qquad \text{(IV-3)}$$

$$\sigma_m = y_t^2 + y_c^2 + 2y_t y_c \cos\phi \qquad \text{(IV-4)}$$

To find the mean of the measured cross section the expected value of the above expression is taken. To find the expected value of the second term, the basic definition of

expected value for two independent variables is used.

$$E[ab] = \int_a \int_b u\ v\ f_a(u)\ f_b(v)\ du\ dv \qquad \text{(IV-5)}$$

where

$f_a(u)$ = probability distribution of the first variable
$f_b(v)$ = probability distribution of the second variable

Into Equation (IV-5) the above expressions are substituted. The limits of integration are the same as the limits on the variables. Where the cross section amplitude, x, is defined for all non-negative values and the random phase is defined from 0 to 2π radians.

$$E[y_t \cos\phi] = \int_0^{\infty} \int_0^{2\pi} (y_t \cos\phi) \left[\frac{2y_t}{\sigma_m} \exp(-y_t^2/\sigma_m)\right] \left(\frac{1}{2\pi}\right) d\phi\ dy \qquad \text{(IV-6)}$$

This integral, of course, is equal to zero because a cosine term is being integrated over one period.

The expected value of the first term of Equation (IV-4) has already been found. This is simply the second moment of a Rayleigh distributed variable, Equation (III-45), and is equal to the power, or cross section, of the variable. Therefore, the mean, simplifies to:

$$\bar{\sigma}_m = \bar{\sigma}_t + y_c^2 \qquad \text{(IV-7)}$$

$$\bar{\sigma}_m = \bar{\sigma}_t + \sigma_c \qquad \text{(IV-8)}$$

Next, the standard deviation and the variance of the measured cross section are found. The variance is the expected value of the square of the difference between the measured cross section and its mean.

$$s_m^2 = E[|\sigma_m - \bar{\sigma}_m|^2] \qquad \text{(IV-9)}$$

Into this equation the expression for the measured cross section, Equation (IV-4), and the expression for the mean, Equation (IV-8) are substituted.

$$s_m = E[|\sigma_t + \sigma_c + 2y_t y_c \cos\phi - (\bar{\sigma}_t + \sigma_c)|^2] \qquad \text{(IV-10)}$$

Cancelling like terms, squaring, and expanding the variance simplifies to:

$$s_m^2 = E[\sigma_t + \sigma_c - 2\sigma_t\sigma_c + 4\sigma_t\sigma_c\cos^2\phi + 4(\sigma_t - \bar{\sigma}_t)y_t y_c\cos\phi] \qquad \text{(IV-11)}$$

Because of the independence of the variables and because the phase is uniformly distributed, the last term is zero. Also, because the second moment of a Rayleigh amplitude distributed cross section, Equation (III-46), is known and the expected value of cosine squared of a uniform distributed variable is 1/2, the variance can be further simplified.

$$s_m^2 = \bar{\sigma}_t^2 + 2\bar{\sigma}_t\sigma_c \qquad \text{(IV-12)}$$

The standard deviation is given by:

$$s_m = \sqrt{\bar{\sigma}_t^2 + 2\bar{\sigma}_t\sigma_c} \qquad \text{(IV-13)}$$

It can be seen at this point that if the clutter or constant term were allowed to go to zero, the expressions for the variance and standard deviation would approach that of a strictly Rayleigh amplitude distributed source.

Probability Density Functions

Not only are the statistics of this new target with clutter model of interest, the probability density functions, pdf's, that describe this new model are of interest also.

In this section the pdf of the measured cross section is derived. To do this and to do other related operations the joint pdf between the measured cross section and the target cross section must first be found. The joint pdf is given by [Ref 8:67]:

$$f_{mt}(\sigma_m,\sigma_t) = f_m(\sigma_m\ \sigma_t)\ f_t(\sigma_t) \qquad \text{(IV-14)}$$

where

$f_t(\sigma_t)$ = pdf of the target cross section
$f_{m|t}(\sigma_m|\sigma_t)$ = conditional pdf of the measured cross section
$f_{mt}(\sigma_m,\sigma_t)$ = joint pdf of the measured and target cross section

The pdf of the target cross section is known to be exponential, Equation (III-41), so the first step is to find the conditional pdf.

Again, the expression for the measured cross section, Equation (IV-4), is the starting point:

$$\sigma_m = \sigma_t + \sigma_c + 2\sqrt{\sigma_t\sigma_c}\cos\phi \qquad \text{(IV-15)}$$

This time, however, it can be assumed that both the clutter and target cross sections are known. This leaves only the phase term as probabilistic. To simplify the expression some new terms will be defined:

let

$$a = \sigma_t + \sigma_c$$
$$b = \sqrt{2\sigma_t\sigma_c}$$
$$u = \cos\phi$$
$$v = \sigma_m / \sigma_t$$

leaving:

$$v = au + b \qquad \text{(IV-16)}$$

First, the pdf of u is found. If the phase is uniformly distributed between 0 and 2π radians standard transform techniques [Ref 10:132] can be used:

$$f_u(u) = \frac{1}{\pi\sqrt{1 - u^2}} \quad , \quad -1<u<1 \qquad \text{(IV-17)}$$

To find the conditional pdf, the transformation of u scaled by a constant and biased by another constant [Ref 10:127], as in Equation (IV-16), is used:

$$f_v(v) = \frac{1}{|a|} f_u\left(\frac{v-b}{a}\right) \qquad \text{(IV-18)}$$

substituting into this expression:

$$f_v(v) = \frac{1}{[a\,\pi\sqrt{1 - (\,v-b\,/a)^2}]}\,, \qquad (b-a) < v < (b+a) \quad \text{(IV-19)}$$

simplifing this expression the pdf becomes:

$$f_v(v) = \frac{1}{[\pi\sqrt{a^2 - (v - b)^2}]}\,, \qquad (b-a) < v < (b+a) \quad \text{(IV-20)}$$

and substituting back the original variables:

$$f_{mt}(\sigma_m|\sigma_t) = \frac{1}{[\,\pi\sqrt{4\sigma_t\sigma_c - (\sigma_m - (\sigma_t + \sigma_c))^2}]} \quad \text{(IV-21)}$$

This conditional pdf is valid for:

$$\sigma_t + \sigma_c - 2\sqrt{\sigma_t\sigma_c} < \sigma_m < \sigma_t + \sigma_c + 2\sqrt{\sigma_t\sigma_c} \quad \text{(IV-22)}$$

The next step, of course, is to find the joint pdf. This is merely the product of the conditional pdf, Equation (IV-21), and the target cross section pdf, Equation (III-41).

$$f_{mt}(\sigma_m,\sigma_t) = \frac{\exp(-\sigma_t/\bar{\sigma}_t)}{\bar{\sigma}_t\pi\sqrt{4\sigma_t\sigma_c - (\sigma_m - (\sigma_t + \sigma_c))^2}} \quad , \qquad \text{(IV-23)}$$

for $\sigma_t > 0$ and $\sigma_t + \sigma_c - 2\sqrt{\sigma_t\sigma_c} < \sigma_m < \sigma_t + \sigma_c + 2\sqrt{\sigma_t\sigma_c}$

Once the joint pdf between the measured and target cross sections have been found, the pdf of the measured cross section alone can be obtained. This is done by integrating the joint pdf over the region defined for the target cross section.

The limits of integration need to be transformed. If the measured cross section is held constant, the upper and lower limits of the target cross section are defined below:

let

$$l1 = \sigma_m + \sigma_c - 2\sqrt{\sigma_m\sigma_c}$$
$$l2 = \sigma_m + \sigma_c + 2\sqrt{\sigma_m\sigma_c}$$

Now, taking only the factor in the square root of the joint pdf and rewriting it:

$$4\sigma_t\sigma_c - (\sigma_m - (\sigma_t + \sigma_c))^2 \qquad \text{(IV-24)}$$

Expanding, cancelling, combining, and isolating the target cross section the square root term becomes:

$$-\sigma_t^2 + 2\sigma_t(\sigma_m + \sigma_c) - (\sigma_m - \sigma_c)^2 \qquad \text{(IV-25)}$$

Now the following substitutions are made to simplify the expression.

let

$$a = 2(\sigma_m + \sigma_c)$$
$$b = (\sigma_m - \sigma_c)$$
$$c = 1/\sigma_t$$

The argument of the square root becomes:

$$-\sigma_t^2 + a\sigma_t - b \qquad \text{(IV-26)}$$

Regrouping and completing the square:

$$(a^2/4 - b) - (\sigma_t - a/2) \qquad \text{(IV-27)}$$

Again, the following simplifing substitutions are made:

let

$$d = (a^2/4 - b)$$
$$u = \sigma_t - a/2$$

where $d = 2\sqrt{\sigma_m \sigma_c}$

The limits of integration using these new substitutions need to be defined. The new transformed limits become:

$$L1 = u \qquad \text{[evaluated for } \sigma_m = 11\text{]}$$
$$= (\sigma_m + \sigma_c - 2\sqrt{\sigma_m \sigma_c}) - (\sigma_m + \sigma_c)$$
$$= -2\sqrt{\sigma_m \sigma_c}$$

or rather $L1 = -d$

and similarly:

$$L2 = u \quad [\text{evaluated for } \sigma_m = 12]$$
$$= d$$

Putting all of these substitutions back into the original joint pdf the pdf becomes:

$$f_{mt} = \exp(-ac/2) \frac{c \exp(-cu)}{\pi \sqrt{d^2 - u^2}} \quad , \quad -d < u < d \qquad \text{(IV-28)}$$

This is the function which will be integrated. This integral becomes:

$$f_m = c \exp(-ac/2) \frac{1}{\pi} \int_{-d}^{d} \frac{\exp(-cu)}{\sqrt{d^2 - u^2}} \, du \qquad \text{(IV-29)}$$

Again, a new set of variables will be defined:

let

$$u = d \cos\theta$$
$$du = -d \sin\theta$$

therefore:

$$\sqrt{d^2 - u^2} = \sqrt{d^2 - d^2\cos^2\theta}$$
$$= d \sin\theta$$

the new limits of integration become:

$$L1 = \cos(u/d) \quad [\text{evaluated for } u = -d]$$
$$= \cos(-d/d)$$
$$= \pi$$

and similarly:

$$L2 = \cos(u/d) \quad [\text{evaluated for } u = d]$$
$$= 0$$

With these last substitutions the integral becomes:

$$f_m = c \exp(-ac/2) \frac{-1}{\pi} \int_{\pi}^{0} \frac{\exp(-cd \cos\theta)}{d \sin\theta} (d \sin\theta) d\theta \qquad \text{(IV-30)}$$

simplifing and rearranging:

$$f_m = c \exp(-ac/2) \left[\frac{1}{\pi} \int_{0}^{\pi} \exp(-cd \cos\theta)\, d\theta\right] \qquad \text{(IV-31)}$$

The factor inside the brackets of the above expression is a modified Bessel function of order zero [Ref 1:376]. Therefore the expression becomes:

$$f_m = c \exp(-ca/2) I_0(cd) \qquad \text{(IV-32)}$$

Replacing all of the substitutions, the pdf of the measured

cross section becomes:

$$f_m(\sigma_m) = \frac{1}{\bar{\sigma}_t} \exp[-\frac{(\sigma_m + \sigma_c)}{\bar{\sigma}_t}] \; I_0(\frac{2\sqrt{\sigma_m \sigma_c}}{\bar{\sigma}_t}), \qquad \sigma_m > 0 \qquad \text{(IV-33)}$$

This pdf will now be verified by taking the Nakagami-Rice distribution [Ref 11:101] and making the appropriate transformations. The Nakagami-Rice distribution was derived by Rice and is the distribution for the instanteous amplitude of the sum of a constant vector and a Rayleigh distributed vector. The distribution of the amplitude is given by [Ref 9:1357, 2:928]:

$$f_x(x) = \frac{2x}{k^2} \exp[-\frac{(y_c^2 + x_2)}{k_2}] \; I_0(\frac{2y_c x}{k^2}) \qquad \text{(IV-34)}$$

where

x = amplitude of the Rayleigh source
y_c = amplitude of the constant, deterministic source
$\bar{k}$ = mean of the Rayleigh source
$I_0(z)$ = modified Bessel function of order zero

But the goal here is to find the pdf of the measured cross section, which is the square of the measured amplitude. Again, standard variable transformation techniques can be used to obtain the pdf of the measured cross section.

For the transformation of:

$$v = u^2 \tag{IV-35}$$

where

u = original random variable
v = new, transformed random variable

The distribution of v is given by [Ref 10:129]:

$$f_v(v) = \frac{1}{2\sqrt{v}} [f_u(\sqrt{v}) + f_u(-\sqrt{v})], \quad v>0 \tag{IV-36}$$

But in this case the original random variable is only defined for positive values leaving just the first term in the above expression.

$$f_v(v) = \frac{1}{2\sqrt{v}} f_u(\sqrt{v}), \qquad v>0 \tag{IV-37}$$

And making the following substitutions:

$$v = \sigma_m$$
$$u = x^m$$

the pdf becomes:

$$f_m(\sigma_m) = \frac{2x}{2\sqrt{\sigma_m}\, k^2} \exp[-\frac{(y_c^2 + \sigma_m)}{k^2}] \; I_0(\frac{2y_c\sqrt{\sigma_m}}{k^2}), \quad \sigma_m>0 \tag{IV-38}$$

Making further substitutions and cancellations the pdf of the measured cross section is obtained:

$$f_m(\sigma_m) = \frac{1}{\bar{\sigma}_t} \exp\left[-\frac{(\sigma_m + \sigma_c)}{\bar{\sigma}_t}\right] I_0\left(\frac{2\sqrt{\sigma_m \sigma_c}}{\bar{\sigma}_t}\right), \qquad \sigma_m > 0 \qquad \text{(IV-39)}$$

The above pdf, Equation (IV-39), is the same as the pdf derived from the new model of a Rayleigh distributed target with constant clutter, Equation (IV-33).

It can be seen that as the power from the deterministic source approaches zero, the modified Bessel function approaches unity, and the entire distribution function approaches the exponential distribution of the Rayleigh target alone.

Computer Generated Probability Density Functions

In the previous sections the probability density function for the new model of a target with constant clutter was derived. In this section the computer generated data will be used to demonstrate this pdf. Again, all of the data was obtained by using the RCSBSC program on a triangluar flat plate model rotated from 15 to 95 degrees aspect angle above a flat plate target support. The cross section data was obtained for every tenth of a degree in this region. Figure IV-1 represents the pdf of the cross section amplitude for the case of a target in a low average signal to clutter ratio environment. This graph was obtained by plotting the number of occurances in a particular range of cross section versus the range of cross section amplitudes. This was done for the case of when the target support was at a tilt angle of 66 degrees. This pdf looks quite different from the pdf of the cross section amplitude when there was no clutter. Figure IV-2 provides something to compare Figure IV-1 with. This figure represents the pdf of the cross section amplitude for the case of a target in a high signal to clutter ratio environment (tilt angle of 68 degrees). As predicted theortically, when the clutter contribution is small, the model is similar to that of there being no clutter at all.

Again, when the data that is used to generate these pdf graphs is averaged first, the pdf's begin to take on a Gaussian shape. Figures IV-3, IV-4, and IV-5 show the simulated pdf curves for the case of a low signal to clutter

ratio after averaging over a window of 11 points (1.1 degrees), 25 points (2.5 degrees), and 51 points (5.1 degrees) respectively. Notice that the more the data is sampled, the more the curves take on a Gaussian shape.

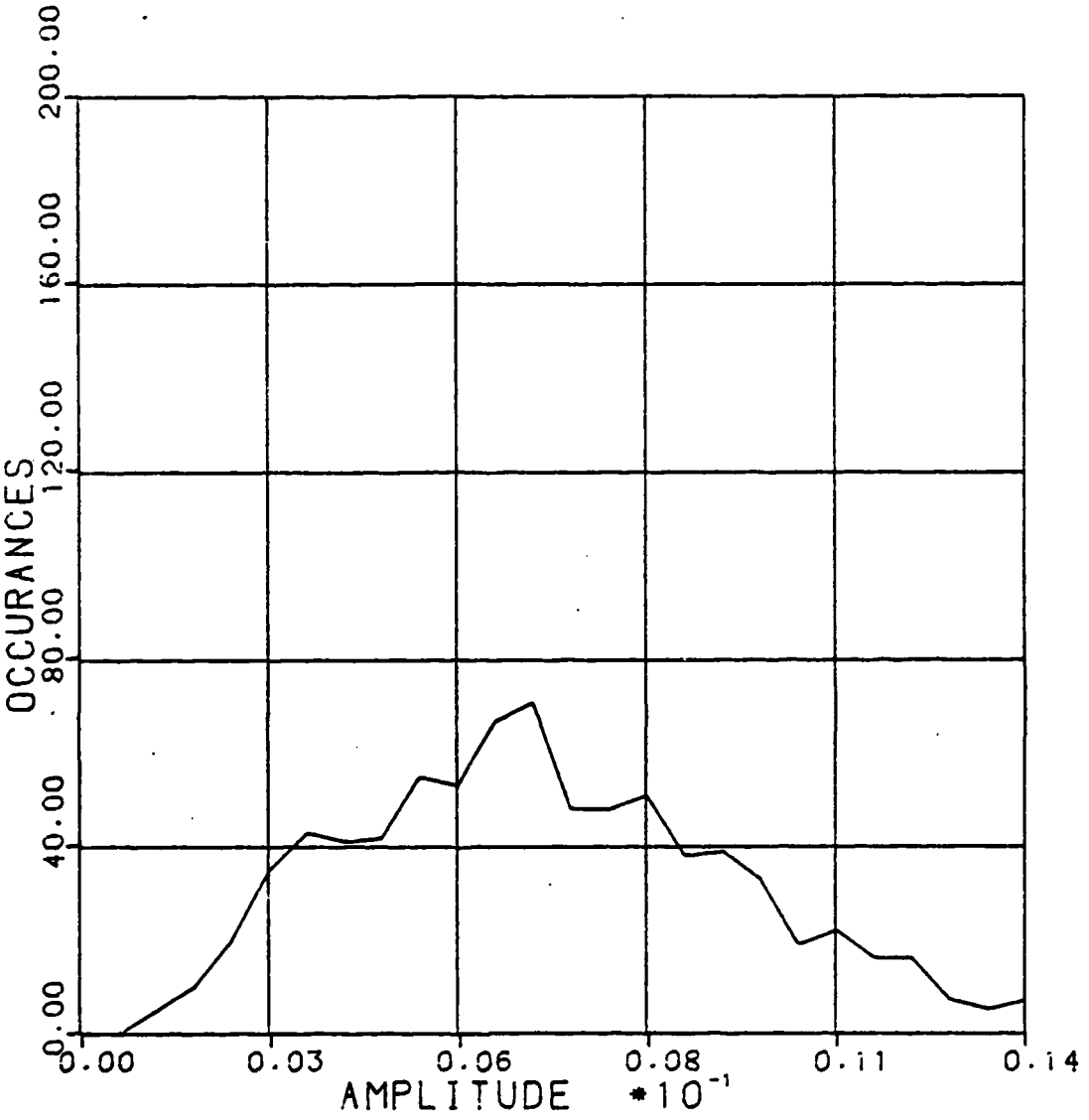

Figure IV-1 Probability Density Function (from Computer Generated Data) of a Target and Target Support Cross Section Amplitude for Low (2.1 dB) Signal to Clutter Ratio

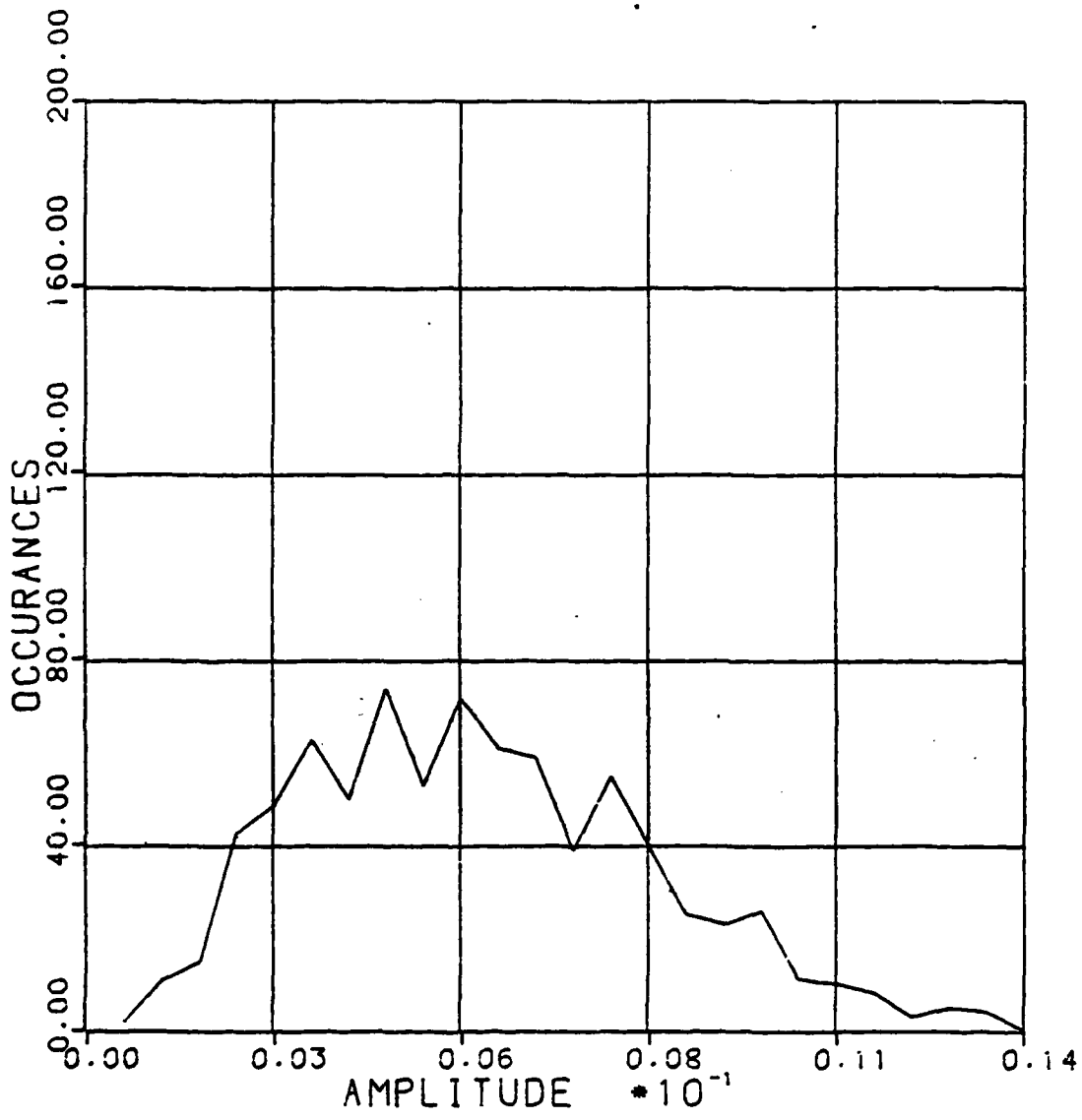

Figure IV-2 Probability Density Function (from Computer Generated Data) of a Target and Target Support Cross Section Amplitude for High (13.6 dB) Signal to Clutter Ratio

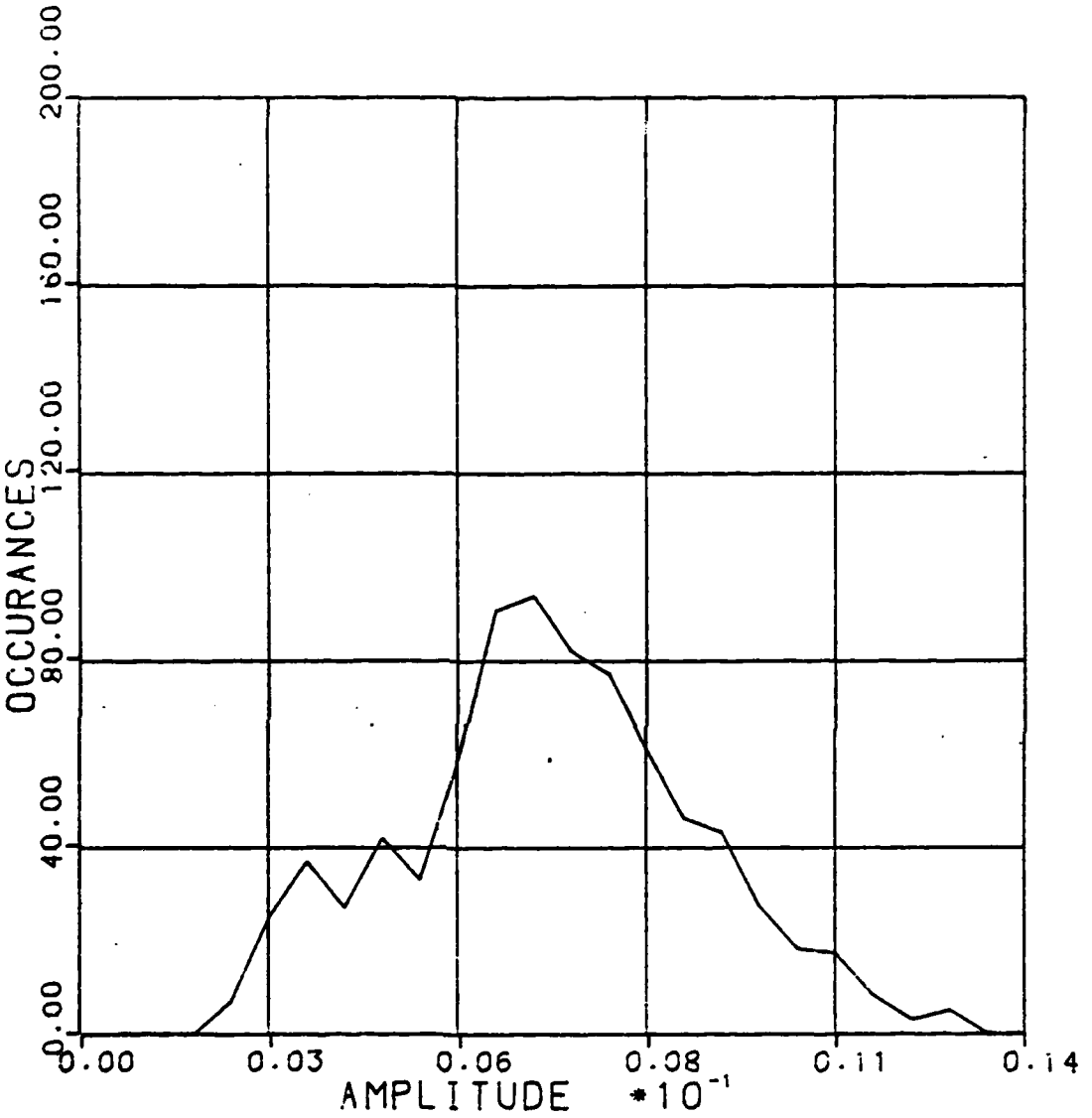

Figure IV-3 Probability Density Function (from Computer Generated Data) of a Target and Target Support Cross Section Amplitude for Low (2.1 dB) Signal to Clutter Ratio After Averaging Over an 11 Point (1.1 degree) Window

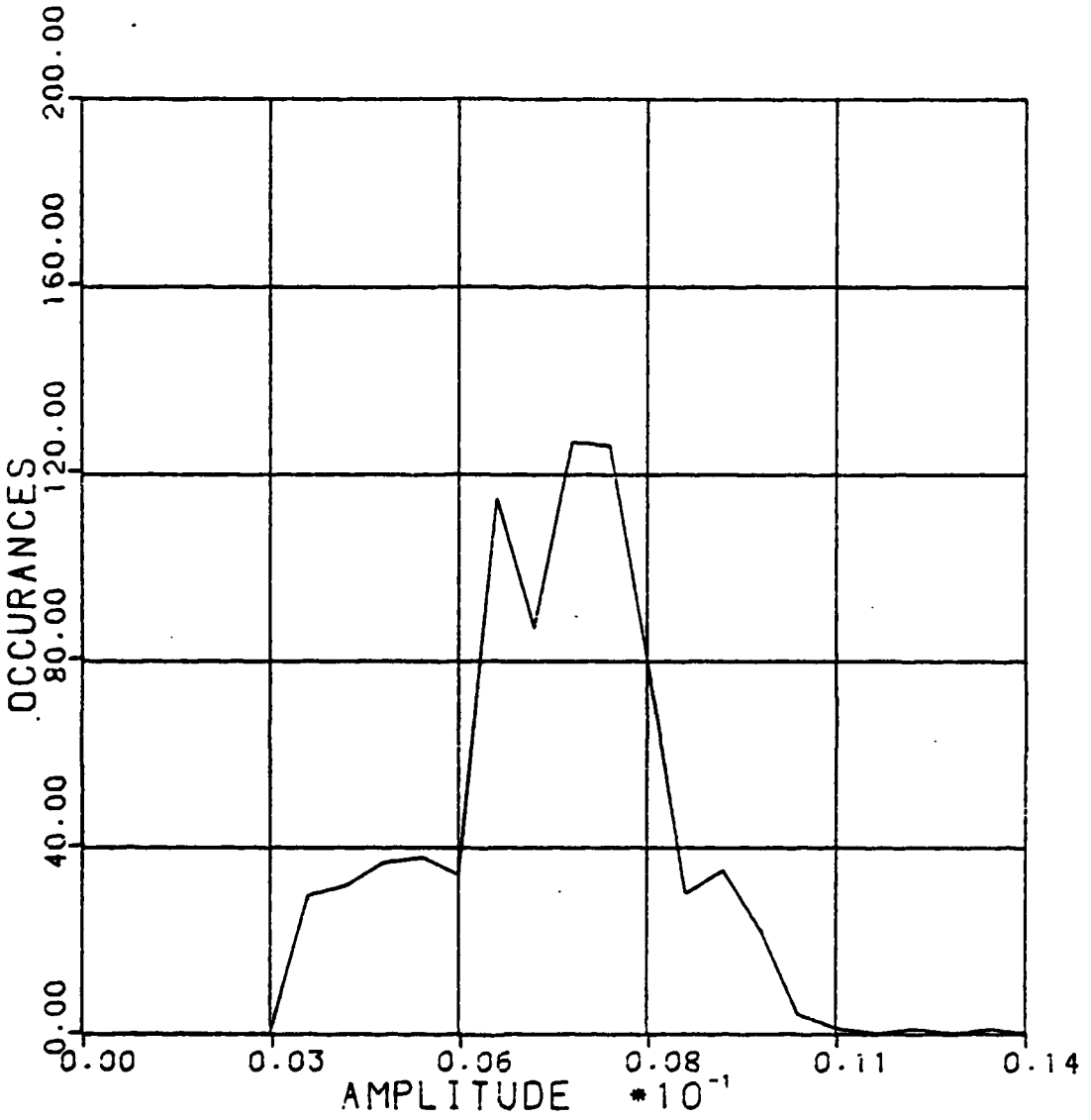

Figure IV-4 Probability Density Function (from Computer Generated Data) of a Target and Target Support Cross Section Amplitude for Low (2.1 dB) Signal to Clutter Ratio After Averaging Over a 2.5 Point (2.5 degree) Window

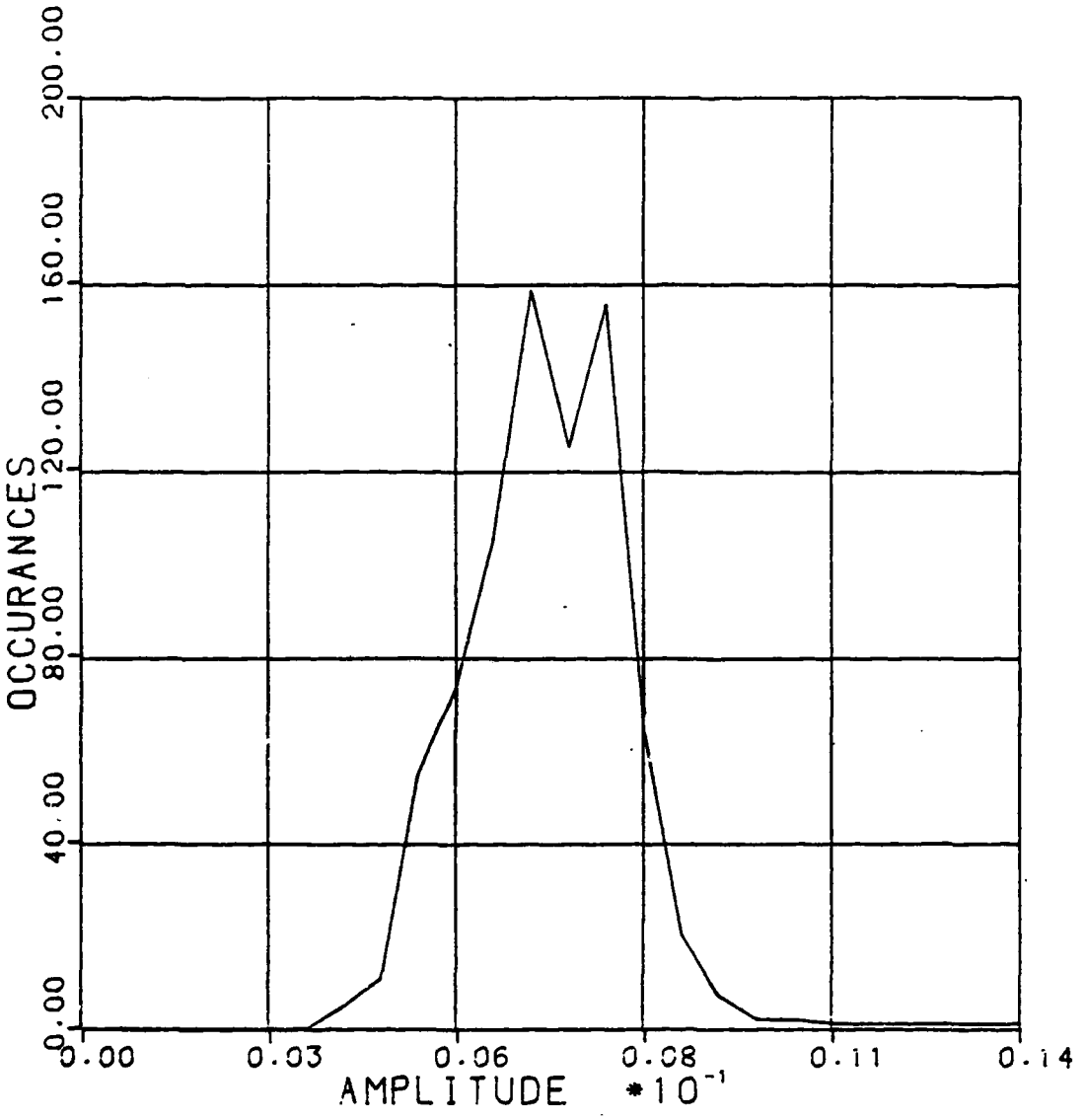

Figure IV-5 Probability Density Function (from Computer Generated Data) of a Target and Target Support Cross Section Amplitude for Low (2.1 dB) Signal to Clutter Ratio After Averaging Over a 51 Point (5.1 degree) Window

V. Analysis of the Probability Distribution of the Ratio of the Measured to Target Cross Sections

In this chapter a new approach for estimating the error is derived. In the traditional approach the error estimate was based on measured cross section normalized by the measured cross section's average, where the average cross section is the sum of the clutter cross section and the target cross section. This traditional approach also is based on deterministic sources and therefore the returns are assumed to be known at every point.

In the new approach, the sources are assumed to be probabilistic, using the model derived in Chapter IV. This probablistic model is a much more accurate model of the system. Furthermore, measurement of cross sections does not require the hard requirement of accuarcy at every point. This new approach assumes that the data from the cross section measurement is run through a running average processor.

Just as in the traditional approach, the new approach is based on the normalized measured cross section. This time, however, the measured cross section is normalized to the target cross section alone. This ratio will be the new

indictor of the magnitude of error that the constant clutter introduces in the measured cross section. The smaller the effect of the constant clutter, the closer the measured cross section will be to the target cross section. As the measured cross section becomes closer to the target cross section, the ratio of the two will approach unity. Of course, if there is no contribution from the constant clutter, the ratio will be indentically unity.

If the probability density function, pdf, of this ratio were plotted, the result would be a curve whose variance grows smaller with smaller constant clutter. In the limiting case of there being no constant clutter, the pdf should be an impulse centered at unity. On the other hand, as the contribution of the constant clutter becomes more significant, the pdf of the ratio will become "washed out" and the variance will grow larger. As can be seen by the above discussion, the variance of the ratio of the measured cross section to the target free space cross section is a good indicator of the error in the measured cross section.

Gaussian Approximation

To find the pdf of the ratio of the exact measured cross section to the exact target cross section would be very difficult due to the complicated limits of integration. However, the measurements are not to be based on the exact, point to point data, but rather, on the data from averaged

versions of the measured cross section and the target cross section. If these cross sections are averaged over enough points, the Central Limit Theorem can be used to assume that the distribution of the average is Gaussian. This Gaussian approximation makes the integration required to find the pdf of the ratio much more managable. Of course, the question arises of how many samples is enough before the Gaussian approximation is valid. According to the Central Limit Theorem, if the pdf's are already nearly Gaussian it takes fewer samples to satisfiy the Gaussian approximation. As can be seen from Figures III-8 and IV-1 the shape of the pdf's from the computer generated data is already roughly Gaussian. This application of the Central Limit Theorem is demostrated in Figures III-9, III-10, III-11 and Figures IV-2, IV-3, IV-5. These figures show the free space target amplitude pdf and the target with clutter amplitude pdf for increasing levels of averaging. For this paper it will be assumed that 11 samples will be sufficient to satisfy the Central Limit Theorem. This assumption is not proved in this paper.

Correlation Coefficient

To find the pdf of the ratio of the averaged measured cross section to the averaged target cross section, the bivariate joint Gaussian distribution will be needed. The correlation coefficient is a parameter of this joint Gaussian distribution. In this section the correlation coefficient of

AD-A138 075 ACCURACY ESTIMATE FOR RADAR CROSS SECTION MEASUREMENTS OF TARGETS MODELLE..(U) AIR FORCE INST OF TECH WRIGHT-PATTERSON AFB OH SCHOOL OF ENGI.. J N LINK 2/2

UNCLASSIFIED DEC 83 AFIT/GE/EE/83D-39 F/G 17/9 NL

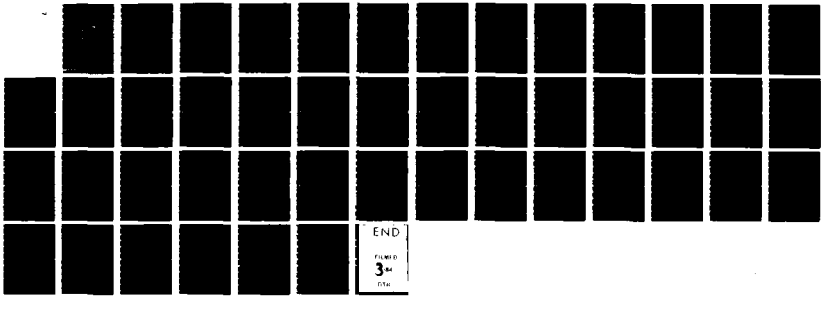

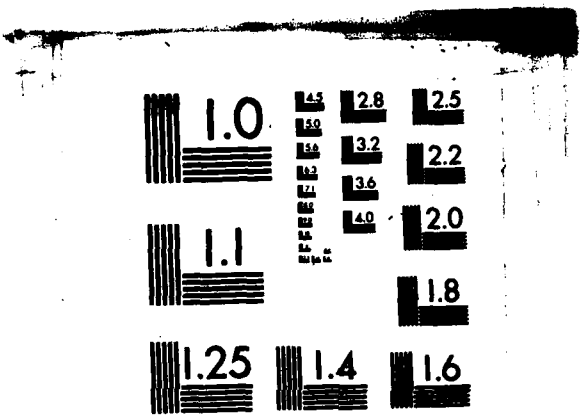

the exact distributions will be found. It will be also assumed that this coefficient will work for the averaged distributions. This assumption turns out to be a good one. The correlation coefficient for the computer generated data was found and compared to the cofficient of the averaged data. These two coefficients were found to be nearly identical.

The correlation coefficient is defined as [Ref 8:73]:

$$r_{xy} = \frac{E[(x - \bar{x})(y - \bar{y})]}{\sqrt{E[(x - x)^2]\ E[(y - y)^2]}} \qquad (V-1)$$

Expanding this expression:

$$r_{xy} = \frac{E[xy] - \bar{x}\bar{y}}{s_x\ s_y} \qquad (V-2)$$

where

$\bar{x}$, $\bar{y}$ = means of x and y
E[xy] = cross correlation of x and y
s_x, s_y = standard deviations of x and y

Finding the cross correlation between the measured cross section and the target cross section is the first step in finding the correlation coefficient.

$$E[\sigma_m \sigma_t] = \iint \sigma_m \sigma_t f_{mt}(\sigma_m, \sigma_t) d\sigma_m d\sigma_t \qquad \text{(V-3)}$$

Substituting the limits of integration and the joint pdf this integral becomes:

$$E[\sigma_m \sigma_t] = \int_0^{\infty} \int_{m1}^{m2} \frac{\sigma_t \ \sigma_m}{\bar{\sigma}_t \ \pi \sqrt{4 \ \sigma_t \sigma_c - (\sigma_m - (\sigma_t + \sigma_c))^2}} \frac{\exp(-\sigma_t / \bar{\sigma}_t) \quad d\sigma_m d\sigma_t}{} \qquad \text{(V-4)}$$

where

$$m1 = \sigma_t + \sigma_c - 2\sqrt{\sigma_t \sigma_c}$$
$$m2 = \sigma_t + \sigma_c + 2\sqrt{\sigma_t \sigma_c}$$

Expanding the expression in the square root:

$$4\sigma_t \sigma_c - (\sigma_m^2 + \sigma_t^2 + \sigma_c^2 + 2\sigma_t \sigma_c - 2\sigma_m(\sigma_t + \sigma_c)) \qquad \text{(V-5)}$$

Rewriting and isolating the measured cross section:

$$-\sigma_m^2 + 2\sigma_m(\sigma_t + \sigma_c) - (\sigma_t - \sigma_c)^2 \qquad \text{(V-6)}$$

Now, the following substitutions are made to simplify the expression.

let

$$a = 2(\sigma_t + \sigma_c)$$
$$b = (\sigma_t - \sigma_c)^2$$

The square root term becomes:

$$-\sigma_m^2 + a\sigma_m - b \qquad \text{(V-7)}$$

Completing the square and rearranging terms:

$$(a^2/4 - b) - (\sigma_m - a/2)^2 \qquad \text{(V-8)}$$

Making the following simplifing substitutions:

let

$$d^2 = a^2/4 - b$$
$$u = \sigma_m - a/2$$

where $d = 2\sigma_t\sigma_c$

The square root term becomes:

$$d^2 - u^2 \qquad \text{(V-9)}$$

After these substitutions, the limits of integration need to be redefined. The transformed limits become:

$$M1 = u \qquad [\text{evaluated for } \sigma_m = m1]$$
$$= \sigma_t + \sigma_c - 2\sqrt{\sigma_t\sigma_c} - (\sigma_t + \sigma_c)^m$$
$$= -2\sqrt{\sigma_t\sigma_c}$$
$$= -d$$

And similarly:

$$M2 = u \quad = d \qquad \text{[evaluated for } \sigma_m = m2\text{]}$$

Putting all of these substitutions back, the original integral becomes:

$$E[\sigma_m \sigma_t] = \int_0^{\infty} \int_{-d}^{d} \frac{\sigma_t (u + a/2)}{\bar{\sigma}_t \pi} \frac{\exp(-\sigma_t/\bar{\sigma}_t)}{\sqrt{d^2 - u^2}} \, du \, d\sigma_t \qquad \text{(V-10)}$$

Separating the inside integral into two parts:

$$E[\sigma_m \sigma_t] = \frac{\sigma_t \exp(-\sigma_t/\bar{\sigma}_t)}{\bar{\sigma}_t} \int_0^{\infty} \left[\frac{1}{\pi} \int_{-d}^{d} \frac{u \, du}{\sqrt{d^2 - u^2}} + \frac{a}{2\pi} \int_{-d}^{d} \frac{du}{\sqrt{d^2 - u^2}} \right] d\sigma_t \qquad \text{(V-11)}$$

Both integrals on u are in standard integral tables. Solving the integrals and substituting the values of the limits of integration the integral becomes:

$$E[\sigma_m \sigma_t] = \int_0^{\infty} \frac{\sigma_t \exp(-\sigma_t/\bar{\sigma}_t)}{\bar{\sigma}_t} \left[\frac{-1}{\pi} \sqrt{d^2 - u^2} \Big|_{u=-d}^{u=d} + \frac{a}{2\pi} \sin^{-1}(u/d) \Big|_{u=-d}^{u=d} \right] d\sigma_t \quad \text{(V-12)}$$

Simplifing this integral:

$$E[\sigma_m \sigma_t] = \int_0^{\infty} (\sigma_t/\bar{\sigma}_t) \exp(-\sigma_t/\bar{\sigma}_t) \ (a/2) \ d\sigma_t \quad \text{(V-13)}$$

Substituting the value of the constant a and expanding again into two integrals:

$$E[\sigma_m \sigma_t] = (1/\bar{\sigma}_t) \int_0^{\infty} \sigma_t^2 \exp(-\sigma_t/\bar{\sigma}_t) \ d\sigma_t + (\sigma_c/\bar{\sigma}_t) \int_0^{\infty} \sigma_t \exp(-\sigma_t/\bar{\sigma}_t) \ d\sigma_t \quad \text{(V-14)}$$

Solving these two integrals the expression for the cross correlation is finally obtained:

$$E[\sigma_m \sigma_t] = 2\bar{\sigma}_t^2 + \sigma_c \bar{\sigma}_t \quad \text{(V-15)}$$

The expression for the correlation coefficient also requires the means and standard deviations of the two variables, the measured cross section and the target free space cross section. But these have already been found in Chapters III and IV. Substituting these into Equation (V-2) the correlation coefficient becomes:

$$r_{mt} = \frac{(2\bar{\sigma}_t^2 + \sigma_c\bar{\sigma}_t) - (\bar{\sigma}_t + \sigma_c)\bar{\sigma}_t}{\sqrt{(\bar{\sigma}_t^2 + 2\bar{\sigma}_t\sigma_c)\bar{\sigma}_t^2}} \qquad \text{(V-16)}$$

Simplifing the above expression, the correlation coefficient can be written soley as a function of the signal to clutter ratio:

$$r_{mt} = \sqrt{\frac{X}{X + 2}} \qquad \text{(V-17)}$$

where

$X = \bar{\sigma}_t/\sigma_c$ or the signal to clutter ratio

A graph of this correlation coefficient for a range of signal to clutter ratios is given in Figure V-1.

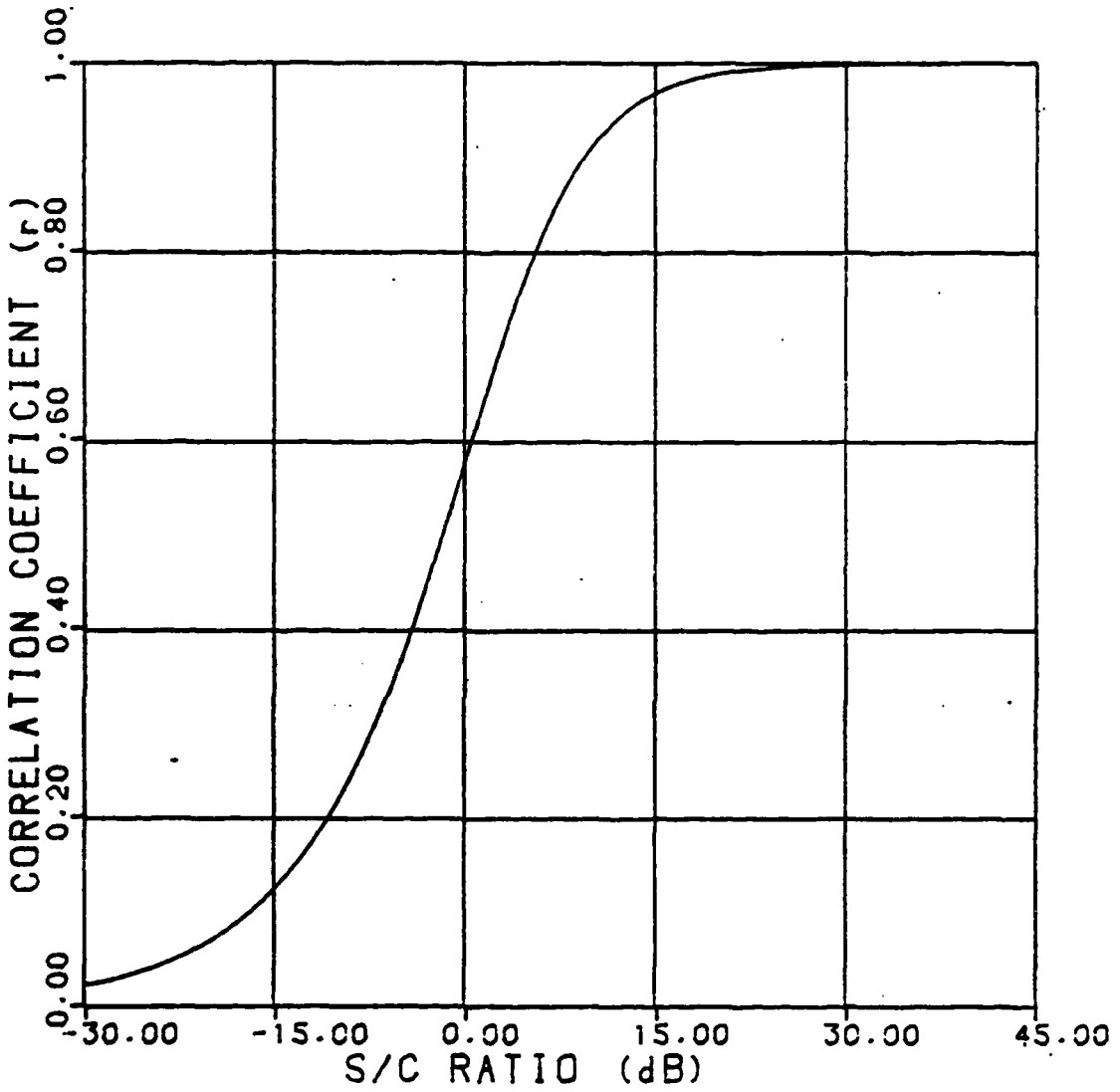

Figure V-1 Correlation Coefficient vs. Signal to Clutter Ratio

Bivariate Joint Gaussian Distribution

Now, all of the necessary parameters for the joint Gaussian pdf have been derived. The joint pdf is given by [Ref 8:117]:

$$f_{\hat{m}\hat{t}}(\hat{\sigma}_m, \hat{\sigma}_t) = \frac{1}{2\pi \; s_{\hat{m}} \; s_{\hat{t}} \; \sqrt{1 - r^2}} \exp(Q) \qquad \text{(V-18)}$$

where

$$Q = \frac{-1}{2(1 - r^2)} \left[\frac{\hat{\sigma}_m - \bar{\hat{\sigma}}_m}{s_{\hat{m}}}\right]^2 + \left[\frac{\hat{\sigma}_t - \bar{\hat{\sigma}}_t}{s_{\hat{t}}}\right]^2 - 2r \left[\frac{\hat{\sigma}_m - \bar{\hat{\sigma}}_m}{s_{\hat{m}}}\right] \left[\frac{\hat{\sigma}_t - \bar{\hat{\sigma}}_t}{s_{\hat{t}}}\right]$$

But recall that the Gaussian distribution is assumed after each of the two individual distributions are sampled and averaged. Therefore, the variables of this joint Gaussian distribution, $\hat{\sigma}_m$ and $\hat{\sigma}_t$, are the averaged values and are only estimates of the true values. It has already been assumed that the correlation coefficient, r_{mt}, is not affected by the averaging. It is also known that the sampled means, $\bar{\hat{\sigma}}_m$ and $\bar{\hat{\sigma}}_t$, are equal to the exact means [Ref 10:246] and the sampled standard deviations, $s_{\hat{m}}$ and $s_{\hat{t}}$, are the exact standard deviations scaled by the square root of the number of samples, or rather:

$$s_{\hat{m}} = s_m/\sqrt{N}$$
$$s_{\hat{t}} = s_t/\sqrt{N}$$

Probability Density Function of the Ratio

All of the necessary information has now been found to find the pdf of the ratio of the averaged versions of the measured cross secton and the target cross section. To find the pdf of the ratio the area in the $\hat{\sigma}_m\hat{\sigma}_t$ plane is found such that:

$$\hat{\sigma}_m/\hat{\sigma}_t \leq z \qquad \text{(V-19)}$$

is the shaded area of Figure V-2 below because:

if $\hat{\sigma}_t > 0$ then $\hat{\sigma}_m \leq \hat{\sigma}_t z$
if $\hat{\sigma}_t < 0$ then $\hat{\sigma}_m \geq \hat{\sigma}_t z$

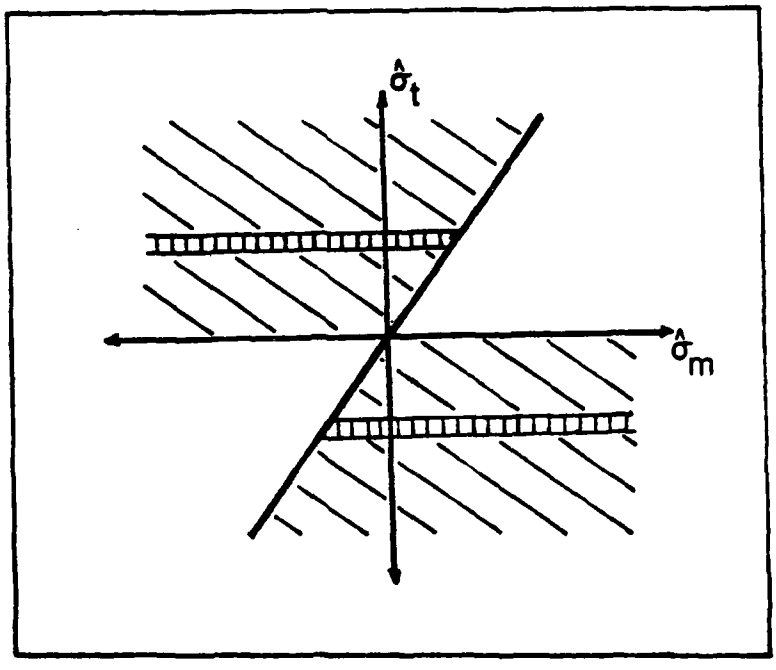

Figure V-2 $\hat{\sigma}_m$, $\hat{\sigma}_t$ Plane

The area can be found by integrating over the horizontal strips. This area represents the cumlative distribution function given below:

$$F(z) = \int_0^{\infty} \int_{-\infty}^{\hat{\sigma}_t z} f_{\hat{m}\hat{t}}(\sigma'_m, \sigma'_t)\, d\sigma'_m d\sigma'_t + \int_{-\infty}^{0} \int_{\hat{\sigma}_t z}^{\infty} f_{\hat{m}\hat{t}}(\sigma'_m, \sigma'_t)\, d\sigma'_m d\sigma'_t \quad \text{(V-20)}$$

Differentiating with respect to z the pdf of the ratio is found.

$$f_z(z) = \int_0^{\infty} \sigma'_t f_{\hat{m}\hat{t}}(\sigma'_t z, \sigma'_t)\, d\sigma'_t - \int_{-\infty}^{0} \sigma'_t f_{\hat{m}\hat{t}}(\sigma'_t z, \sigma'_t)\, d\sigma'_t \quad \text{(V-21)}$$

Now recall that the exact distributions of the measured cross section and the target cross section are zero for negative values. The Gaussian approximation assumes values that are positive or negative. However, since the joint Gaussian distribution has non-zero means most of the area under the pdf curve is in the positive quadrant. In fact, it turns out that there is practically no contribution to the pdf of the ratio for negative values. Therefore, th second integral in the above expression is essentially zero, leaving only the first integral.

$$f_z(z) = \int_0^\infty \sigma_t' f_{\hat{m}\hat{t}}(\sigma_t' z, \sigma_t') d\sigma_t' \qquad \text{(V-22)}$$

To simplify the expression the following substitutions will be used:

let

$$\begin{aligned} \hat{\sigma}_m &= x \\ \bar{\hat{\sigma}}_m &= \bar{x} \\ s_{\hat{m}} &= s_x \\ \hat{\sigma}_t &= y \\ \bar{\hat{\sigma}}_t &= \bar{y} \\ s_{\hat{t}} &= s_y \end{aligned}$$

Taking these substitutions and the joint Gaussian pdf and putting them into the above integral expression for the pdf of the ratio:

$$f_z(z) = \int_0^\infty \frac{y}{2\pi s_x s_y \sqrt{1 - r^2}} \exp(Q)\, dy \qquad \text{(V-23)}$$

where

$$Q = \frac{-1}{2(1 - r^2)} \left[\frac{yz - \bar{x}}{s_x}\right]^2 + \left[\frac{y - \bar{y}}{s_y}\right]^2 - 2r\left[\frac{yz - \bar{x}}{s_x}\right]\left[\frac{y - \bar{y}}{sy}\right]$$

Taking this expression and expanding the argument of the expontial term, all of the factors containing y can be isolated.

$$f_z(z) = \frac{1}{2\pi s_x s_y \sqrt{1 - r^2}} \int_0^\infty y \exp\left[\left(\frac{1}{2(1 - r^2)}\right) y^2 \left(\frac{z^2}{s_x^2} + \frac{1}{s_y^2} - 2r\frac{z}{s_x s_y}\right) + y\left(\frac{-2\bar{x}z}{s_x s_y} - \frac{2\bar{y}}{s_x^2} + \frac{2r\bar{y}z}{s_x s_y} + \frac{2r\bar{x}}{s_x s_y}\right) + \left(\frac{\bar{x}^2}{s_x^2} + \frac{\bar{y}^2}{s_y^2} - \frac{2r\bar{x}\bar{y}}{s_x s_y}\right)\right] dy \quad \text{(V-24)}$$

This integral can be simplified greatly with the following substitutions:

let

$$a = \frac{1}{2(1 - r^2)}$$

$$b = \frac{z}{s_x^2} + \frac{1}{s_y^2} - 2r\frac{z}{s_x s_y}$$

$$c = \frac{2r\bar{y}z}{s_x s_y} + \frac{2r\bar{x}}{s_x s_y} - \frac{2\bar{y}z}{s_x s_y} - \frac{2\bar{y}}{s_x^2}$$

$$d = \frac{\bar{x}^2}{s_x^2} + \frac{\bar{y}^2}{s_y^2} - \frac{2r\bar{x}\bar{y}}{s_x s_y}$$

$$K = \frac{1}{2\pi s_x s_y \sqrt{1 - r^2}}$$

where

$$r = \sqrt{X/(X + 2)}$$
$$X = \bar{\sigma}_t/\sigma_c$$

After a great deal of algebra the expressions for the means, standard deviations, correlation coefficient, and signal to clutter ratio can be substituted into these

expressions and they can all be written soley as functions of the ratio, z, and the signal to clutter ratio, X.

$$a = \frac{X + 2}{4}$$

$$b = N\frac{X}{X + 2}\,(z^2 - 2z + 1 + 2/X)$$

$$c = -2N\,\frac{1 + z}{X + 2}$$

$$d = N\,\frac{1 + 2X}{X(X + 2)}$$

$$K = \frac{N}{\pi}\sqrt{\frac{X}{2}}$$

Putting all of these simplifications back into the original integral it becomes:

$$f_z(z) = \int_0^\infty K\, y\, \exp[-a(by^2 + cy + d)]\, dy \qquad \text{(V-25)}$$

Taking out the constant terms this integral can be rewritten as:

$$f_z(z) = K \exp(-ad) \int_0^\infty y \exp(-aby^2) \exp(-acy)\, dy \quad \text{(V-26)}$$

This integral has the exact form of a known Laplace transform [Ref 5:146]. Thus the pdf of the ratio of the averaged measured cross section to the averaged target cross section becomes:

$$f_z(z) = K \exp(-ad)\left(\frac{1}{2ab} - \frac{\sqrt{\pi}\, c}{4b\sqrt{bc}} \exp\left[\frac{ac^2}{4b}\right] \text{Erfc}\left[\frac{c}{2}\sqrt{\frac{a}{b}}\right]\right) \quad \text{(V-27)}$$

Where Erfc(x) is the Error Function Compliment and is defined here as:

$$\text{Erfc}(x) = 2/\sqrt{\pi} \int_x^\infty \exp(-t^2)\, dt \quad \text{(V-28)}$$

Because this pdf contains the error function compliment, it can not be integrated in closed form and the moments cannot be found in closed form. To find the standard deviation of z, therefore, numerical integration on a computer must be used.

The next two figures show the pdf of the ratio, Equation

(V-26), for various values of averaging (N samples) and for various signal to clutter ratios. Figure V-3 represent the pdf of the ratio for several signal to clutter ratios while holding N constant at 11 samples. Just as expected, for higher signal to clutter ratios the pdf approaches a spike centered at unity, and for lower signal to clutter ratios the pdf's mode shifts further from unity and the standard deviation grows. Figure V-4 represent the pdf of the ratio for several sampling levels while holding the signal to clutter ratio constant at 2 (3 dB). Again, just as expected, for more averaging the peak of the curve grows higher and the standard deviation decreases. When the signal to clutter ratio is held constant at 2 the mode of the pdf is held constant at about 1.5 just as expected.

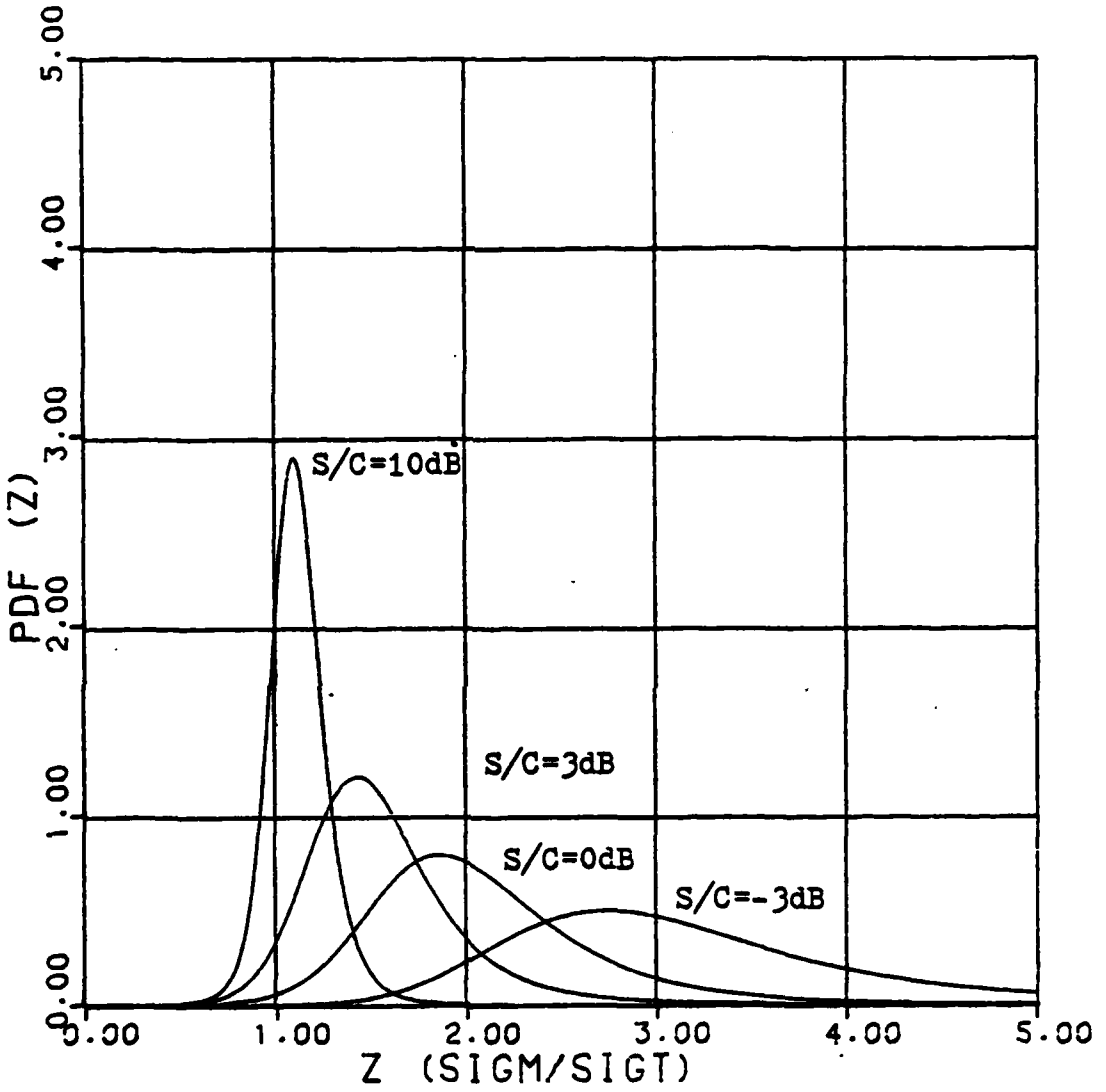

Figure V-3 Probability Density Function of the Ratio of the Averaged Measured Cross Section to the Averaged Target Cross Section for Several Signal to Clutter Ratios and Constant Averaging (N=11)

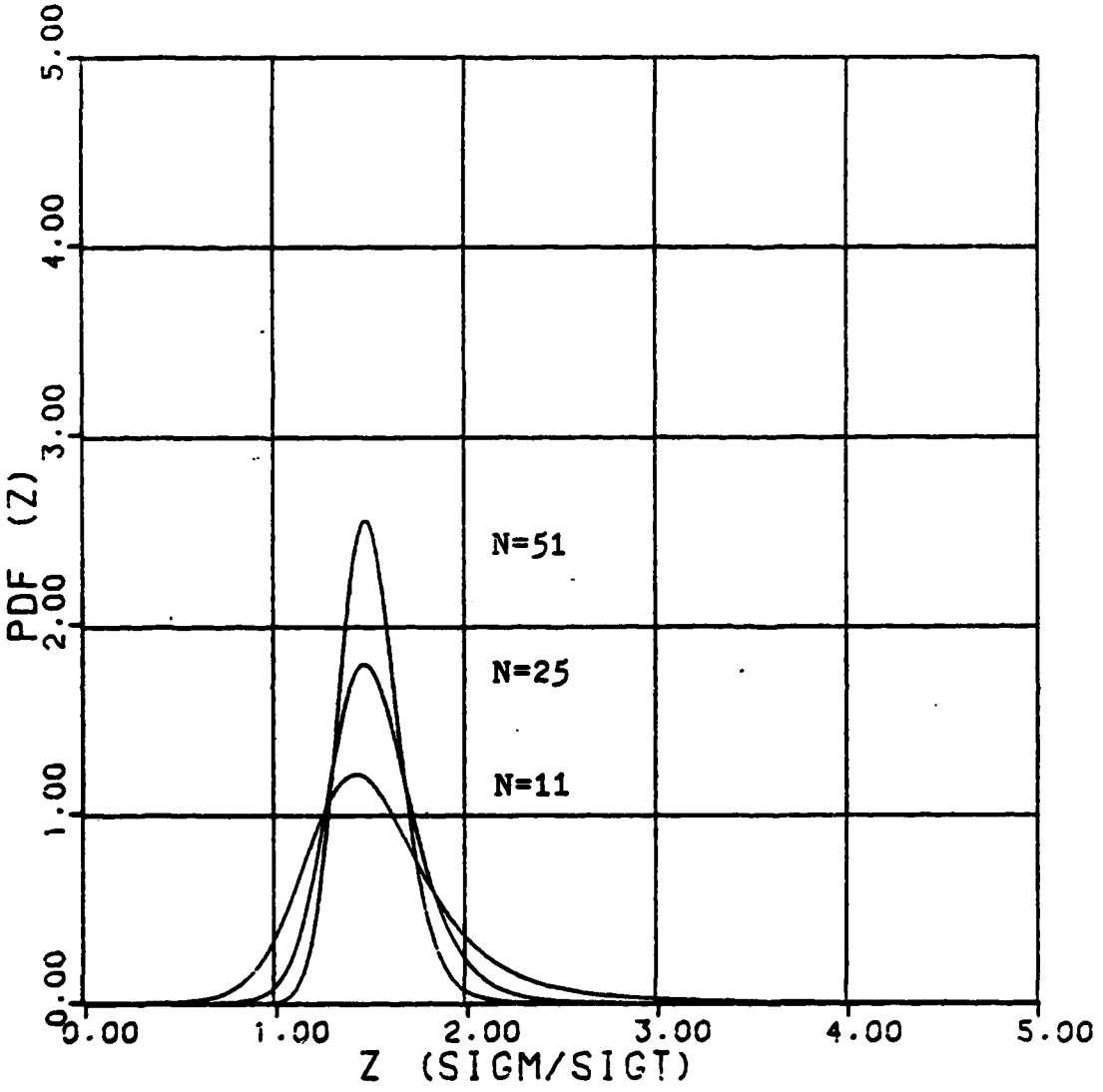

Figure V-4 Probability Density Function of the Ratio of the Averaged Measured Cross Section to the Averaged Target Cross Section for Several Averaging Levels and Constant Signal to Clutter (S/C=2, 3 dB)

It can be seen from all of these past curves that the standard deviation of the pdf becomes smaller for more averaging and for higher signal to clutter ratios. The standard deviation of the ratio, therefore, can be used as a measure of confidence in the measurement of the cross section. With smaller standard deviations more confidence can be placed in the cross section measurement.

Comparison with Computer Generated Data

In this section the theoretical pdf curves will be compared to the pdf curves obtained from the computer generated data for similar averaging and signal to clutter ratios. It is important to bear in mind, however, that the theoretical curves are somewhat artificial in that the entire curve is generated for one particular signal to clutter ratio. On the other hand, the computer generated data for a particular tilt angle will have signal to clutter ratios that vary rapidly from point to point. To deal with this problem only data points that are within 25 percent of the desired signal to clutter ratio are used to compare with the theoretical curves.

Figure V-5 shows the pdf curve from the computer generated data for an average signal to clutter ratio of 1 (0 dB) and for N=11 samples. Figure V-6 shows the theoretical pdf curve for the same signal to clutter ratio and averaging level.

The next two figures (Figures V-7 and V-8) show the pdf curves, from the computer generated data and theoretical, for the same low signal to clutter ratio but for a high level of averaging (N=51). These curves represent the low signal to clutter ratio case.

The next set of figures are for an average signal to clutter ratio of 10 (10 dB). This signal to clutter ratio is used to demostrate the high signal to clutter ratio case. Figure V-9 shows the pdf curve from the computer generated data for this average signal to clutter ratio and for N=11 samples. Figure V-10 shows the theoretical pdf curve for the same signal to clutter ratio and averaging level.

The computer generated and theoretical pdf curves are shown next for the same high signal to clutter ratio but now for a high averaging level (N=51).

It can be seen from these past curves that the theoretical and computer generated pdf curves roughly correspond. The curves match best for higher signal to clutter ratios. Whether the shape of the curves match exactly or not, the means of the theoretical and computer generated pdf's do match.

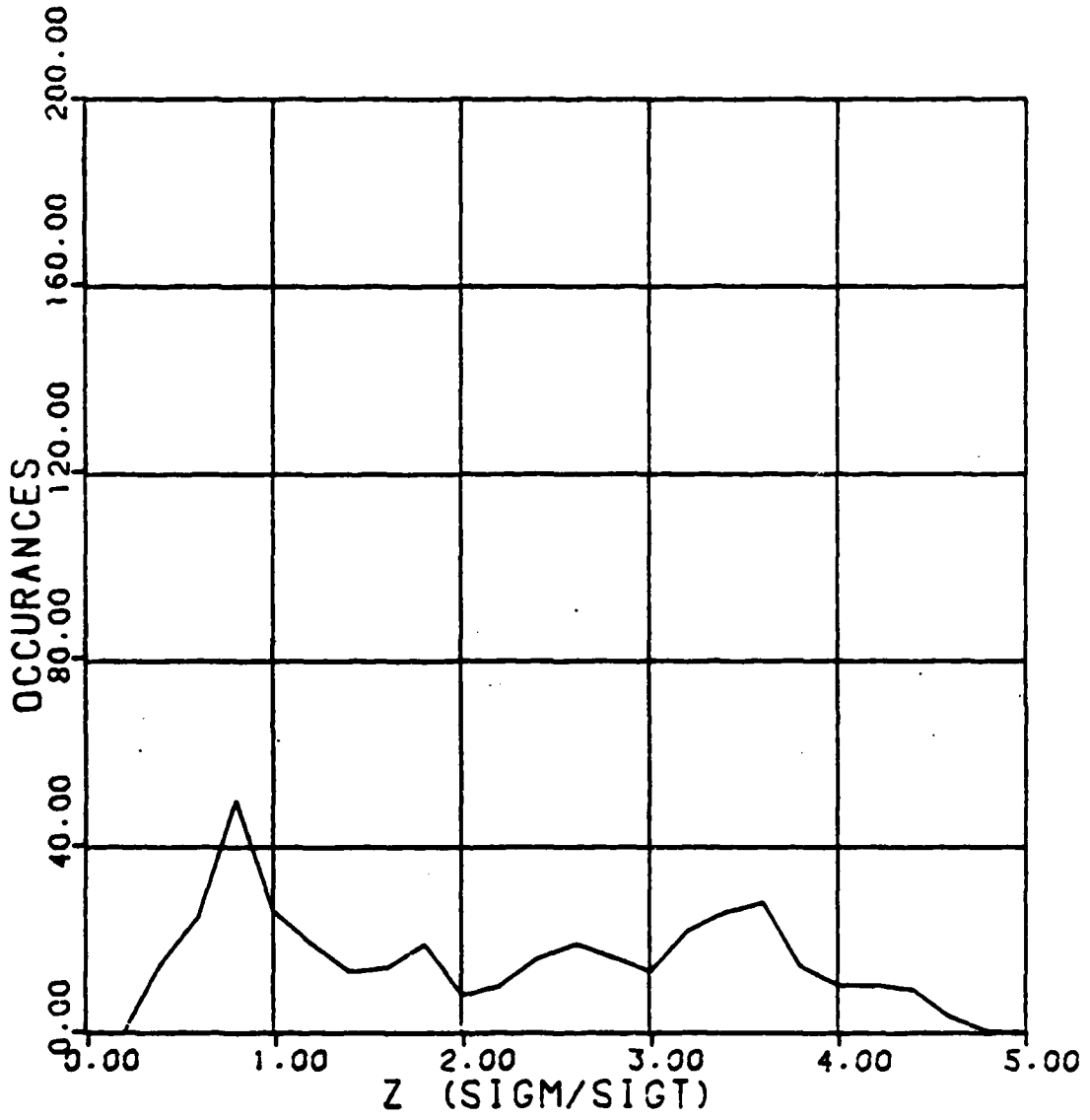

Figure V-5 Probability Density Function (from Computer Generated Data) of the Ratio of the Averaged Measured Cross Section to the Averaged Target Cross Section for an Average Signal to Clutter Ratio of 1 (0 dB), and Averaging of N=11 Samples

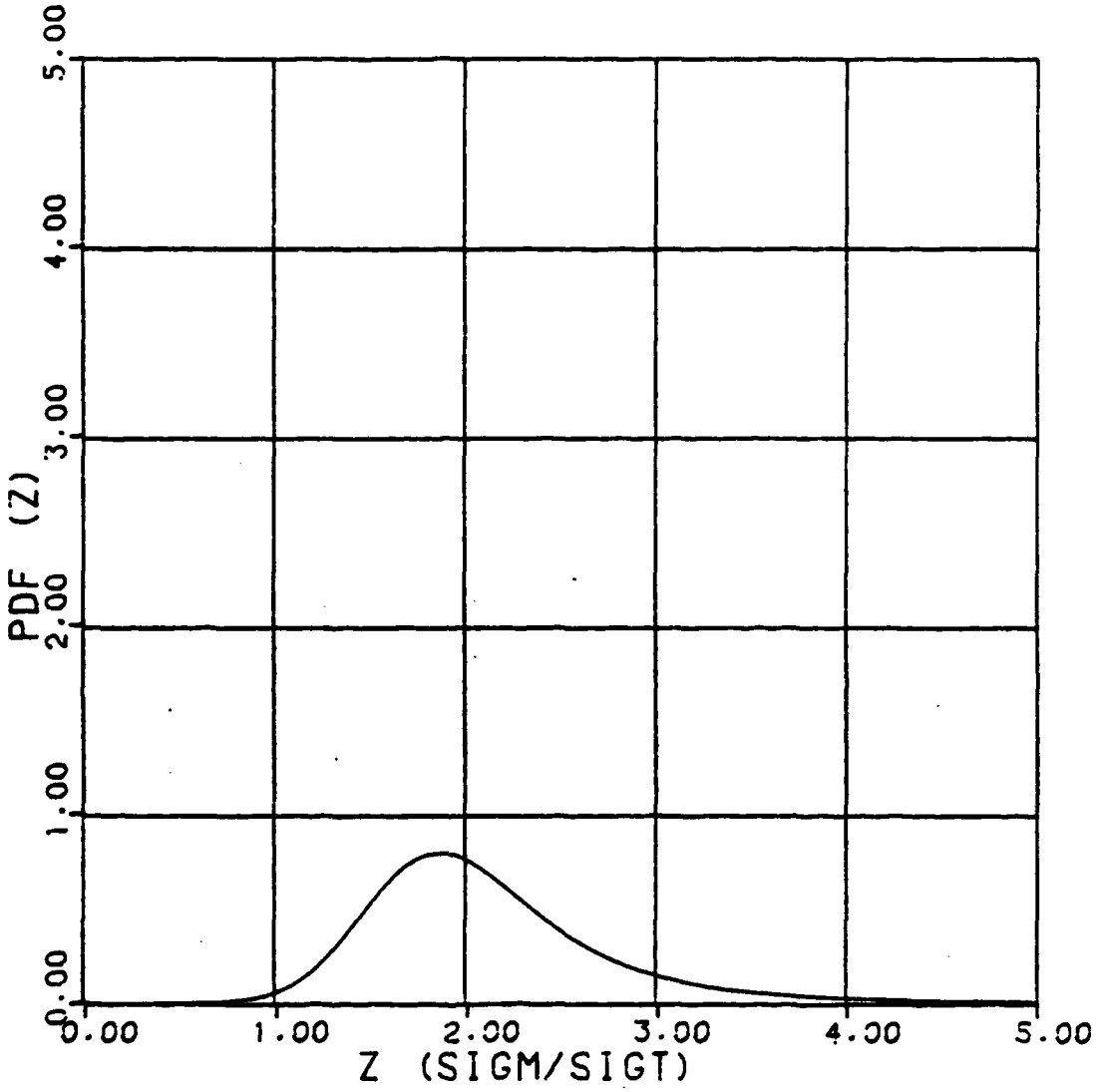

Figure V-6 Probability Density Function (Theortical) of the Ratio of the Averaged Measured Cross Section to the Averaged Target Cross Section for a Signal to Clutter Ratio of 1 (0 dB) and Averaging of N=11 Samples

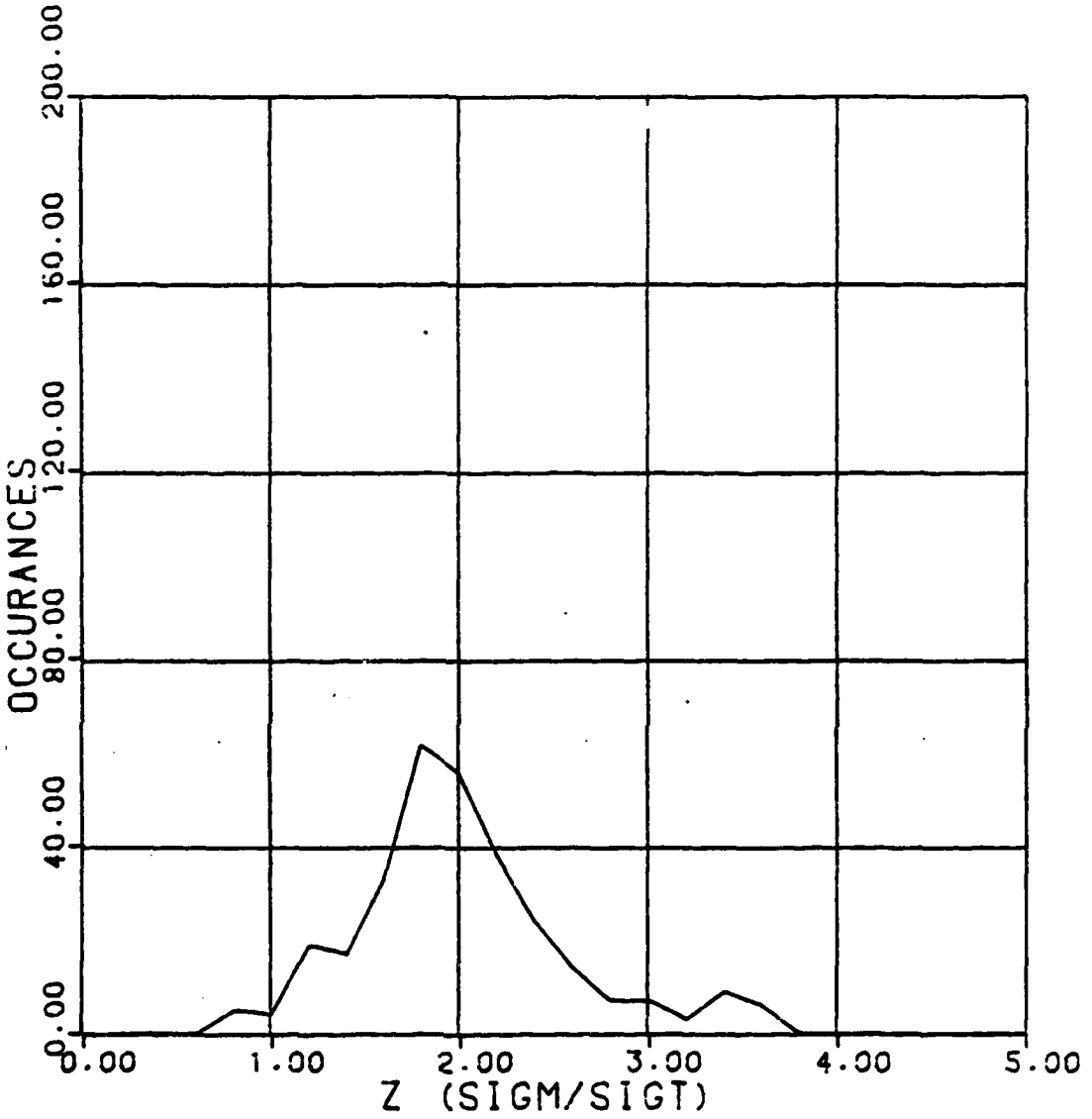

Figure V-7 Probability Density Function (from Computer Generated Data) of the Ratio of the Averaged Measured Cross Section to the Averaged Target Cross Section for an Average Signal to Clutter Ratio of 1 (0 dB), and Averaging of N=51 Samples

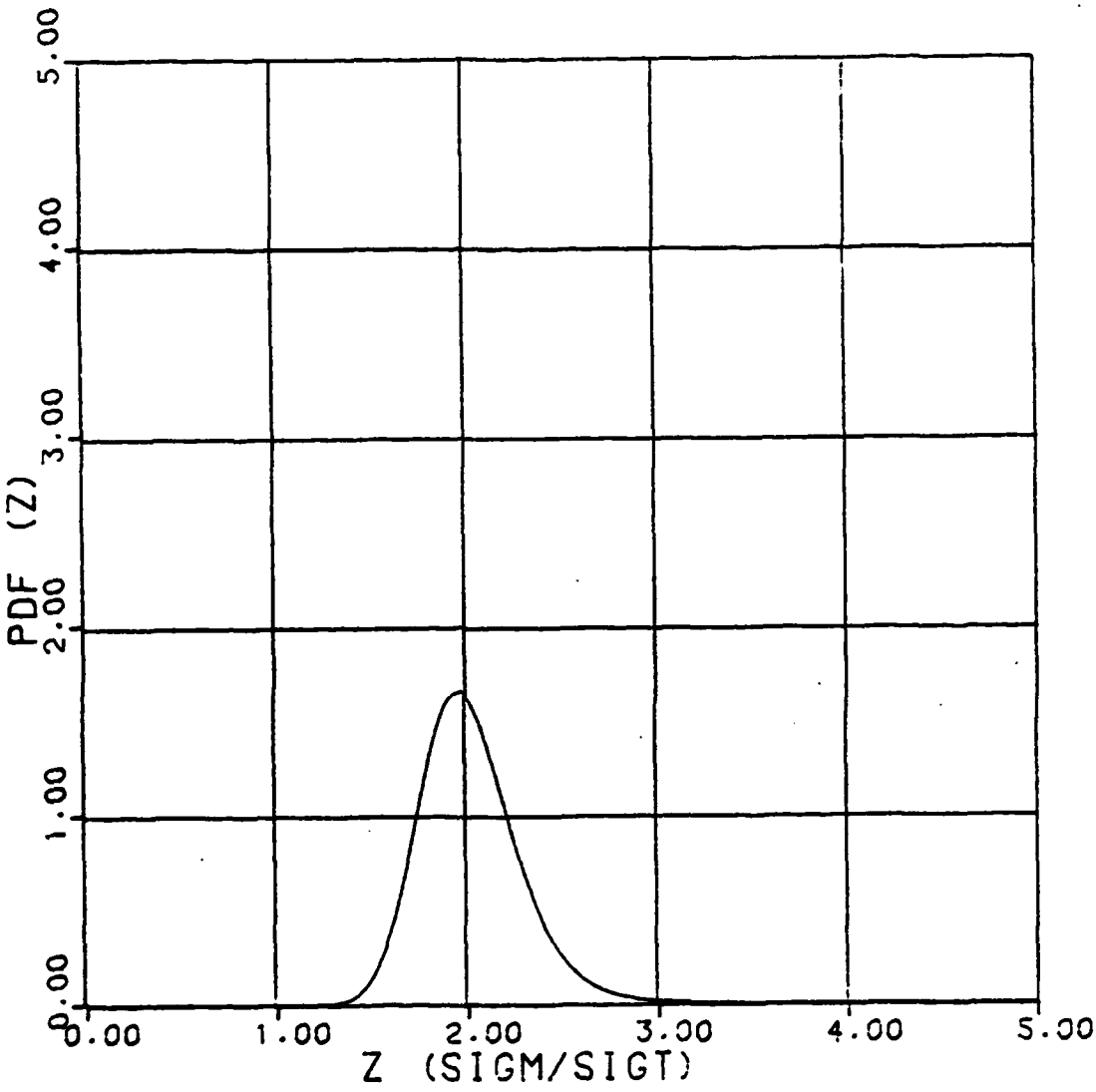

Figure V-8 Probability Density Function (Theortical) of the Ratio of the Averaged Measured Cross Section to the Averaged Target Cross Section for a Signal to Clutter Ratio of 1 (0 dB) and Averaging of N=51 Samples

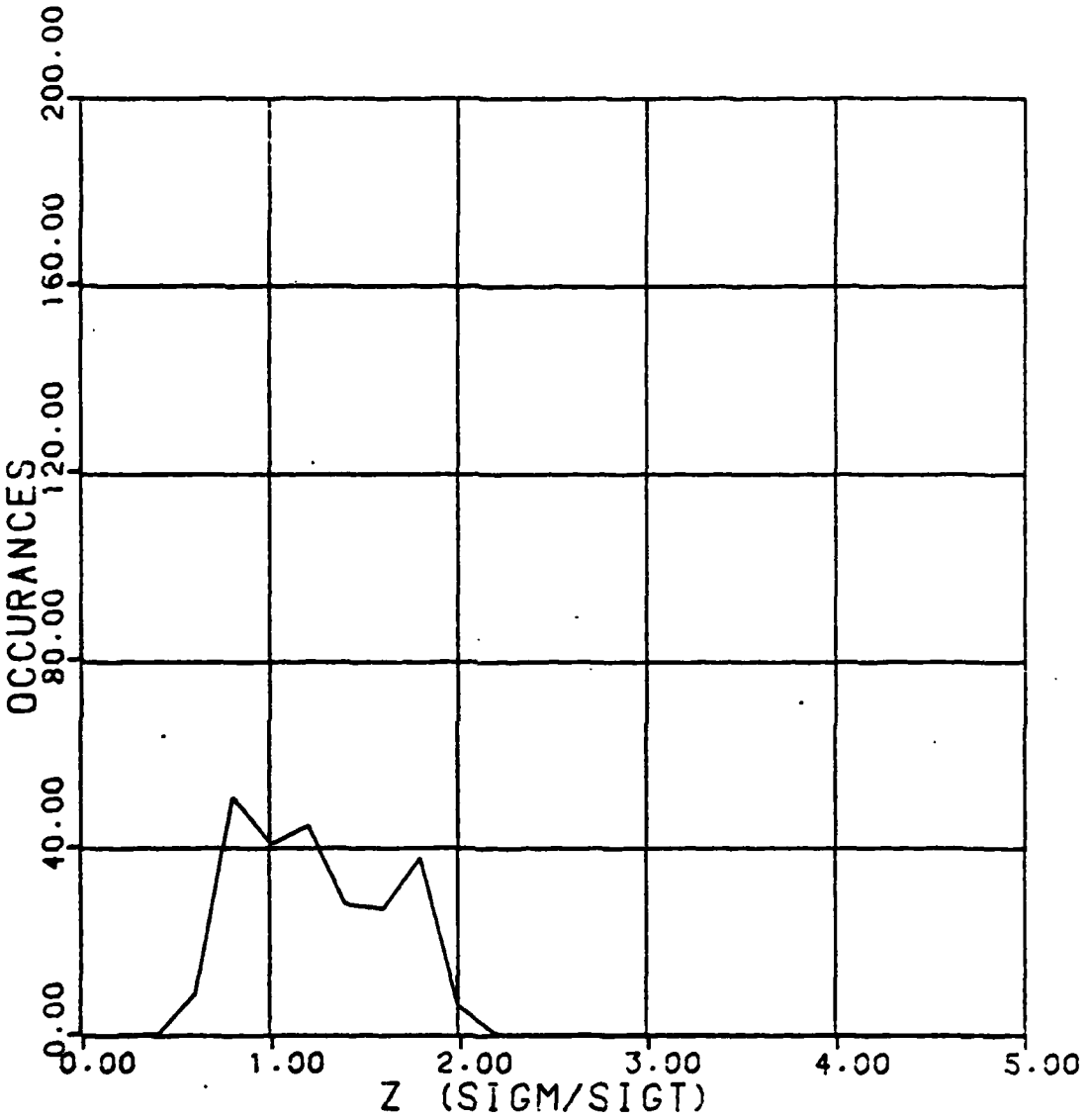

Figure V-9 Probability Density Function (from Computer Generated Data) of the Ratio of the Averaged Measured Cross Section to the Averaged Target Cross Section for an Average Signal to Clutter Ratio of 10 (10 dB), and Averaging of N=11 Samples

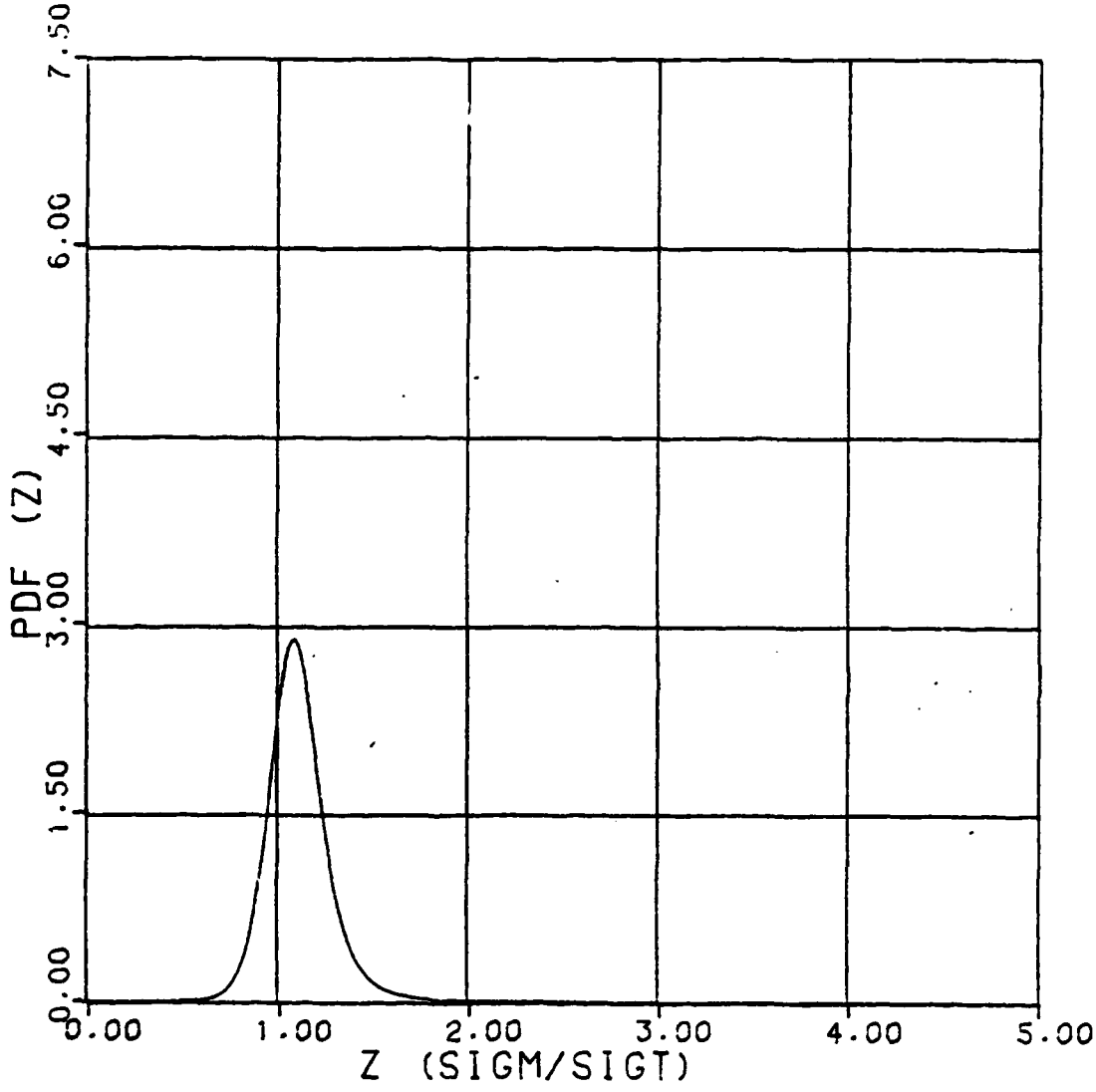

Figure V-10 Probability Density Function (Theortical) of the Ratio of the Averaged Measured Cross Section to the Averaged Target Cross Section for a Signal to Clutter Ratio of 10 (10 dB) and Averaging of N=11 Samples

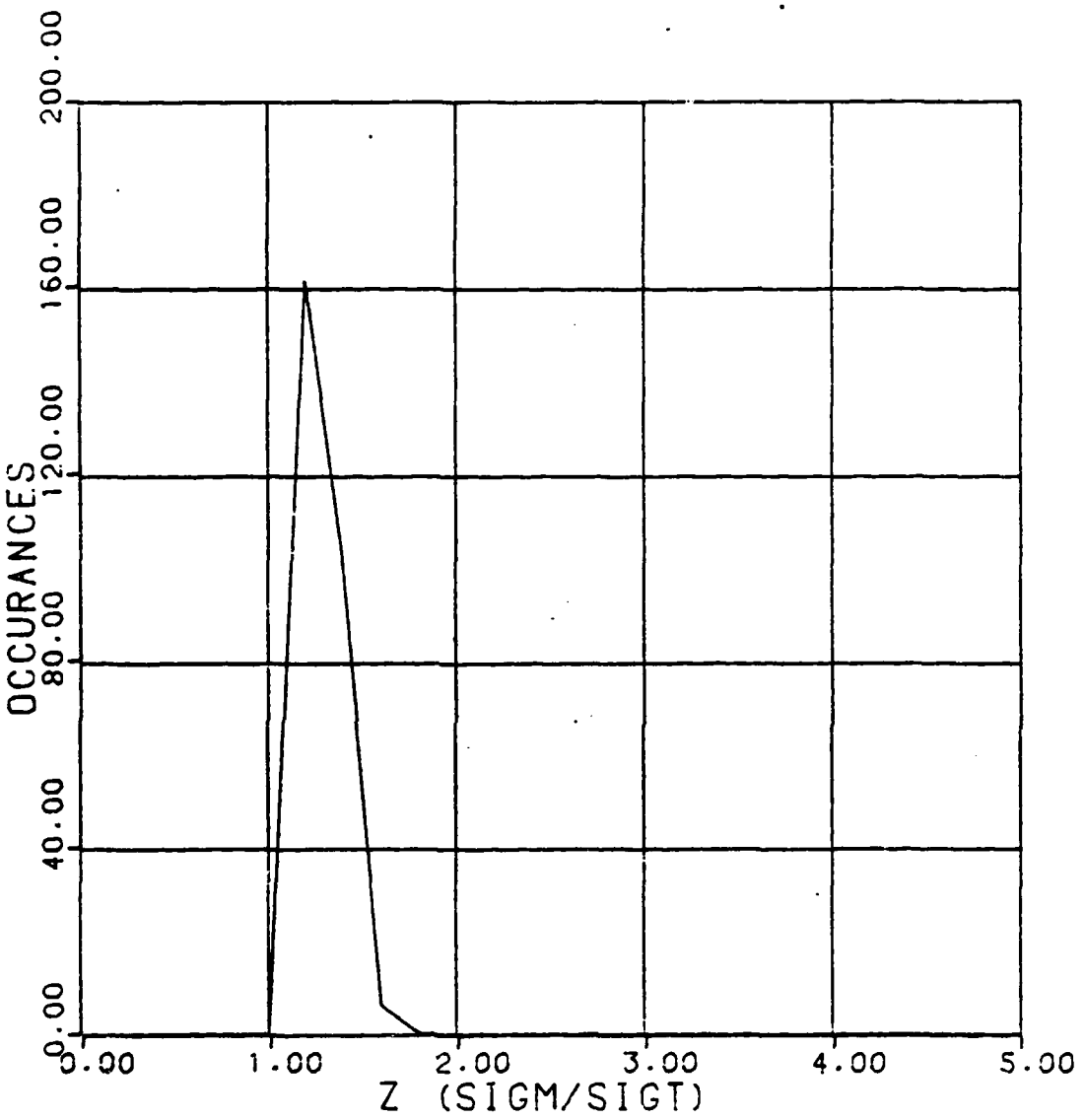

Figure V-11 Probability Density Function (from Computer Generated Data) of the Ratio of the Averaged Measured Cross Section to the Averaged Target Cross Section for an Average Signal to Clutter Ratio of 10 (10 dB), and Averaging of N=51 Samples

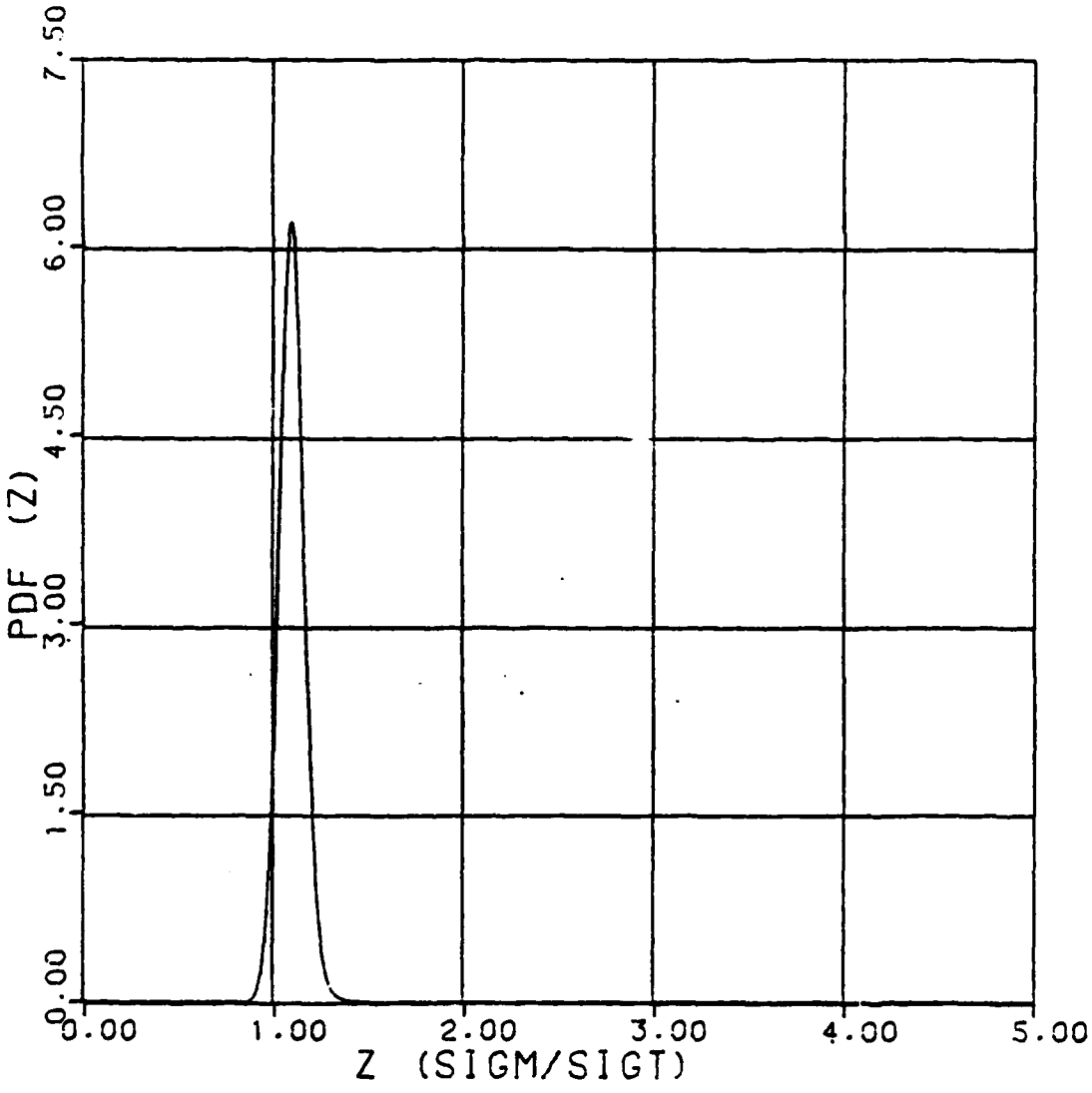

Figure V-12 Probability Density Function (Theortical) of the Ratio of the Averaged Measured Cross Section to the Averaged Target Cross Section for a Signal to Clutter Ratio of 10 (10 dB) and Averaging of N=51 Samples

VI. Results and Conclusions

In this chapter the problem and the outline of the procedure used to solve the problem will be reviewed. Next, the results and conclusions obtained from this procedure will be given.

Problem

The goal of this paper was to develop an error estimate of the cross section measurement of a diffracting target in constant clutter. This clutter was assumed to be caused soley by the target support. Because the target was diffracting in nature, it could be modelled by multiple independent scatterers and these many scatterers are statistical in nature. In the traditional approach the error was derived assuming two determinisic sources, with uniform random phase, and accuracy at every point. In this paper the new approach assumed statistical properties for the sources, and relaxed the hard requirement of accuracy at every point by incorperating an averaging techinque.

Procedure

The following is a list of the steps that went into the solution of the problem of this paper.

1. Derive the probability density function (pdf) and statistics of the target in free space.
2. Derive the pdf and statistics of the new model of the target with support.
3. Derive the pdf and statistics of the ratio of averaged measured cross section to the averaged target free space cross section.
4. Compare all of these theortical pdf's to pdf curves obtained from computer generated data.
5. Use the results obtained to find the level of confidence that can be placed in the measured data.

The properties of the target in free space, step one above, were derived in the chapter on the traditional approach, Chapter III. In this chapter it was shown that the target in free space has a Rayleigh distribution on the amplitude and an exponential distribution on the amplitude squared, or cross section. It was also shown that the mean of the cross section is simply the sum of the means of the cross sections of the contributing sources. Also in this chapter, the traditional approach of accuracy estimation was reviewed. Not only is the traditional accuracy estimate based on deterministic sources and no averaging, the estimate only shows how closely the measured data values are to the mean of the measured cross section. Of more interest is how

closely the measured data values are to the true free space target cross section.

The properties of the target with support, step two above, were derived in the chapter on the new model, Chapter IV. In this chapter the model of a Rayleigh distributed source added to a constant source was used to represent the target and target support. It was shown that the amplitude of the measured cross section, the combination of the target and support, has a Nakagami-Rice distribution. It was also shown that the mean of this measured cross section is simply the sum of the mean of target cross section and the support, or clutter, cross section.

The properties of the ratio of the averaged measured cross section to the averaged target cross section, step three above, were derived in the chapter on the new model, Chapter V. In this chapter the assumption was made that tne distributions of both the measured and free space target cross sections approach a Gaussian distribution after they are averaged over a minimum number of points. The correlation coefficient of the measured cross section and the target cross section was derived and used to complete the joint Gaussian pdf. This joint pdf was used to obtain the pdf of the ratio.

Every one of the pdf's that were derived were compared to pdf curves obtained from the computer generated data, step four above. The chapter on the computer generated data, Chapter II, explains the techinques used to obtain this data.

In all cases the theortical pdf's and the computer generated pdf's compare closely.

The results are used to obtain a measure of confidence that can be placed in the measured data, step five above. It turns out that the standard deviation of the ratio of the averaged measured cross section to the averaged target free space cross section is this measure of confidence. These results are summarized in the following section.

Results

In Chapter V it was shown that for a given level of clutter, increasing the amount of averaging lowered the standard deviation of the ratio of the averaged measured to the averaged free space target cross section. Of course, increasing the signal to clutter ratio also decreased the standard deviation, but on a measurement range one is usually limited to a particular value, or average value, of clutter. When the standard deviation of this ratio becomes less the spread of possible values of data around the mean becomes smaller. Therefore, the standard deviation can be used as a measure of confidence of how close the actual measured data will be to true target data.

Figure VI-1 shows a family of plots of standard deviations versus signal to clutter ratio for several values of averaging. It can be seen from this family of plots that the confidence, or rather, the standard deviation, of the measured data improves not only with increasing signal to clutter ratio, but also with increasing averaging.

Also shown on the same figure is a similar curve of the ratio of the measured cross section to the free space target cross section using the traditional approach assumptions. These assumptions, of course, are determinisic sources, except for uniform random phase, and no averaging. It can be seen that even for the moderately low level of 11 samples, the new approach shows a dramatic improvement over the traditional approach in the amount of confidence that can be

placed in the measured data.

Another way of showing the new accuracy estimate, that may be more familiar, is to show the rms bounds. These rms error bounds are similar to the traditional rms bounds (see Chapter III) in that they show, in dB, the spread one standard deviation above and below the normalized mean. Figure VI-2 shows the rms bounds from the new approach for a sampling level of N=11. At first, these bounds appear to be worse, especially at very low signal to clutter levels, than the traditional approach's rms bounds. But the thing to remember is that the traditional approach determines how far the data can be from the mean of the measured cross section. Of more interest is how far the data can be from the true free space target cross section, which is what is shown here. Figure VI-3 and Figure VI-4 show the rms bounds from the new approach for sampling of N=25 and N=51 points respectively.

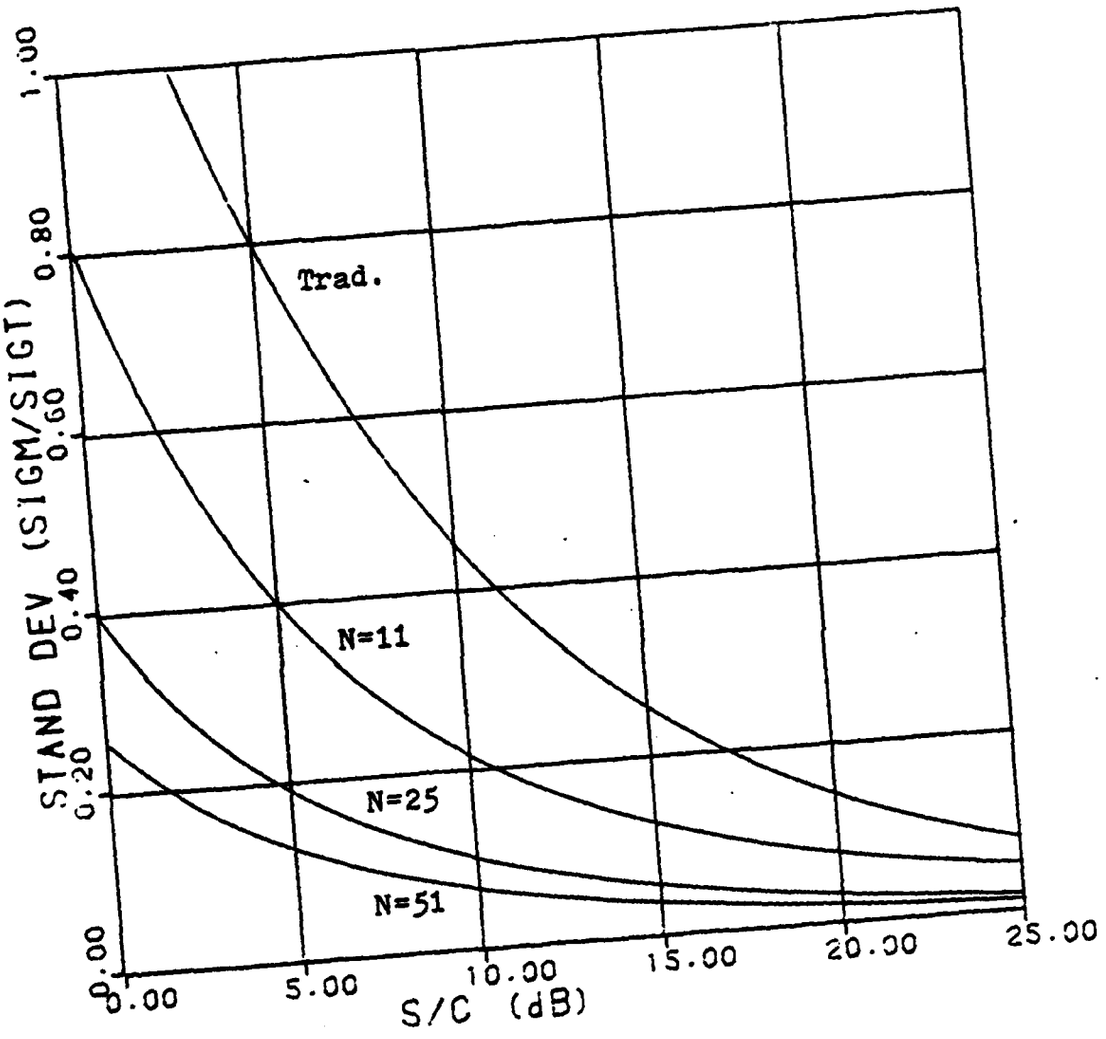

Figure VI-1 Standard Deviation vs. Signal to Clutter Ratio of the Ratio of the Averaged Measured Cross Section to the Averaged Free Space Target Cross Section for Several Values of Averaging and for Traditional Approach Assumptions.

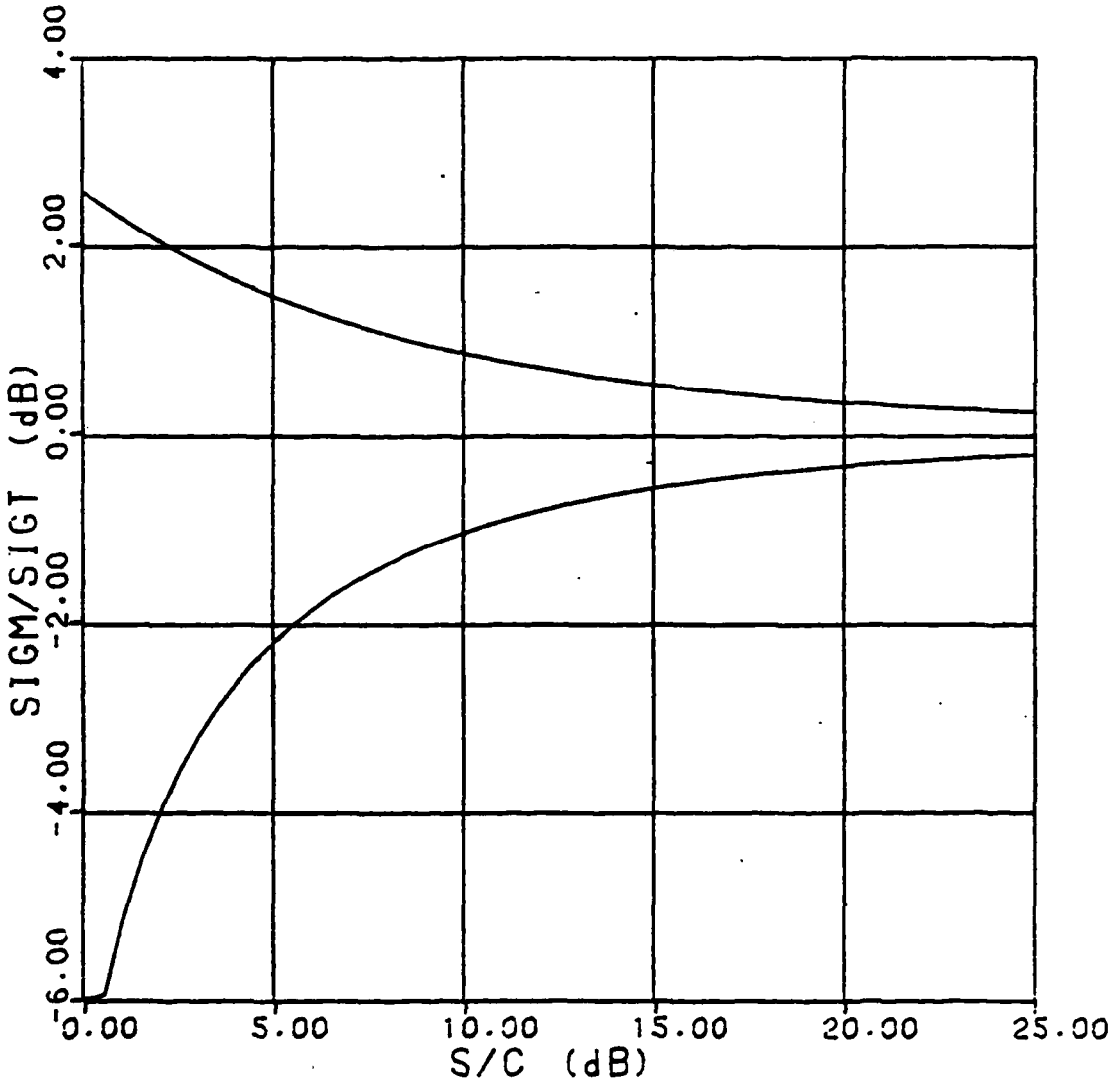

Figure VI-2 RMS Bounds for New Approach Assumptions (N=11)

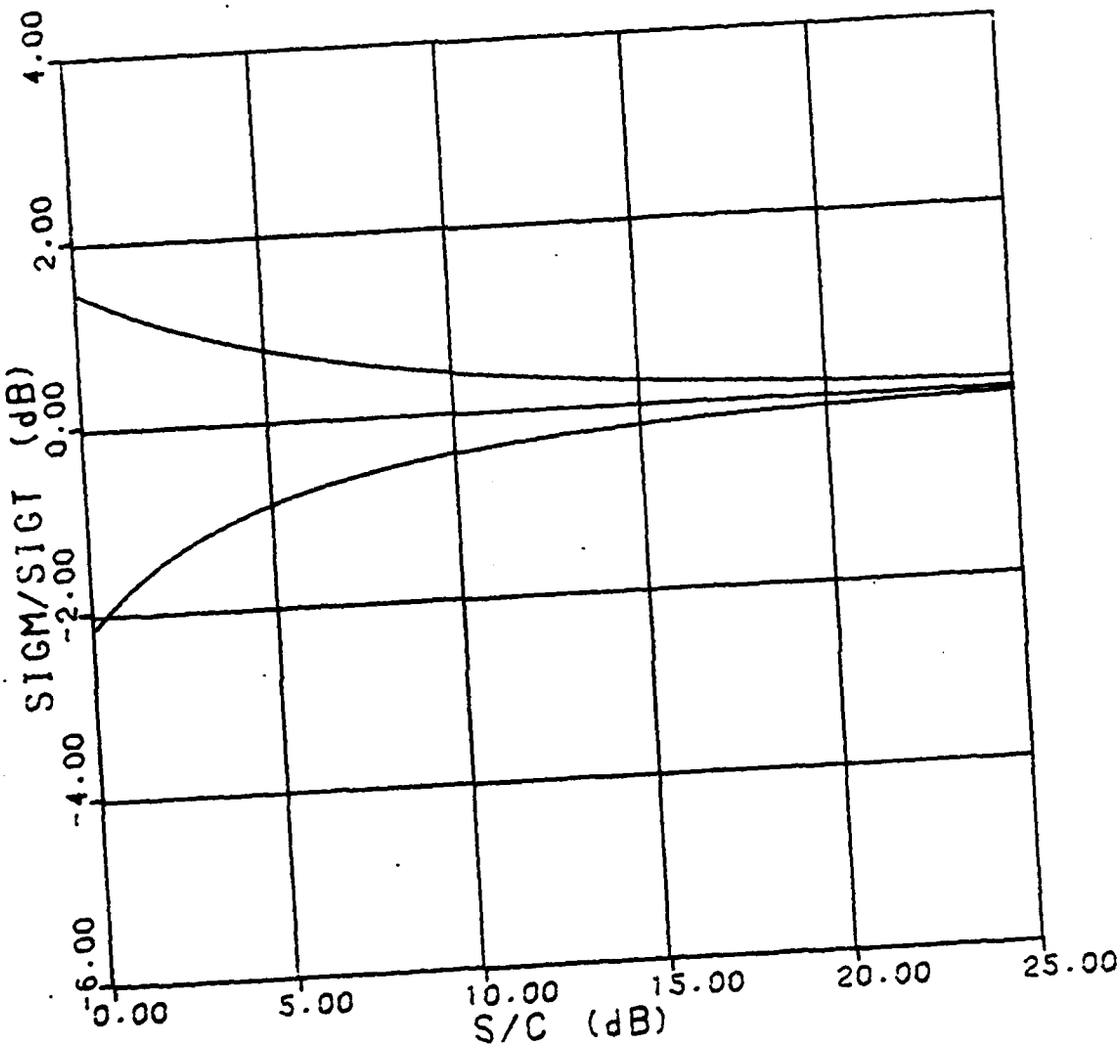

Figure VI-3 RMS Bounds for New Approach Assumptions (N=25)

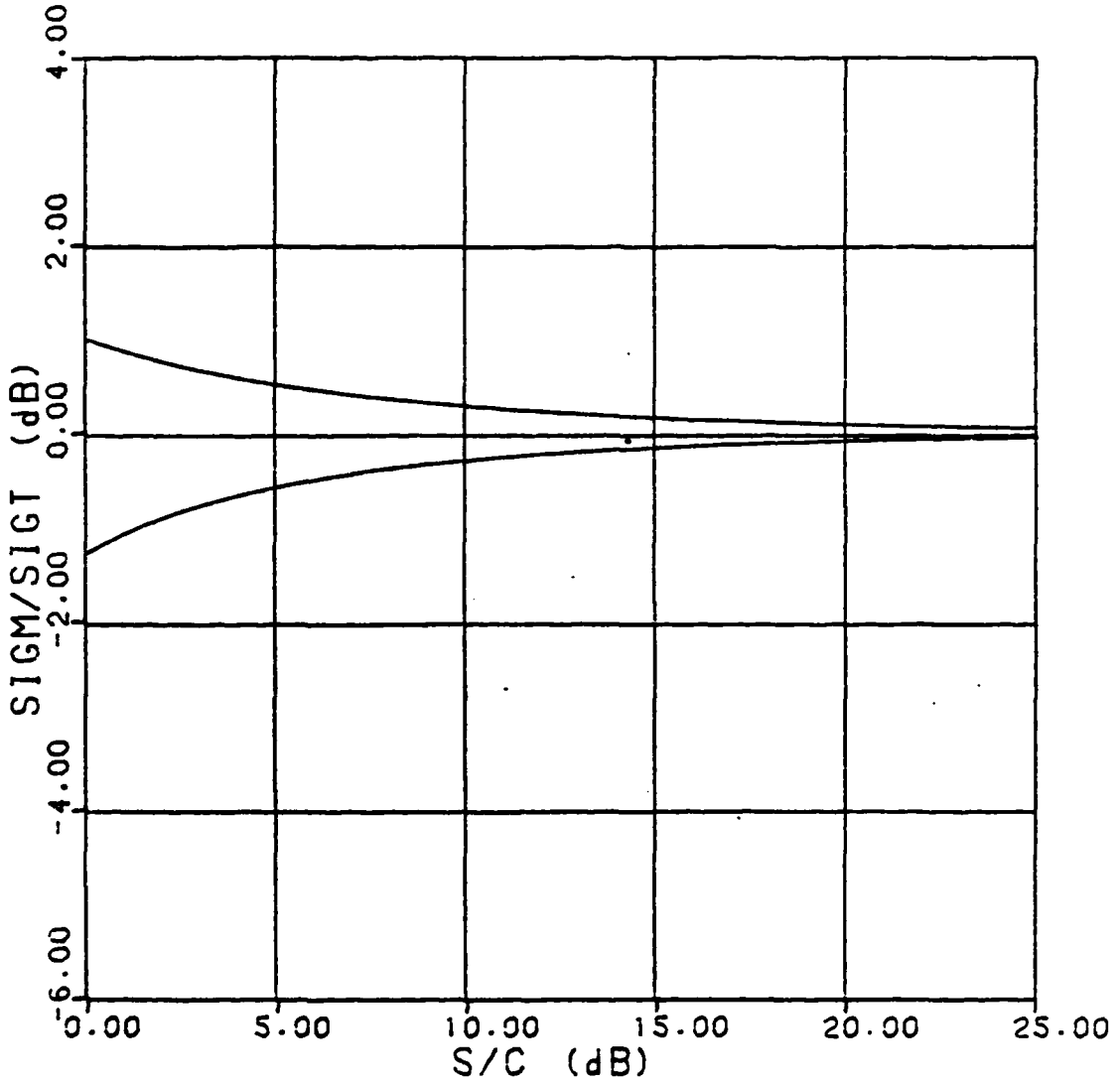

Figure VI-4 RMS Bounds for New Approach Assumptions (N=51)

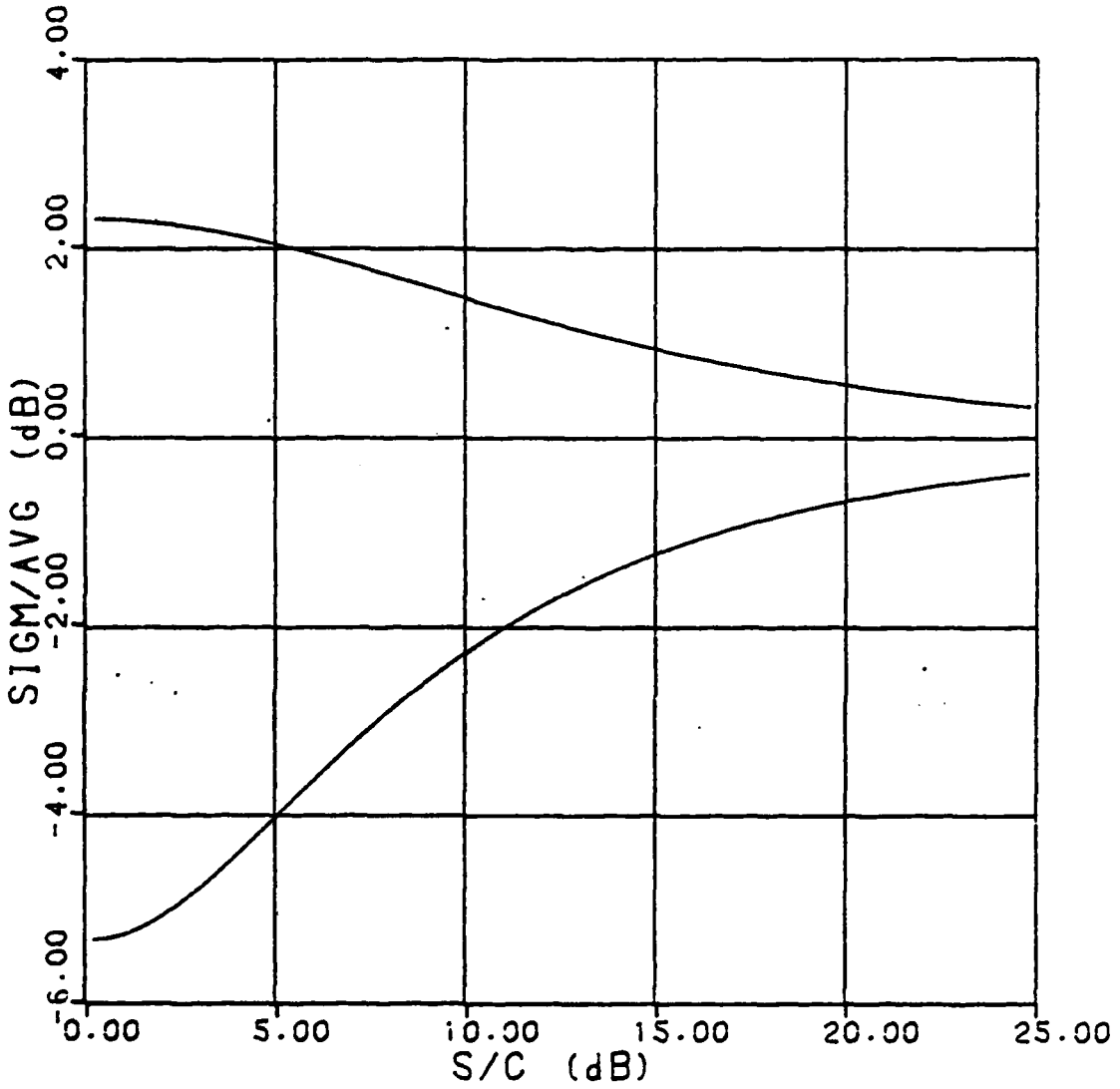

Figure VI-5 RMS Bounds for Traditional Approach Assumptions

Example

To illustrate the use of Figures VI-1, VI-2, VI-3, and VI-4 in determining the level of confidence of the measured data, an example will be worked. In this example the following assumptions will be made:

1. The background clutter is only from the target support.
2. This clutter level can be accurately measured.
3. The number of averaging points is known and is greater or equal to 11.
4. An average value of the return from the target with clutter can be obtained.

First, the use of standard deviation curves (Figure VI-1) will be demonstrated. In this example suppose that the average target and target support return was measured at -46 dB, and suppose that the clutter, or support, was measured at -52.2 dB. Recall that the mean of the measured cross section is simply the sum of the mean of the free space target cross section and the clutter cross section, Equation (IV-8). Converting these cross section levels from dB and subtracting, the average target cross section is found to be -47.2 dB. This makes an average signal to clutter ratio of 5 dB. If the values of the measured cross section are shifted by the value of the clutter level, the mean of the ratio of the averaged measured and averaged target cross sections will be unity. Another way of visualizing this is to shift the pdf curve of the ratio so that the mode is at unity (the mode

and medium of these pdf curves are all very close). Suppose now that the averaging is 11 samples. With these values of averaging and signal to clutter ratio, it can be seen from Figure VI-1 that the standard deviation is 0.40. In other words, a majority of the cross section data will be withing 0.40 of the mean of the ratio. In fact, numerical integration has shown that 84 percent of the values will be within this rms bound.

To demonstrate the rms bounds curves the same assumptions will be made. Using a signal to clutter ratio of 5 dB and sampling of N=11 one can look on Figure VI-2 to see how many dB's of accuracy one can expect in a measurement. From Figure VI-2 one would expect 84 percent of the measured data points to be within 1.5 dB above and 2.1 dB below the true free space target cross section.

This can be contrasted with the confidence limits of the traditional approach, shown in Figure VI-5, which gives the rms spread of the data for this case as being within 0.6 of the measured value, or falling in a range of 4.0 dB below and 2.0 dB above the measured value. The difference is that Figure VI-5 says that about 84 percent of the raw data points will fall in the range of -4.0 dB to 2.0 dB of the measured data, while Figure VI-2 says that after averaging over 11 samples the data will be within -1.5 dB to 2.1 dB of the true mean 84 percent of the time.

Conclusions

The following is a summary of the conclusions that are obtained from this paper.

1. The new approach more accurately describes the error than the traditional approach.
2. The amplitude of the model for the target with support used in the new approach has a Nakagami-Rice distribution.
3. If the data of cross section points is taken for too small of an increment of aspect angle, the values of cross section will no longer be independent and the all assumptions about the probabilistic nature of the cross section are no longer valid.
4. The standard deviation of the ratio of the averaged measured cross section to the averaged free space target cross section is a good measure of confidence for the measured data.
5. This measured of confidence not only improves with increasing signal to clutter ratio, but also improves as the data is averaged over more points.
6. This measure of confidence, or standard deviation of the ratio, is shown for several values of averaging in Figure VI-1. The measure of confidence is also shown in the form of rms bounds for several values of averaging in Figures VI-2, VI-3, and VI-4.

Bibliography

1. Abramowitz, M. and Stegun, I. A. Handbook of Mathematical Functions. NBS Applied Mathematical Service, v55 (1970).

2. Beckmann, P. "Rayleigh Distribution and Its Generalizations," Radio Science Journal of Research NBS, v68D (9): 927-932 (September 1964).

3. Crispin, J. W. and Maffett, A. L. "Radar Cross Section Estimation for Complex Shapes," Proceedings IEEE, v53: 972-982 (August 1965).

4. Crispin, J. W. and Siegel, K. M. Methods of Radar Cross Section Analysis. New York: Academic Press, 1968.

5. Erdeyli, A. et al. Tables of Integral Transforms v1. New York: McGraw-Hill Book Co., 1954.

6. Freeny, C. C. "Target Support Parameters Associated With Radar Reflectivity Measurements," Proceedings IEEE, v53: 929-936 August 1965).

7. Heidbreder, G. R. and Mitchel, R. L. "Detection Probabilities for Log-Normally Distributed Signals," IEEE Transactions on Aerospace and Electronic Systems, v3 (1): 5-13 (January 1967).

8. Hogg, R. V. and Craig, A. T. Introduction to Mathematical Statistics, (fourth edition). New York: Macmillan Publishing Co, Inc., 1978.

9. Norton, K. A. et al. "The Probability Distribution of a Constant Vector Plus a Rayleigh Distributed Vector," Proceedings of the IRE, v43: 1354-1361 (October 1955).

10. Papoulis, A. Probability, Random Variables, and Stochastic Process. New York: McGraw-Hill Book Co., 1965.

11. Rice, S. O. "Mathematical Analysis of Random Noise," Bell System Technical Journal, v24: 46-156 (1945).

12. Ruck, G. T. et al. Radar Cross Section Handbook v2. New York: Plenum Press, 1970.

Bibliography (continued)

13. Senior, T. A. et al, "Designing Foamed Plastic Target Supports," Microwaves: 38-43 (December 1964).

14. Skolnik, M. Introduction to Radar Systems, (second edition). New York: McGraw-Hill Book Co., 1980.

15. Swerling, P. "Probability of Detection for Fluctuating Targets" RAND Corp., Santa Monica, CA, Research Memo. RM-1217, March 17, 1954.

Vita

Jon Nelson Link was born 11 April 1960 in Grand Island, Nebraska. He Graduated from high school in Ravenna, Nebraska in 1978 and attended the University of Colorado from which he received the degree of Bachelor of Electrical Engineering in May 1982. Upon graduation, he received a commission in the United States Air Force through the ROTC program. He went directly into active duty and entered the School of Engineering, Air Force Institue of Technology, in June 1982.

Permanent address: Route 3, Box 23
Ravenna, Nebraska 68869

UNCLASSIFIED

SECURITY CLASSIFICATION OF THIS PAGE (When Data Entered)

REPORT DOCUMENTATION PAGE		READ INSTRUCTIONS BEFORE COMPLETING FORM
1. REPORT NUMBER AFIT/GE/EE/83D-39	2. GOVT ACCESSION NO. AD-A138075	3. RECIPIENT'S CATALOG NUMBER
4. TITLE (and Subtitle) ACCURACY ESTIMATE FOR RADAR CROSS SECTION MEASUREMENTS OF TARGETS MODELLED BY MULTIPLE INDEPENDENT SCATTERERS IN CONSTANT CLUTTER		5. TYPE OF REPORT & PERIOD COVERED MS THESIS 6. PERFORMING ORG. REPORT NUMBER
7. AUTHOR(s) Jon N. Link 2Lt USAF		8. CONTRACT OR GRANT NUMBER(s)
9. PERFORMING ORGANIZATION NAME AND ADDRESS Air Force Institute of Technology (AFIT/EN) Wright-Patterson AFB, Ohio 45433		10. PROGRAM ELEMENT, PROJECT, TASK AREA & WORK UNIT NUMBERS
11. CONTROLLING OFFICE NAME AND ADDRESS		12. REPORT DATE December 1983 13. NUMBER OF PAGES 141
14. MONITORING AGENCY NAME & ADDRESS(if different from Controlling Office)		15. SECURITY CLASS. (of this report) Unclassified 15a. DECLASSIFICATION DOWNGRADING SCHEDULE

16. DISTRIBUTION STATEMENT (of this Report)

Approved for public release; distribution unlimited

17. DISTRIBUTION STATEMENT (of the abstract entered in Block 20, if different from Report)

18. SUPPLEMENTARY NOTES

Approved for public release: IAW AFR 190-17.

Lynn E. Wolaver
Dean for Research and Professional Development
Air Force Institute of Technology (AFIT)
Wright-Patterson AFB OH 45433

7 Dec 84

19. KEY WORDS (Continue on reverse side if necessary and identify by block number)

Radar Cross Section
Measurement Errors
Background Clutter

20. ABSTRACT (Continue on reverse side if necessary and identify by block number)

The error bounds for accuracy of radar cross section (RCS) measurements of targets in clutter are examined in detail. Traditional error bounds are based on precision at every individual aspect angle and on two deterministic sources (target and clutter). In this thesis a model is developed that describes the target and clutter probibilistically. The requirement of

(continued on back)

DD FORM 1 JAN 73 1473 EDITION OF 1 NOV 65 IS OBSOLETE

UNCLASSIFIED

SECURITY CLASSIFICATION OF THIS PAGE (When Data Entered)

(continued from Block 20)

accuracy at every point is replaced by a requirement for accuracy of a running average of measured RCS values. The probability distribution of the ratio of the averaged, measured RCS to the averaged, true, free space target RCS is calculated. The standard deviation of this ratio represents how much the averaged, measured RCS data diverages from the averaged, true, free space target RCS.

The results show that accuracy improves for increasing signal to clutter ratios, and also for increasing levels of averaging. Even averaging as few as eleven points, this new measure is shown to give more confidence in the measured, averaged results than the traditional approach.


FILM
3-8